

Kristoffer Gustad Landsem

Investigation of the diffusion barrier properties in mixtures of mammalian and cold-water fish gelatin

Master's thesis in Chemical Engineering and Biotechnology (MTKJ)

Supervisor: Catherine Taylor Nordgård

Co-supervisor: Kurt Ingar Draget

June 2023

Kristoffer Gustad Landsem

Investigation of the diffusion barrier properties in mixtures of mammalian and cold-water fish gelatin

Master's thesis in Chemical Engineering and Biotechnology (MTKJ)
Supervisor: Catherine Taylor Nordgård
Co-supervisor: Kurt Ingar Draget
June 2023

Norwegian University of Science and Technology
Faculty of Natural Sciences
Department of Biotechnology and Food Science



Preface

This master thesis was conducted at the Department of Biotechnology and Food Science at the Norwegian University of Science and Technology (NTNU) from January to June of 2023. The thesis was written as part of the research network iFOODnet, a multi-disciplinary research network with the goal of furthering a long-term Norway-Japan research partnership, with a focus on zero-waste food systems.

I would like to thank my supervisors Dr. Catherine Taylor Nordgård and Professor Kurt Ingar Draget for supporting me and guiding me through this project, and for taking the time to teach me and help me when I have needed it, I want to thank them for being patient and understanding to me, and for giving me the freedom to develop my own skills as well, something that has been very valuable for me. I feel as though I have learnt a lot throughout this entire project, both theoretical and practical.

I would also like to thank all of the students and Professor Shingo Matsukawa at the BUSSEI group at the Tokyo University of Marine Science and Technology for being so kind and helpful to me during my visit at their university. Lastly I would also like to thank my family, friends and fellow students for all the help and support throughout this entire process.

NTNU, Trondheim

June 2023

Kristoffer Gustad Landsem

Abstract

The diffusion barrier properties of a gel is one of several important factors that helps to define the behaviour and functionality of that gel. Gelatin is one of many gelling agents that are commonly used in the industry today, with the majority of the gelatin used coming from mammalian sources. Gelatin has a wide array of uses both in food and pharmaceutical contexts, many of which the diffusion barrier properties are highly important for. Gelatin is a biopolymeric material that can be obtained from the hydrolysis of collagen, the source of which highly affects the properties of the resulting gelatin. Collagen can be obtained from the skin and bones of most animals, with fish being one such example. With the fishing industry constantly growing on a yearly basis, the amounts of rest raw materials produced is naturally increasing as well, something that's of a growing concern due to the lack of high-profit applications for these raw materials. Despite much of this raw material containing large amounts of collagen, the production of gelatin from cold-water fish sources is still relatively uncommon. The main reason for this is the low gelling and melting temperatures that it exhibits, as this is undesirable for many common industrial applications. For this reason, there is a need to find a way to improve the gelling capabilities of cold-water fish gelatin if it is to see any significant use. One such method could potentially be mixing cold-water fish gelatin with mammalian gelatin to obtain a mixed system with desirable properties, a method which has shown some promise.

The aim of this thesis was to examine the diffusion barrier properties of mixtures containing cold-water fish gelatin and mammalian gelatin, with the goal of determining how these properties are affected by the presence of cold-water fish gelatin. To do this, samples containing both gelatin types were tested with the use of several different methods, and compared to samples of pure mammalian gelatin. The purpose of this was to establish how the diffusion barrier properties are affected when substituting part of a mammalian gelatin gel with cold-water fish gelatin. The methods employed to test this were particle tracking of fluorescent particles added to the gels, and the measurement of the release of coloured compounds from the gels in an aqueous medium. It was also suggested that the addition of oil to the mixed gelatin systems via emulsification affected the distribution of the two gelatin types. To explore if the distribution was affected when the mixed gels were used in an oil emulsion, fluorescence recovery after photobleaching was utilised.

The results obtained from the particle tracking indicated that the diffusion barrier properties were heavily shifted towards the behaviour seen in mammalian gelatin gels when measured at room temperature, even for mixtures containing just 10% mammalian gelatin. These results indicated that even with as much as 90% of the gelatin matrix being cold-water fish gelatin, which should melt well below room temperature, the gels were still able to form a seemingly mixed and stable system. The same thing was seen when measuring the release in an aqueous environment as well, where mixed gels containing 50% cold-water fish gelatin showed a slow release of both small and large compounds similar to pure mammalian gels. Both of these experiments gave no indication that there was phase separation in the mixed gels, which would suggesting that they are able to form mixed matrices. These result seem to imply that a relatively large amount of cold-water fish gelatin can be used in place of mammalian gelatin without any significant effect on the diffusion barrier properties. The FRAP experiments did not provide any significant difference between the diffusion properties of the oil emulsions and regular gels, though they did also seem to show no sign of any phase separation, further strengthening the other findings.

Sammendrag

Diffusjonsbarriereegenskapene til en gel er en av flere viktige faktorer som bidrar til å definere oppførselen og funksjonaliteten til den. Gelatin er en av mange geleringsmiddel som er vidt brukt i industrien i dag, og det aller meste av dette gelatinet kommer fra pattedyr. Gelatin har et bredt spekter av bruksområder både innenfor mat og legemidler, hvor diffusjonsbarriereegenskapene er viktige for mange av dem. Gelatin er et biopolymert material som lages ved hydrolyse av kollagen, hvorav kollagenkilden har stor effekt på egenskapene til det resulterende gelatinet. Kollagen kan bli hentet ut av skinn og ben til de aller fleste dyr, blant annet fisk. Gitt at fiskeindustrien er stadig voksende for hvert år er det også naturlig at mengden restråstoff produsert øker, noe som er en økende bekymring på grunn av mangelen på høyprofittapplikasjoner for disse råvarene. Til tross for at store deler av dette råmaterialet inneholder mye kollagen, er produksjon av gelatin fra kaldtvannsfisk fremdeles relativt uvanlig. Den største årsaken til dette er den lave gelerings- og smeltetemperaturen som den viser, siden dette er uønsket for mange vanlige industrielle bruksområder. På grunn av dette så er det et stadig behov for å finne en måte å forbedre geleringsvevnen til gelatin fra kaldtvannsfisk på for at det skal kunne se en større industriell bruk. En potensiell metode for å oppnå dette er ved å blande kaldtvannsfiskegelatin med pattedyrgelatin for å få et blandet system med gode egenskaper, en metode som har vist seg å være lovende.

Målet med denne oppgaven var å undersøke diffusjonsbarriereegenskapene til blandinger av gelatin fra kaldtvannsfisk og pattedyr, med et håp om å kunne finne ut hvordan disse egenskapene påvirkes av kaldtvannsfiskegelatin. For å gjøre dette ble prøver som inneholdt begge gelatintyper testet ved bruk av flere ulike metoder, og deretter sammenlignet med prøver fra ren pattedyrgelatin. Hensikten med dette var å undersøke hvordan diffusjonsbarriereegenskapene påvirkes når deler av pattedyrgelatinet erstattes med kaldtvannsfiskegelatin. Metodene anvendt for å gjøre dette var partikkelsporing av tilsatte fluorescerende partikler i gelene, og måling av frigjøring av fargede stoffer fra gelene i et vandig medium. Det ble også antydnet at tilsetning av olje til de blandede gelene via emulgering påvirket fordelingen av de to gelatintypene. For å undersøke om fordelingen ble påvirket når gelene ble brukt i en oljeemulsjon, ble det brukt fluorescence recovery after photobleaching.

Resultatene fra partikkelsporingen indikerte at diffusjonsbarriereegenskapene var relativt stekt forskjøvet mot den oppførselen sett i ren pattedyrgelatin når målingene ble utført ved romtemperatur. Dette ble observert selv for blandinger med bare 10% pattedyrgelatin, som antydnet at selv med 90% kaldtvannsfiskegelatin i blandingen, som i utgangspunktet burde smelte ved romtemperatur, var gelene fremdeles i stand til å danne et blandet og stabilt system. Det samme ble observert når frigjøringen fra gelene i et vannholdig miljø ble testet, da geler med 50% kaldtvannsfiskegelatin viste en langsom frigjøring av både små og store forbindelser i lik linje med ren pattedyrgelatin. Begge disse metodene ga ingen indikasjon på at det oppsto en faseseparasjon i de blandede gelene, noe som tyder på at de dannet blandede matriser. Disse resultatene ser også ut til å antydne at en relativt stor mengde kaldtvannsfiskegelatin kan brukes i stedet for pattedyrgelatin uten at det har en vesentlig effekt på diffusjonsbarriereegenskapene. FRAP-eksperimentene ga ingen betydelig forskjell mellom diffusjonsegenskapene til emulsjonene og de vanlige gelene. Det var heller ingen tegn til faseseparasjon i FRAP-resultatene, noe som ytterligere styrker de andre funnene over.

List of abbreviations

FITC	Fluorescein isothiocyanate
FRAP	Fluorescence recovery after photobleaching
MSD	Mean squared displacement
NTNU	Norwegian University of Science and Technology
TUMSAT	Tokyo University of Marine Science and Technology

Table of Contents

List of Figures	7
List of Tables	11
1 Introduction	1
1.1 Gels	1
1.2 Collagen & gelatin	1
1.2.1 Collagen	1
1.2.2 Gelatin	2
1.2.3 Cold-water fish skin gelatin	4
1.2.4 Gelatin usage	5
1.3 Fluorescence and light absorption	5
1.3.1 Light absorption	5
1.3.2 Fluorescence	6
1.4 Methods for studying particle motion in liquid and semi solid systems	7
1.5 Dissolution measurements	9
1.6 Fluorescence laser scanning microscopy	10
1.6.1 Confocal laser scanning microscopy (CLSM)	10
1.6.2 Fluorescent recovery after photobleaching (FRAP)	11
1.7 Motivations and goals for the thesis	12
2 Materials and methods	13
2.1 Materials	13
2.1.1 Porcine gelatin	13
2.1.2 Cold-water fish gelatin	13
2.1.3 Fluospheres™ microbeads, 1 μm yellow-green	13
2.1.4 Tartrazine	13
2.1.5 Blue dextran	13
2.1.6 Fluorescein isothiocyanate–dextran	13
2.1.7 Corn oil	14
2.2 Methods	14
2.2.1 Particle tracking	14
2.2.1.1 Sample preparation	14
2.2.1.2 Imaging of particles	14

2.2.1.3	Tracking of particles and mean squared displacement analysis . . .	15
2.2.1.4	Overview of particle tracking protocol	16
2.2.2	Release from gels in aqueous environment	17
2.2.2.1	Introduction	17
2.2.2.2	Determination of standard curves	17
2.2.2.3	Sample preparation	20
2.2.2.4	Protocol for release measurements	21
2.2.2.5	Overview of release measurement protocol	22
2.2.3	Fluorescence recovery after photobleaching	23
2.2.3.1	Introduction	23
2.2.3.2	Sample preparation	23
2.2.3.3	Protocol for measurements and analysis	24
2.2.3.4	Overview of fluorescence recovery after photobleaching protocol . .	24
3	Results discussion	26
3.1	Particle tracking	26
3.1.1	Particle tracking at Tokyo University of Marine Science and Technology . .	26
3.1.2	Particle tracking conducted at the Norwegian University of Science and Technology	42
3.2	Release from gelatin in an aqueous environment	52
3.2.1	Pure porcine gelatin	53
3.2.2	Gel containing equal parts pig skin and cold-water fish skin gelatin	59
3.2.3	Comparison and interpretation of results	62
3.3	Emulsion tests	65
4	Conclusion	70
5	Possible implications of findings	71
6	Further work	72
	References	73
	Appendix	77
A	Particle tracking MSD data	77
A.1	Particle tracking performed at TUMSAT	77
A.1.1	Particle tracking at 5 °C	77
A.1.1.1	Porcine gels	77

A.1.1.2	Cold-water fish gels	79
A.1.1.3	50-50 mixed gels	81
A.1.2	Particle tracking at 20 °C	84
A.1.2.1	Porcine gels	84
A.1.2.2	Cold-water fish gels	86
A.1.2.3	50-50 mixed gels	88
A.2	Particle tracking preformed at NTNU	91
A.2.1	Porcine gels	91
A.2.2	Cold-water fish gels	93
A.2.3	50-50 mixed gels	95
A.2.4	90-10 mixed gels	98
B	MATLAB code used for particle tracking	101
C	Release in aqueous environment - Raw data	105
C.1	Release after heating to 40 °C	105

List of Figures

1	A simplified illustration of the gelling process of gelatin. The image on the left represents the dissolved gelatin, while the image on the right represents the resulting gel network created after the formation of the triple-helical junction zones. ²¹ . . .	3
2	A simple Jablonski energy diagram illustrating the fluorescence process. The electron absorbs the excitation energy, causing it to go from its ground state, to a high-energy excited state. This state is unstable, causing some energy loss to the system as the electron remains excited. The rest of the energy is then rapidly released in the form of a photon, causing the energy level to return to the ground state. The released photon is observed as fluorescent light.	6
3	Simplified illustrations of the four basic types of motion a particle can have in a liquid or gas system. The curves are given alongside examples showing how the particles could be moving in the system. ⁷	8
4	A simple schematic representation showing how the lag time affects the step sizes used when measuring the MSD. The black squares represent images of the particle, The lag time τ is given on the left hand side of the figure, with the corresponding step sizes illustrated on their right.	9
5	A simplified visualization of the characteristic curve obtained from a FRAP analysis. The pre-bleach, bleach and post-bleach areas of the curve are indicated in the figure. The images above the curve represents the general look of the images obtained at each stage, where the solid black dot in the second to left image is the bleached area. ⁷	11
6	A flowchart summarising all major steps involved in the particle tracking protocol. The starting point is marked with green, while the final step is marked with red. .	16

7	Absorbance spectrum for tartrazine, with the absorbance plotted against the wavelengths between 300 and 800 nm. The peak of the absorbance curve was deemed to lay around 425-427 nm.	18
8	Absorbance spectrum for blue dextran, with the absorbance plotted against the wavelengths between 300 and 800 nm. The peak of the absorbance curve was deemed to lay around 618-620 nm.	18
9	Standard curve found for tartrazine at a wavelength of 425 nm, The coefficient of determination and the equation for the curve fit is given below the curve. The absorbance for a dilution series of tartrazine starting at 22 $\mu\text{g}/\text{ml}$ was used to create the standard curve.	19
10	Standard curve found for blue dextran at a wavelength of 620 nm, The coefficient of determination and the equation for the curve fit is given below the curve. The absorbance for a dilution series of blue dextran starting at 1.12 mg/ml was used to create the standard curve.	20
11	A flowchart summarising all major steps involved in the release measurement protocol. Volumes and weights used are not specified.	22
12	A flowchart summarising all major steps involved in the FRAP measurement protocol.	25
13	Mean Squared Displacement curve for cold-water fish gelatin at 5°C, tracking a total of 58 individual particles for 110 seconds. A linear reference line with a slope of 1 is included at the top of the figure.	27
14	Four of the tracks found for 1 micron particles in pure cold-water fish gelatin with an 18 w% concentration. Tracking was preformed at 5 °C for 110 seconds.	28
15	Drift corrected Mean Squared Displacement curve for cold-water fish gelatin at 5°C, tracking a total of 58 individual particles for 110 seconds. A linear reference line with a slope of 1 is included at the top of the figure.	29
16	Slope α plotted against $\log(\text{MSD})$ for all tracked particles in cold-water fish skin gelatin at 5°C.	30
17	Drift corrected Mean Squared Displacement curves for porcine gelatin at 5°C, tracking a total of 41 individual particles for 110 seconds. A linear reference line with a slope of 1 is included at the top of the figure.	32
18	Slope α plotted against $\log(\text{MSD})$ for all tracked particles in porcine gelatin at 5°C.	33
19	Four of the tracks found for 1 micron particles in pure porcine gelatin with an 18 w% concentration. Tracking was preformed at 5 °C for 110 seconds.	34
20	Drift corrected Mean Squared Displacement curves for mixtures of equal part porcine and cold-water fish gelatin 5°C, tracking a total of 40 individual particles for 110 seconds. A linear reference line with a slope of 1 is included at the top of the figure.	35
21	Four of the tracks found for 1 micron particles in in a mixture of equal parts porcine and cold-water fish gelatin with an 18 w% total concentration. Tracking was preformed at 5 °C for 110 seconds.	36
22	Slope α plotted against $\log(\text{MSD})$ for all tracked particles in a mixture of equal parts cold-water fish gelatin and porcine gelatin at 5°C.	37
23	Slope α plotted against $\log(\text{MSD})$ for all tracked particles in porcine gelatin, cold-water fish gelatin and a mixture of equal parts cold-water fish gelatin and porcine gelatin at 5°C.	38

24	Drift corrected MSD curves for pure porcine gelatin (top left), a 50-50 mixture between porcine and cold-water fish gelatin (top right), and pure cold-water fish gelatin. All MSD curves were obtained at 20 °C.	39
25	Slope α plotted against $\log(\text{MSD})$ for all tracked particles in porcine gelatin, cold-water fish gelatin and a mixture of equal parts cold-water fish gelatin and porcine gelatin at 20°C.	40
26	MSD curves for particles tracked in an 18 w% solution of porcine gelatin at room temperature. The solution was allowed to gel for 20 hours at 5 °C before analysis. The curves on the left side represent the raw MSD curves, with the drift corrected curves shown on the right.	42
27	Mean Squared Displacement curve for porcine gelatin at 20°C, tracking a total of 46 individual particles for 110 seconds. A linear reference line with a slope of 1 is included at the top of the figure.	43
28	MSD curves for particles tracked in a mixture of equal parts porcine and cold-water fish gelatin with a total gelatin concentration of 18 w%, measured at room temperature. The solution was allowed to gel for 20 hours at 5 °C before analysis. The curves on the left side represent the raw MSD curves, with the drift corrected curves shown on the right.	44
29	The slope α plotted against the $\log(\text{MSD})$ values for all tracked particles in porcine gelatin and a mixture of equal parts cold-water fish gelatin and porcine gelatin. The figure consists of data compiled from 5 separate measurements in each sample. The measurements were conducted at room temperature.	45
30	MSD curves for particles tracked in an 18 w% solution of cold-water fish gelatin at room temperature. The solution was allowed to gel for 20 hours at 5 °C before analysis. The curves on the left side represent the raw MSD curves, with the drift corrected curves shown on the right.	46
31	Slope α plotted against $\log(\text{MSD})$ for all tracked particles in porcine gelatin, cold-water fish gelatin and a mixture of equal parts cold-water fish gelatin and porcine gelatin. The figure consists of data compiled from 5 separate measurements in each sample. The measurements were conducted at room temperature.	46
32	MSD curves for particles tracked in a mixture of 10% porcine and 90% cold-water fish gelatin by weight, with a total gelatin concentration of 18 w%. All measurements were performed at room temperature. The solution was allowed to gel for 20 hours at 5 °C before analysis. The curves on the left side represent the raw MSD curves, with the drift corrected curves shown on the right.	47
33	MSD curves for particles tracked in a mixture of 10% porcine and 90% cold-water fish gelatin by weight, with a total gelatin concentration of 18 w%. All measurements were performed at room temperature. The solution was allowed to gel for 20 hours at 5 °C before analysis. The curves on the left side represent the raw MSD curves, with the drift corrected curves shown on the right.	48
34	Slope α plotted against $\log(\text{MSD})$ for all tracked particles in porcine gelatin, cold-water fish gelatin and mixtures containing 50% and 10% porcine gelatin mixed with 50% and 90% cold-water fish gelatin, respectively. All samples had a total gelatin concentration of 18 w%. The figure consists of data compiled from 5 separate measurements in each sample. The measurements were conducted at room temperature.	49
35	A copy of Figure 25: Slope α plotted against $\log(\text{MSD})$ for all tracked particles in porcine gelatin, cold-water fish gelatin and a mixture of equal parts cold-water fish gelatin and porcine gelatin at 20 °C.	49

36	Slope α plotted against $\log(\text{MSD})$ for all measurements preformed at TUMSAT and NTNU. The figure contains data for porcine gelatin, cold-water fish gelatin and mixtures containing 50% and 10% porcine gelatin mixed with 50% and 90% cold-water fish gelatin, respectively.	50
37	Concentration of blue dextran over time in liquid medium kept at room temperature. Each point corresponds to a measurement, with the final measurement taken after 48 hours.	54
38	Concentration of Tartrazine over time in liquid medium kept at room temperature. Each point corresponds to a measurement, with the final measurement taken after 48 hours.	54
39	Concentration of blue dextran over time in liquid medium kept at room temperature. Each point corresponds to a measurement, with the final measurement taken after 48 hours. The average measured concentration after complete melting of the gel matrix is given as a dotted line.	56
40	Concentration of Tartrazine over time in liquid medium kept at room temperature. Each point corresponds to a measurement, with the final measurement taken after 48 hours. The average measured concentration after complete melting of the gel matrix is given as a dotted line.	57
41	Concentration of blue dextran over time in liquid medium surrounding a mixed gel containing equal parts porcine and cold-water fish gelatin at room temperature. Each point corresponds to a measurement, with the final measurement taken after 46.5 hours.	59
42	Concentration of Tartrazine over time in liquid medium surrounding a mixed gel containing equal parts porcine and cold-water fish gelatin at room temperature. Each point corresponds to a measurement, with the final measurement taken after 46.5 hours.	60
43	Concentration of blue dextran over time in liquid medium kept at room temperature. Each point corresponds to a measurement, with the final measurement taken after 46.5 hours. The average measured concentration after complete melting of the gel matrix is given as a dotted line.	61
44	Concentration of Tartrazine over time in liquid medium kept at room temperature. Each point corresponds to a measurement, with the final measurement taken after 46.4 hours. The average measured concentration after complete melting of the gel matrix is given as a dotted line.	61
45	Concentration of blue dextran over time in solvent medium surrounding the mixed gel containing equal parts porcine and cold-water fish gelatin, and the pure porcine gel, measured at room temperature. Each point corresponds to one measurement.	62
46	Concentration of Tartrazine over time in solvent medium surrounding the mixed gel containing equal parts porcine and cold-water fish gelatin, and the pure porcine gel, measured at room temperature. Each point corresponds to one measurement.	63
47	Suggested distribution of cold-water fish gelatin and mammalian gelatin in oil emulsions. The black lines represent mammalian gelatin, the red lines represent cold-water fish gelatin and the yellow circles represent oil droplets. Pure gel is shown on the left, while the emulsion is shown on the right.	65
48	Images captured at 0 and 50 seconds during a fluorescence recovery after photobleaching experiment in a gelatin-oil emulsion. The black areas are the oil droplets. The red and blue circles show the positions of the same two sets of oil droplets at both time points.	66

49	A simplified illustration showing how oil droplets under the region of interest (ROI) could interfere with the bleaching during a fluorescence recovery after photobleaching experiment. The flat side of the triangle represents the ROI.	69
----	--	----

List of Tables

1	The melting and gelling temperatures of mammalian gelatin and cold-water fish gelatin, for 10 % (w/v) solutions with cooling- and heating rates of 0.5°C/min. ²¹ .	4
2	Information about the pixel size, resolution and frame rate for images captured in particle tracking experiments at TUMSAT and NTNU.	15
3	An overview of the data obtained from the particle tracking, including a brief description for each one.	16
4	The resulting halftime of recovery, mobile fraction and diffusion coefficients for all parallels and repetitions performed in the 18 w% control gelatin. The gelatin consisted of equal parts pig skin and cold-water fish skin gelatin by weight.	67
5	The resulting halftime of recovery, mobile fraction and diffusion coefficients for all parallels and repetitions performed in the 20% oil emulsion. The control solution was used as the base, adding oil to an end concentration of 20% by weight.	68

1 Introduction

1.1 Gels

Gels are a result of a phenomenon called gelation, a process which can turn liquid systems, usually a polymer solution into something that is solid, which is called a gel. Gels can be seen as a sort of intermediary between a solid and a liquid, generally consisting of two distinct components, the solvent and the polymer. The solvent is the liquid portion of the gel, which makes up most of the gel. This liquid portion exists only within the polymer portion, which forms a continuous solvent swollen matrix giving the material solid dominant properties. Polymers are the very reason why gelling occurs. While the mechanisms by which the gelling happen varies between polymers, they all share one commonality, namely the ability to form links between molecules to form large, continuous networks of polymers. These networks form within the liquid as the gelling starts to occur, which ends up enveloping and trapping the solvent within this network of polymers. For biopolymers (polymers of biological origin) the solvent is most commonly water.¹³

Gelling occurs commonly in food, particularly foods that are rich in proteins and polysaccharides, as these are the most common gelling biopolymers. Gelling is the reason why eggs turn solid when boiled, or why cakes turn solid when they are baked. Simply put, gelling is a very common phenomenon in food. Gelling agents are widely used to thicken or solidify foods, from desserts like mousse or pudding that are kept cold, to candies and sweets that sit at room temperature. While all of this is highly important, gels are used in many other areas outside of food as well. They see uses within all kinds of cosmetic products, and they can be used to create moulds and capsules, like for example medicine capsules. They might even be used to form soft, chewable medicines by suspending the medicine within a gel.^{35,59}

Biopolymers might gel in similar ways, but the frequency and strength of the cross-linking bonds is what in many cases determines exactly how the gel behaves, This means that while gels might form in similar ways, they usually exhibit different gel characteristics. Everything from temperature and pH stability to the strength of the gel varies from system to system, and from gelling agent to gelling agent.^{13,59}

No matter the purpose in which the gels are used, it is always highly important that the gels have the properties which that application requires, and something that is highly important in many cases is the diffusion barrier properties of a gel. Diffusion is a term which refers to the undirected movement of something, usually particles and molecules within a system. The barrier properties of a gel is simply put the ability that gel has to hinder diffusion. When talking about the diffusion in a gel, it generally refers to the ability for molecules or particles to move through the liquid phase of the gel. It gives information about how mobile particles can be within the gel, which is highly important in for example drug delivery, where the release rate of the drug is an importance.^{1,48} One example of a gelling biopolymer, and the one studied in this thesis is gelatin, which is obtained from the biopolymer collagen.

1.2 Collagen & gelatin

1.2.1 Collagen

Collagen is a common structural protein that is found predominantly in the white connective tissue of animals. A significant portion of the protein content in skin, cartilage, muscle fibres and the extracellular protein matrix of bone exists as collagen. Due to this, collagen is abundant in many animals, comprising around one third of the total protein content in many mammals.^{21,54} The main function of collagen is to provide mechanical strength and structure to tissue, as collagen has high tensile strength. This comes in large part from the characteristic triple-helical secondary structure of collagen. These triple helixes consist of three individual polypeptide chains referred to as α chains, which are bound together by hydrogen bonds.³⁴

There is currently 28 different types of collagen that have been identified just in vertebrates, however this triple-helical structure is a commonality for all types.⁵⁷ While all three chains in a collagen triple helix may be identical in some cases, they are most often different from one another. This variation in amino acid composition between chains can be utilised as a method of classifying different collagen types. Type(I) collagen is an example of this, which is defined as collagen comprised of two identical α -chains, $\alpha 1(I)$, and one that differs from these two, $\alpha 2(I)$.^{34,57} The amino acid composition is also a distinguishing factor between collagen from different sources, as the composition of the collagen, as well as the stability of the collagen structures may vary depending on the environment of the species in which it comes from. Fish that live in cold-water environments naturally have a different amino acid composition compared to for example cattle, or even fish originating from warm water environments.²¹ Further, these triple helices may form inter-molecular bonds with one another to create higher order structures. This allows for collagen to form for example microfibrils and fibres, which is the form that collagen most often is found as in tissue. The formation of these fibres is essential for providing both strength and flexibility to skin, cartilage and other types of tissue.⁵⁷

1.2.2 Gelatin

Gelatin is a product that is derived via the hydrolysis of collagen, a process which degrades the secondary and higher structures of the collagen, separating the α -chains from one another. The separated chains vary in terms of length, both as a result of the chains being depolymerized and broken down, and also because of covalent binding between chains to form larger ones. This ability to form covalent bonds can be used to distinguish various chain types found in gelatin, and the three most common chain types are referred to as α , β and γ -chains. The α -chains are the chains obtained when the collagen triple helices are broken down. The β -chains on the other hand are defined as two α -chains bound to one another, while the γ -chains consist of three α -chains bound together. The chain lengths also vary depending on the source of the collagen used, as different sources gives collagen with different properties.²¹ What this means is that gelatin cannot be characterised by a singular chain length, but is rather defined by utilizing the average length. Gelatin is therefore a heterogeneous mixture of polypeptide-chains, meaning that it is difficult to define its properties. Factors such as the collagen type, age and perhaps most importantly the collagen source all affect the properties of the final gelatin product.³⁴

As previously mentioned, gelatin is a product obtained via hydrolysis of collagen. There are two primary methods that are commonly used to achieve this, those being alkaline- and acidic hydrolysis, which are named according to the pretreatment utilised to prepare the collagen for gelatin extraction. Gelatin that is obtained after an acidic pretreatment is referred to as Type A gelatin, while Type B gelatin is obtained after an alkaline pretreatment. These methods are differentiated between due to the fact that the gelatin obtained from them differs highly in terms of properties. An example of this would be the average molecular weight M_w of the chain, which is commonly higher for Type B gelatin. In other words, Type B gelatin generally shows a longer average chain length.^{21,44} The two gelatin types also notably differ in bloom strength, with Type A gelatin generally showing a higher average bloom strength. This means that the gels formed with Type A gelatin show a higher strength and rigidity on average.¹⁶

After the pretreatment, the remaining extraction process is typically the same for both extraction methods. The gelatin is first rinsed to remove the acidic or alkaline solutions, before it is placed in the extraction media. This media is commonly warm water, the pH of which is varied depending on the priority of the extraction.²¹ Generally, a lower pH will give a higher extraction yield, but a lower average bloom value for the final gelatin product.⁵¹ After being placed in the extraction media, the collagen is subjected to a series of extractions at increasing temperatures, typically ranging between 55-100 °C. This heating breaks down the secondary and higher structures of the collagen, leaving the singular α chains in the solution. Any remaining collagen and other impurities such as fat are then removed via filtering, while any inorganic salts present are removed by deionization. After this purification process, the remaining gelatin solution is then concentrated and dried to form the final gelatin product.^{21,34}

Unlike collagen, gelatin is a highly water soluble material, with the solution temperature varying

between different gelatin types. For gelatin extracted from mammals, the solution temperature is generally somewhere over 40 °C.²¹ So long as the solution is kept warm, the chains will remain dissolved and freely float in the solution media. When it is cooled down however, the chains will begin to interact with one another to try and reform the triple-helical structures of collagen. While the chains are not able to fully form together to make collagen, they are able to bind together in small junction zones. The fact that the chains are able to form these junction zones via hydrogen bonds is the basis for their gelling capabilities. As the chains bind together in several small junction zones, it creates a network of interconnected polypeptide chains that is able to trap water molecules within, creating a gel. To visualise this process of gelling, a simplified illustration is given in Figure 1.

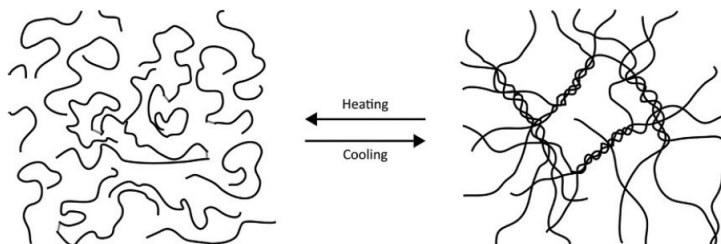


Figure 1: A simplified illustration of the gelling process of gelatin. The image on the left represents the dissolved gelatin, while the image on the right represents the resulting gel network created after the formation of the triple-helical junction zones.²¹

Gelatin gels are usually considered to be homogeneous, particularly on a macroscopic level. Gelatin gels are however by nature non-homogeneous on a microscopic level, meaning that they do not have a repeating, common structure across the whole gel. Gelatin is a mixture of amino-acid chains of various lengths like previously discussed, meaning that they simply cannot form a completely homogeneous system. During gelling, the chains bind together at random as the solution temperature goes down, meaning that they do not follow any strict structure or pattern either. This naturally leads to small variations in the gel matrix, with no two regions of the gel being completely identical. The differences are generally small enough for the gel to be functionally homogeneous in most cases, simply due to the sheer number of chains that makes up the network. For most use cases gelatin can therefore be assumed homogeneous, though some minor functional differences between smaller areas of the gel is highly plausible when examining the gel at a microscopic level.^{21,34}

One factor that is important for the properties of gelatin is the amino acid composition of the chains, as this plays a large role in determining the gelling capabilities. The general amino acid sequence of an α -chain in both collagen and gelatin is Gly-X-Y, where the glycine acts as a sort of backbone for other amino acids that may inhabit the X and Y positions. The most common amino acids occupying the X and Y positions is proline and hydroxyproline, respectively. Other common amino acids that may be found in these amino acid triplets is arginine for the Y position, and leucine for the X position. The triplets tend to distribute into separate regions on the chain depending on whether they contain polar or non-polar amino acids, leading to the chains having distinct polar and non-polar regions. The polar regions are hydrophilic by nature, while the non-polar regions are hydrophobic. The existence of these regions is the main reason as to why gelatin is highly surface active.^{21,34,57}

When considering the gelling capabilities of gelatin, the proline and hydroxyproline contents in the gelatin is highly important. Like stated they are among the most common amino acids in gelatin, but there is also strong evidence to suggest that they play a large role in providing thermal stability to the gelatin. In particular, hydroxyproline has been found to play a large role in stabilising gelatin gels, which likely comes from its ability to easily form hydrogen bonds. Gelatin gels are held together by the formation of triple helical junction zones, which are a result of hydrogen bonds between chains. For this reason, it is believed that the hydroxyproline plays a large role in the

gelling process. This is the reason why the proline and hydroxyproline contents often are taken in account when discussing the physical properties of a gelatin gel. Generally, a decrease in these amino acids would suggest a decrease in both thermal stability and gel strength.^{17,50}

1.2.3 Cold-water fish skin gelatin

Cold-water fish (CWF) gelatin refers to gelatin created from cold-water fish species such as cod or salmon, and is not widely used in industrial applications. The consumption of fish on a worldwide basis is continuously growing each year, which is naturally also leading to an increase in the amount of waste generated by the fishing industry. While there is a general desire to decrease the amount of waste generated, it still poses a large challenge.²⁶ A large amount of fish is processed to remove several byproducts such as skin, bones, head, viscera and so on, which all contain valuable compounds such as protein, fat and minerals. The skin in particular is high in protein content, much of which is going to be collagen. Despite this, there is a general lack of high-value commercial applications for these byproducts.¹⁹

The reason why CWF gelatin does not see wide-spread used is often attributed to the poor gelling abilities it exhibits.^{21,68} In comparison to gelatin derived from mammalian sources, of which porcine and bovine are the most common, CWF gelatin shows notably lower gelling and melting temperatures. The gelling and melting temperatures of mammalian and cold-water fish gelatin is shown in Table 1, which shows that the gelling and melting temperatures of CWF gelatin are 4-8 °C and 14-16 °C, respectively. This means that at a relatively normal room temperature of 21 °C, CWF gelatin is going to melt and be unable to form a gel. This is an undesirable trait in many common applications of gelatin, as it is often desirable for the gel to be stable at room temperature. Gelatin capsules is an example of such an application, as it would be highly undesirable for the gelatin capsules to melt at room temperature. The same thing could also be said for many food applications such as pudding, jello and gelatin candies. as it is naturally undesirable for these to completely melt at room temperature.

Table 1: The melting and gelling temperatures of mammalian gelatin and cold-water fish gelatin, for 10 % (w/v) solutions with cooling- and heating rates of 0.5°C/min.²¹

Property	Mammalian gelatin 220g Bloom	Cold-water fish gelatin
Gelling temperature	26-27°C	4-8 °C
Melting temperature	33-34 °C	14-16 °C

Like previously mentioned, the proline and hydroxyproline contents in the gelatin is thought to play a major role in the gelling process, and it is likely the low content of these amino acids that cause the CWF gelatin to have such poor gelling capabilities. A Type A mammalian gelatin has been found to have around 91 residues of hydroxyproline per 1000 residues, while CWF gelatin only appears to have around 60. The same thing is true for proline, where CWF gelatin has roughly 91 residues per 1000, as opposed to the 132 in the Type A mammalian gelatin.²¹ Seeing as these two amino acids are thought to play a major role in stabilising and forming gel networks, this could explain why the CWF gelatin exhibits these significantly lower gelling and melting temperatures seen in Table 1. Having fewer hydroxyproline molecules in particular likely lowers the amount of hydrogen bonds that are able to form, thus making the triple helixes and the gel network as a whole more easy to break apart.

These poor gelling abilities are a key part of the reason for why CWF gelatin is not as widely utilised as mammalian gelatin, as they simply lack the thermal stability and gel strength that is necessary for many applications like previously mentioned. Any use cases that require or desire the gel to remain rigid at room temperature will not work with cold-water fish gelatin. There have been several studies aimed at improving the gelling abilities of CWF gelatin that have shown promising results, such as by the utilisation of cross-linkers, though these methods have yet to see any wide-spread use.^{4,12} Ongoing work conducted by master's students at the Tokyo University of Marine Science and Technology has indicated that gelatin from mammals and cold-water fish is able to mix

together and form a mixed matrix (personal communication Catherine Taylor Nordgård, Hazuku Takagi, Shingo Matsukawa). The same thing has also been seen in previous the specialisation project work which served as a basis for this study, which focused on the barrier properties of these mixed systems.³⁷ What these results have shown is that there are clear, yet small differences in the diffusion within these gels, and thus also the barrier properties in these mixtures when compared to pure mammalian gels. While these results do appear promising, there is still a need to further explore the capabilities and behaviour of these mixed gelatin systems.

1.2.4 Gelatin usage

Gelatin is a common hydrocolloid that is widely used today in a variety of different industrial applications. As of 2021, the global market size for gelatin was estimated to be around 5.8 Billion USD,⁵² with it having a higher market share within food applications than any other hydrocolloid.^{28,53}

For food applications gelatin is commonly used as a thickening agent in many store bought desserts such as mousse or pudding, and even in gummy candies to provide texture and firmness to them. Gelatin is also used in some cases to extend shelf life of products, by for example hindering water separation in some dairy products like sour cream, or even hindering the crystallisation of sugar in products like marshmallows.^{32,35,60} In addition to use cases like these, it is also been considered and conducted research on using gelatin in food packaging. The goal with this is to create biodegradable and edible films that can be used to package food products, extending their shelf lives.^{31,40}

While gelatin is mostly used in food applications, it also used in other areas such as pharmaceuticals as well. One of the most common pharmaceutical applications is gel capsules, which are used to encapsulate medicine. it is also starting to see more use in the creation of chewable gel-based medicines,²² Even outside of pharmaceuticals, gelatin is often used in cosmetic products to increase water binding, provide a better skin feel, and for a variety of other different reasons as well. Gelatin is even used to some extent in photography to create photographic films, with the production of x-ray film being the most common in this case.²¹ In order to further study the barrier properties of mixed gelatin matrices a number of techniques were employed, namely multiple particle tracking of fluorescent particles, aqueous release of coloured molecules in a dissolution apparatus and fluorescence recovery after photobleaching.

1.3 Fluorescence and light absorption

1.3.1 Light absorption

Light absorption refers to the absorption of photons, and it can be performed by any electrically charged particle such as electrons. Photons are what is observed as light, and are defined as elementary particles that have the ability to carry electromagnetic energy. The energy that these photons carry determines the wavelength of the light, and it is the variation in these wavelengths that are the basis for colour. Different wavelengths are perceived as different colours. In practice, all materials have the capability to absorb light, The perceived colour of a material is determined by the wavelengths which it is capable of absorbing, as the observed colour is a result of the wavelengths which are reflected by the material. A blue object reflects wavelengths corresponding to the colour blue, and therefore must absorb other wavelengths. The absorption of light leads to its energy getting transferred to the material, meaning that the photons cease to exist. This energy can cause a variation of different effects depending on the material, such as atomic transition, ionisation and heating. Atomic transition in particular is the basis for what is called luminescence.²⁰

1.3.2 Fluorescence

Fluorescence is a term which falls under the broader category of luminescence, which describes the ability certain materials have to emit light. Luminescence is a result of the ability for electrons to be excited, which happens when they absorb energy, leaving them in a higher energy state compared to their normal. This high energy state leaves the electrons unstable, and thus it is desirable for them to return to the more stable ground state. To do this, the absorbed energy has to be released, which is done in the form of photons. There might be some non-radiative energy loss that occurs prior to the photon release as well, but the majority of the energy will be released in the form of photons. A simple Jablonski energy diagram showing illustrating the fluorescence process is shown in Figure 2.

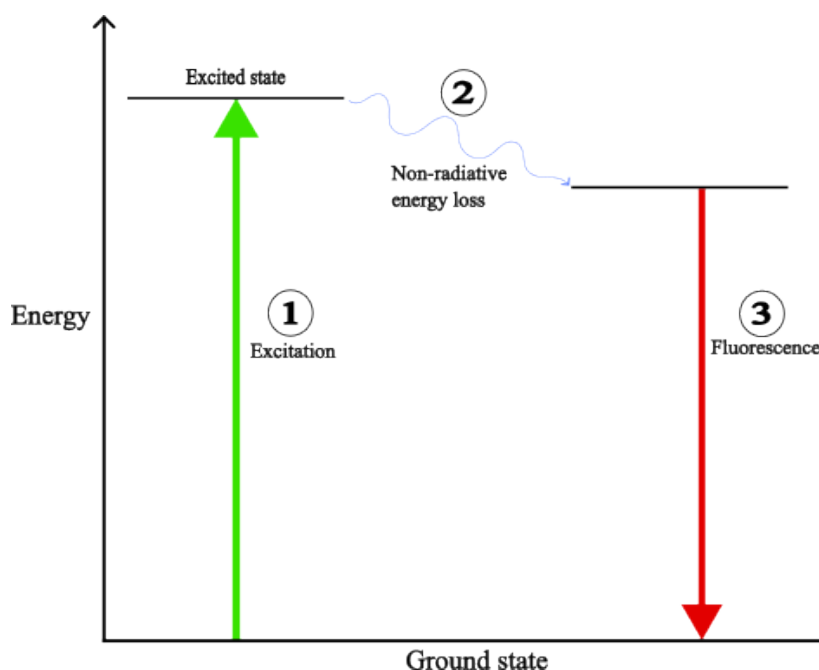


Figure 2: A simple Jablonski energy diagram illustrating the fluorescence process. The electron absorbs the excitation energy, causing it to go from its ground state, to a high-energy excited state. This state is unstable, causing some energy loss to the system as the electron remains excited. The rest of the energy is then rapidly released in the form of a photon, causing the energy level to return to the ground state. The released photon is observed as fluorescent light.

These emitted photons are what is observed as luminescence, and luminescence can be divided into groups depending on the source of the excitation. Chemiluminescence refers to luminescence happening as a result of chemical reactions, while electroluminescence occurs when electric currents cause the excitation. Photoluminescence is another group, and refers to luminescence occurring due to photons exciting the system. It is under the umbrella of photoluminescence that fluorescence exists, alongside another sub-group called phosphorescence.^{9,64} While these sub-groups are closely related, the main difference between them typically lies in the luminescence duration. While phosphorescence usually lasts for a while after the excitation has stopped, up to several minutes, fluorescence stops almost immediately after the excitation has stopped. While this is true for most cases, there are exceptions from this rule. The most accurate way to describe their difference is that phosphorescence occurs when there is a change in the spin multiplicity, unlike fluorescence. While this description is more accurate, their luminescence duration is most often used to distinguish the two.⁶³

Fluorophores is the name given to molecules that have fluorescence capabilities. The wavelength of

the emitted light depends heavily on the molecular composition and conformation of the molecules, meaning that the wavelengths can vary significantly between fluorophores. The excitation energy required also varies between different fluorophores. The excitation energy is typically higher than the resulting emission energy, meaning that for fluorescence, the excitation light generally has to be of a higher wavelength than the wavelengths which the fluorophore emits.⁶³

1.4 Methods for studying particle motion in liquid and semi solid systems

Particle tracking refers to the general idea of measuring the movement of particles in a medium. The goal with particle tracking is to obtain positional data for one or more particles over a time series, and using this positional data to obtain their trajectories over that time series. The positional data may be both two- and three-dimensional, or even one-dimensional in certain cases if it is desirable. The trajectories can be used to obtain information regarding the dynamics of the particle, which in turn can provide information about the system which the particle exists within. It can show whether there is active transport happening for the particle, whether the particle is confined or freely moving within the system, what the diffusion coefficient of the particle is, and even if it is interacting with other particle.^{25,67}

A common method of performing particle tracking is using particles that can be observed via microscopy methods, such as fluorescent beads, and capturing images of these particles at set time intervals. These images may then be used to determine the position of the particles over time, whether by manual methods, with the use of software like ImageJ⁵⁵ or via the use of tools like Python and MATLAB. Regardless of the method in which the trajectories are determined, the end result is a 2D trajectory for one or more particles, which can then further be used to obtain the desired information.^{25,56}

To interpret the particle tracking data, it is important to understand the principles behind how the particles can move in liquid or semi-solid systems like gels. Brownian motion is a term used to describe the random movement of particles in a liquid or gas phase. This type of movement only occurs when there are no external forces applied to the system, and the only driving force for motion is thermal energy. This means that there is no common direction or speed for the particles. The particles are constantly moving and colliding with one another, which leads to their paths and momentum changing as a result of each collision. The distance each particle in a system has from its starting position generally follows a Gaussian distribution, the width of which increases the longer the particles are observed. This means that the displacement over time relative to the starting point becomes increasingly more random as time goes on, which is a result of the particles freely diffusing.¹⁰

The mean squared displacement (MSD) of a particle is commonly used to determine whether a particle is following the principles of Brownian motion. By measuring the mean squared displacement of a particle over time, these values can be plotted together, and the curve used to determine the diffusion behaviour of a particle. Generally, the MSD curves can be used to classify the motion of a particle into 4 main classes, which are Brownian, anomalous, confined and directed motion.⁴⁶ Examples of how the MSD curves could look for each of these types of motion are shown in Figure 3.

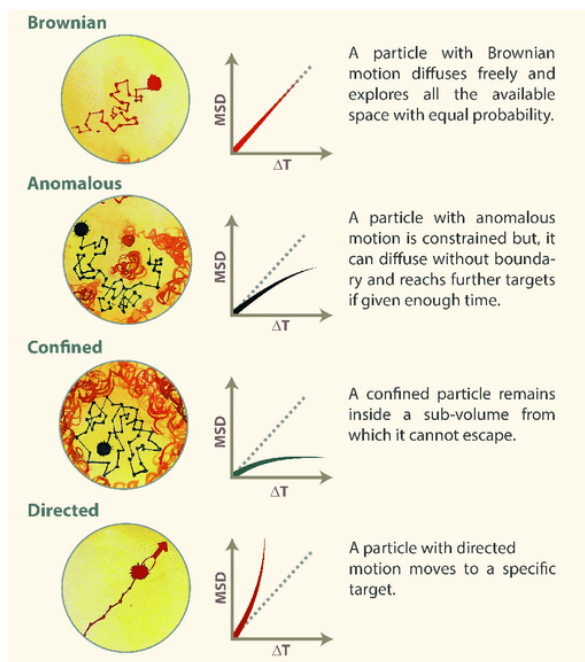


Figure 3: Simplified illustrations of the four basic types of motion a particle can have in a liquid or gas system. The curves are given alongside examples showing how the particles could be moving in the system.⁷

When plotted in a log-log curve, Brownian motion has been found to give a completely linear curve over time. The distance which the particle is displaced continuously increases with time, however the speed at which it does remains constant. This means that if a particle exhibits Brownian motion, the MSD curve should in theory have a slope equal to 1, as the MSD value is directly proportional to the time. Anomalous and confined motion plotted in the same way gives curves that generally exhibit a decreasing slope over time. Anomalous motion describes particles that are partially constrained, but that have the ability to escape said confinement if given enough time. This causes the curve to generally decrease in slope, but not to the point of flattening out. Confined motion on the other hand describes particles that are fully constrained within a structure, meaning that they cannot travel further than the edges of the confined area. This generally gives a curve that quickly rises up to a maximum value, before flattening out. The maximum value in that case depends entirely on the size of the area in which the particle is confined, increasing as the area increases. Lastly, directed motion describes particles that move in a set direction as a result of external force acting on them. Instead of moving around at random such as the other cases, the particles are directed or pushed in a specific direction. The MSD curve for directed motion generally shows an exponential rise in the MSD over time, as the particle moves in a more steady, linear fashion when compared to Brownian motion.^{46,67}

The important thing to note about the MSD curves is that the x-axis does not represent the time since the start of the experiment, but rather the lag time, which is usually given as τ or ΔT . The lag time represents the size, or rather duration of the steps used when calculating the MSD. For example, if a particle's position is tracked once a second over a duration of 100 seconds, a total of 100 images will be taken to make up that particle's trajectory. If the lag time is 1 second in this case, it means that the distance the particle moves over 1 second is found along the entire trajectory, and summed up to make the MSD. In this case, that means that the distance between every one of the 100 points is measured to find the average. However, if the lag time is increased to for example 5 seconds, it means that the average distance the particle moves over 5 seconds is what is used to make the MSD at that point. In other words, it means that the distance between every 5 points on the trajectory is what is measured and averaged to make the MSD. To try and show how this works, a simplified schematic showing this concept is given in Figure 4. The figure illustrates how as the lag time increases, so does the time intervals between which the deviations

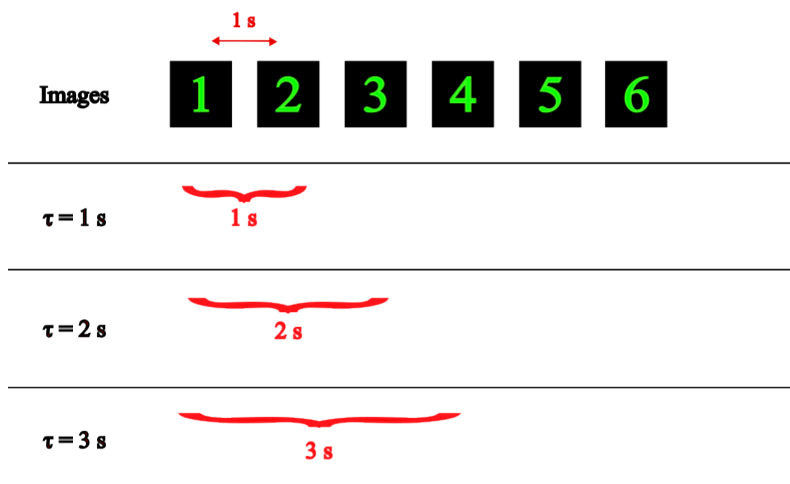


Figure 4: A simple schematic representation showing how the lag time affects the step sizes used when measuring the MSD. The black squares represent images of the particle, The lag time τ is given on the left hand side of the figure, with the corresponding step sizes illustrated on their right.

used to calculate the MSD are found. In practice, this means that as the lag time increases, the number of deviations used to calculate the MSD will also decrease. In the example above, when the lag time is 1, a total of 100 deviations are used to find the MSD. In contrast, at a lag time of 100, only the deviation between the first and last point is used. This often causes the data to become more noisy when approaching higher lag times, as any potential errors or noise in the trajectory will not be masked as well, since there are fewer values to average from.^{46,67}

An example of how particle tracking could be used is for the study of gelling. By tracking the particles in the gelling solution at different stages of the gelling process, it is possible to observe how the motion of the particles changes with increased gelling, which can give information regarding how fast the solution gels.⁴³ In the case of tracking multiple particles in the same gel, it can also provide information regarding whether there is phase separation happening, as this would result in different trajectories depending on which phase the particles are in.²⁹ In use cases like these where there is no active transport of the particles, the particle tracking data is often used to find the mean squared displacement (MSD) of the particles over time. By calculating the MSD from the trajectory, it is possible to construct MSD curves for each tracked particle, which gives information regarding how freely the particles are moving. For more information regarding particle motion and MSD, see Section 1.4. If the observed curve is linear and rising it indicates that the particles are not being confined by the gel matrix, which would imply that that little to no gelling has taken place. As the gelling then takes place, the curves would be expected to start flattening out, getting more horizontal as the particles are getting more confined.¹⁰

1.5 Dissolution measurements

Dissolution refers to the process in which a material, called the solute, is dissolved in a medium, called the solvent. Dissolution is therefore the process in which a solution is created, and the speed of this process is typically quantified by the rate of dissolution. The rate of dissolution is unique

for any given pairing of solute and solvent, in addition to it being dependent on other factors such as temperature and pH. This means that the rate of dissolution is generally quite specific, and therefore it is often necessary to determine it when developing new solutes. A good example of this is the development of drugs, particularly those that are delivered orally. The reason for this is that the bioavailability and drug release kinetics, which are closely related, depend on the dissolution rate. If for example a drug has a low dissolution rate, it means that the bioavailability of the drug compounds will be low, leading to a slower uptake in the body. The opposite is true if the dissolution rate is high. This is highly important information to determine when studying new drugs, as the drug release kinetics are important for the function and effectiveness of the drug. It is important that the drug release rate is suited to provide a stable and optimal concentration of the drug in the body, which is precisely why the rate of dissolution is as important factor to study.^{1,2}

Dissolution tests are usually performed in special equipment made to study dissolution, referred to as dissolution units or apparatus. The general idea of these units is that they keep the solute suspended in the solvent, keep the temperature of the system constant, and provide some circulation or stirring of the solvent. These units most often have valves for extracting samples from the solute as well, with the more advanced ones also having the capability of doing so automatically. These samples can then be analysed to determine the concentration of the solute in the solvent, providing data for how this concentration changes over time. This in turn can be used to find the rate of dissolution, which defines the amount of the compound released per time unit.⁶²

While dissolution units are primarily used for the purpose of measuring dissolution, in practice they may be used to measure release of soluble compounds from materials even when this does not involve dissolution. In this study the dissolution apparatus has been used to measure the release of already solubilised water soluble molecules from gelatin matrices in an aqueous environment. If the parameters, the main ones being the solvent, pH and temperature are adjusted so that the dissolution of the gel matrix material is negligible, then the release of soluble compounds from the material will mainly be as a result of diffusion. In other words, instead of measuring dissolution, the diffusion out of the material is measured instead. While there is no way to guarantee that there will not be some degree of dissolution occurring, doing this could potentially provide information regarding both the stability of the material in a solvent, and to what degree it is able to retain the compound which is measured.

1.6 Fluorescence laser scanning microscopy

1.6.1 Confocal laser scanning microscopy (CLSM)

Confocal laser scanning microscopy (CLSM) is a type of microscopy commonly used within biological and biotechnological research for the purpose of imaging. Conventional widefield microscopy uses light to fully illuminate the sample at all times. In contrast to this, CLSM utilises a laser to perform the imaging point by point, and combining these points to create the full image. The size of these points, the number of points and even the dwelling time at each point can be adjusted to best suit each application. If the goal is to for example study the movement of particles, it might be desirable to have a lower amount of points and dwelling time to allow for more rapid image capture. The imaging being confocal means that the image is only captured in the focal plane, which means the technique is in theory completely independent of sample thickness. The images produced from CLSM are created by measuring the intensity of the fluorescent light from the scanned point, as the laser light will excite fluorescent molecules in that area to release photons more rapidly. The optimal wavelength of the exciting laser depends on what wavelength the fluorescent molecule emits, as the optimal wavelength is usually slightly shorter than this.¹¹ As the fluorescent molecules are excited, the released photons are detected and quantified by a photomultiplier tube (PMT) to determine the intensity of emitted light in that area. This information is then used to create a single pixel in the image, the intensity of which depends on the quantity of photons released.⁴² The dwell time on each point is most often extremely short, usually somewhere around 1-2 μ s or less. This means that a full image of for example 500x500 pixels can be obtained in less than one second. Due to the image being based on the emittance of fluorescent light, the produced image will only show structures and molecules that are fluorescently labelled. Any regions which do not

exhibit any fluorescent properties will not be observed in CLSM. This allows for selective imaging of structures via fluorescently labelling them, which can be useful for observing certain structures in cells for example.

1.6.2 Fluorescent recovery after photobleaching (FRAP)

Fluorescent recovery after photobleaching (FRAP) is a method which utilises confocal laser scanning microscopy to determine the mobility of the fluorescently labelled molecules in a sample. Each measurement in a FRAP analysis follows the same general steps. At first, a series of images are taken of the sample to establish the base fluorescent intensity for the selected region of interest (ROI). The ROI is typically a small circular area in the middle of the image. The ROI is then exposed to intense laser pulses for a brief period of time, typically only a few hundred milliseconds. This bleaches the fluorescent molecules in that region, causing them to rapidly emit all available photons and thus lose their fluorescent capabilities, effectively shortening their fluorescent lifetime dramatically. This step is typically preformed in practice by turning the strength of the imaging laser as high as possible, and scanning the ROI for a short period of time. After the bleaching, images are once again taken of the sample similar to what was done prior to bleaching, measuring the recovery of fluorescence in the bleach region over time. The recovery happens as a result of the fluorescent molecules diffusing, as the bleach molecules are able to diffuse out of the ROI and get replaced by non-bleached molecules, increasing the fluorescence intensity in the ROI again.³

The intensity values in the ROI both pre- and post-bleaching can then be plotted over time, giving a visualisation of how the intensity in the ROI recovered. An example of how this typically looks is shown in Figure 5, which depicts the characteristic shape of a FRAP curve. The curve starts at the base intensity measured pre-bleaching, before rapidly dropping as a result of the bleaching. The curve then slowly recovers up to a maximum intensity, which is typically a little lower than the pre-bleach intensity.

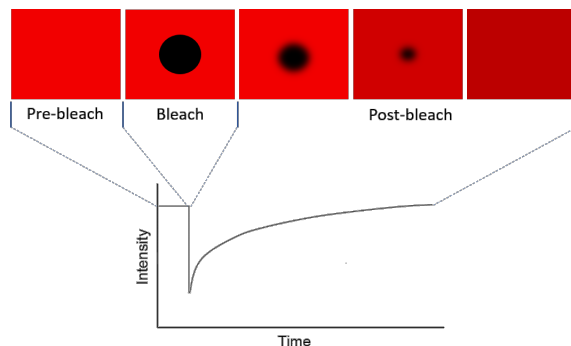


Figure 5: A simplified visualization of the characteristic curve obtained from a FRAP analysis. The pre-bleach, bleach and post-bleach areas of the curve are indicated in the figure. The images above the curve represents the general look of the images obtained at each stage, where the solid black dot in the second to left image is the bleached area.⁷

The shape of this curve provides information regarding the mobility of the fluorescent particles in that sample. If the curve post-bleaching rises quickly up to the maximum, it would indicate that the particles are highly mobile. At the same time, if the recovery curve rises slowly, it indicates that the particles are more constrained. The difference between the pre-bleach intensity and the recovery maximum also gives information as to whether the sample has immobile regions, that being regions where the particles cannot diffuse in or out of. For example, a low maximum recovery would suggest that there is a large fraction of immobile regions within the sample, causing many of the particles to remain immobile. The amount of mobile particles is generally characterised by the mobile fraction, which is the fraction of the particles that are mobile.³ Typically, the FRAP curve

is normalised prior to analysis, setting the pre-bleach intensity as one and the post-bleach intensity as zero. This generally simplifies calculations, and means that the mobile fraction is simply equal to the recovery maximum.

The diffusion rate of the molecules is typically characterised by their diffusion coefficient, which can be calculated from the recovery portion of the FRAP curve.³ There are several equations that have been developed for the purpose of calculating this value, one of those being the Axelrod equation, derived by D. Axelrod et al.⁶ Below, Equation 1 depicts the general Axelrod equation.

$$D = 0.88 \cdot \frac{w^2}{4t_{1/2}} \quad (1)$$

In this equation, D is the diffusion coefficient, w is the radius of the bleached area, and $t_{1/2}$ is the time it takes for the recovery curve to reach half of its maximum value. It is important to note that this equation is only valid for a circular ROI, and for bleaching performed using a Gaussian laser. The equation also assumes that there is no bleaching directly above or below the plane in which the ROI lies. Using this equation, it is possible to obtain the diffusion coefficient, which is only valid for that specific type of fluorescent molecule in that specific sample. Changing either the sample or the type of fluorescent molecule will naturally give a new diffusion coefficient¹.

This method is commonly used to measure the diffusion rate across a membrane, but it can also be used to measure the diffusion rate within a gel. In gels, the diffusion rate is measured for dissolved fluorescent particles which are trapped in the liquid portion of the gel. Immobile fractions in a gel are typically the result of the gel network trapping the particles within a cage-like structure. This also means that the diffusion coefficient and mobile fraction both are strongly dependent on the size and shape of the fluorescent molecule, as larger molecules are more easily hindered and trapped in the gel matrix.

1.7 Motivations and goals for the thesis

This thesis is a continuation of a previous specialisation project, and aims to continue and broaden the scope of this work.³⁷ The aim of this thesis is to study how mixtures of mammalian and cold-water fish gelatin behave in regards to their diffusion barrier properties, as well as determine whether these mixtures form a mixed matrix or result in phase separation between the two gel types. To do this, the main plan is to utilise particle tracking. First, the idea is to develop and adjust the imaging parameters to obtain good quality images which can be used to track the particles. The plan for the tracking itself is to develop a code which can both track the particles in the images, and perform the necessary plotting and calculations with that data. To further study the gels, the rate at which they release compounds to an aqueous medium is also to be studied by the use of a dissolution setup. In addition to this, the difference between the diffusion rates in these mixtures are to be compared to the same values in oil emulsions created from them, the purpose of which is to determine whether the matrix composition changes significantly when used to make oil emulsions.

2 Materials and methods

2.1 Materials

2.1.1 Porcine gelatin

Porcine gelatin purchased from Nitta gelatin Inc. (Gelatin Crystal Collage 2, lot: 200916) was used to create all gelatin gels containing mammalian gelatin in this thesis. The gelatin is sold as a food grade product, and is made purely from pig skin. The gelatin is sold in a powdered form, with a proclaimed protein content of 87%.

2.1.2 Cold-water fish gelatin

High molecular weight cold-water fish gelatin purchased from Kenny & Ross Ltd. (Nova Scotia, Canada, lot: 21027 HMWD) was used to create all gelatin gels containing cold-water fish skin gelatin in this thesis. The gelatin is sold as a pharmaceutical grade product under Pharmacopoeia specifications, with a minimum 85% protein content. The gelatin is produced from the skin of wild caught fish such as cod and pollock. Further technical information is publicly available on the Kenny & Ross Ltd. official website (<https://rb.gy/kc1ln>), alongside safety data for the product.³⁹

2.1.3 Fluospheres™ microbeads, 1 μm yellow-green

Fluospheres™ microbeads purchased from Thermo Fisher Scientific Inc. (Waltham, USA, lot: 1949232) were used for the purpose of particle tracking in this thesis, serving as the tracked particles. The beads were made from polystyrene which is loaded with a variety of dyes to provide fluorescence capabilities, and have a nominal diameter of 1 μm . The excitation and emission maxima for the beads were 505 and 515 nm, respectively. The beads were suspended in distilled water, with the suspension containing a total of 2% solids.

2.1.4 Tartrazine

Tartrazine purchased from Sigma Aldrich Co. (St. Louis, USA, lot 079K1462V) was utilised as a model compound for measuring the release from various gelatin gels in an aqueous environment. Tartrazine is a azo dye with a characteristic yellow color. It has a molecular weight of 534.3 g/mol, and is commonly used for food colouring.⁶⁶

2.1.5 Blue dextran

Blue dextran purchased from Sigma Aldrich Co. (St. Louis, USA, lot 034K0965) was utilised as a model compound for measuring the release from various gelatin gels in an aqueous environment. Blue dextran is a dextran derivative with a characteristic blue color obtained from a covalently bound blue dye. It is commonly used as a volume marker in chromatography, and to some extent as a molecular marker.¹⁴

2.1.6 Fluorescein isothiocyanate–dextran

Fluorescein isothiocyanate (FITC)-dextran was purchased from Sigma Aldrich Co. (St. Louis, USA, lot SLCB8500), and used as a compound for measuring fluorescence recovery after photobleaching (FRAP) in gelatin gels and emulsions in this thesis. The FITC-dextran had a molecular weight average of 70 kDa. FITC-dextran has an excitation maximum at around 493 nm, with the corresponding maximum emission peak at 518 nm.¹⁵

2.1.7 Corn oil

Corn oil purchased from Sigma Aldrich Co. (St. Lois, USA. Product nr. C8267, lot MKCH1635) was used to make gelatin-oil emulsions in this thesis.

2.2 Methods

2.2.1 Particle tracking

2.2.1.1 Sample preparation

To perform particle tracking, samples were created by mixing fluorescent microbeads with dissolved gelatin. Firstly, gelatin was measured by weight and mixed with ultrapure water to provide an 18 w% stock solution of gelatin, to an accuracy of 0.01 grams. Porcine and cold-water fish gels were prepared separately. The solutions were placed in a water bath at 60 °C for 1 hour to dissolve, utilizing a magnetic stirrer to provide constant stirring. After this, a 2 mL volume of the gelatin solution was transferred to a small glass vial to be used for the creation of the sample. For samples containing both porcine and cold-water fish gelatin, the appropriate volume of each was mixed to create a total volume of 2 mL. As an example, in samples containing 50% of each, 1mL each of dissolved cold-water fish gelatin and porcine gelatin was mixed. Any remaining volume of the stock gelatin solutions was refrigerated for later use.

To prepare the microbeads, the microbead suspension was mixed at high speed in a vortex mixer for 1 minute prior to use. To each 2 mL sample of gelatin, a total of 2 μ L of the microbead suspension was added via the use of a micro pipette. This resulted in an approximately 1000x dilution of the microbead suspension, which was found to give an appropriate density of particles for the particle tracking. After the microbeads were added, the solution was mixed gently using a magnetic stirrer for 5 minutes. After mixing, the samples were transferred to the sample plates, which were covered in aluminium foil. The plates were placed in a refrigerated area at 5 °C for 20 hours, after which the samples were analyzed.

2.2.1.2 Imaging of particles

After the samples were created, they were taken to a microscope to perform the imaging of the particles. For samples created at the Tokyo University of Marine Science and Technology (TUMSAT), the imaging was performed utilizing a Keyence BZ-9000E fluorescence microscope. For samples created at the Norwegian University of Science and Technology (NTNU), a ZEISS Axio Observer microscope was utilised. Both of these microscopes utilise mercury arc lamps to induce fluorescence, using green filters to isolate the fluorescence from the yellow-green fluorescing beads.

For samples where temperature control was utilised, a simple cooling system was used to keep the temperature of the microscope stage at a stable temperature. The system consisted of a water bath which could pump cold water through tubes which were connected to channels that ran through the outer edges of the stage. The cooling water was pumped through these channels, which allowed for the metal stage to cool down. The stage had a cylindrical indentation in the middle for the sample to sit in, allowing the stage to have direct contact with both the sides and bottom of the sample plate. The cooling water was kept at 2 °C lower than the desired temperature of the stage, which was observed to give a stable and accurate temperature near the area of the stage where the sample was kept. Temperature sensors were attached both at the edge and centre of the stage to monitor the temperatures during the experiments.

After placing the samples on the stage of the microscope, they were allowed to sit for 30 minutes to ensure a stable and uniform temperature. After this, the imaging of the samples was performed. Each sample was recorded for 110 seconds in 5 separate locations, waiting 10 minutes before recording each time the stage was moved. For the recordings, 40x objective lenses were used. For samples recorded at TUMSAT, a 40x dry objective (Keyence, BZ-PA40) was used. For samples

recorded at NTNU, a 40x oil immersion objective (Zeiss, Plan-Apochromat) was utilised. The resolution, frame rate and pixel sizes for the images captured in the two microscopes is given below in Table 2

Table 2: Information about the pixel size, resolution and frame rate for images captured in particle tracking experiments at TUMSAT and NTNU.

Location	TUMSAT	NTNU
Microscope	Keyence BZ-9000E	ZEISS Axio Observer
Pixel size [$\mu\text{m}/\text{pixel}$]	0.27	0.18
Resolution [pixels]	1360 x 1024	2752 x 2208
Frame rate [frames/s]	4.97	4.87

2.2.1.3 Tracking of particles and mean squared displacement analysis

After the imaging had been completed, the image series were extracted and analysed in MATLAB. The reason MATLAB was chosen was due to the existence of publicly available code for mean squared displacement (MSD) analysis. The one that was used in this case was called *msd_analyzer*, which is a MATLAB class made for performing MSD analysis.⁶¹ This class utilises the trajectories of the particles to calculate, plot and correct for drift, however it does not provide the tools for tracking the particles from the image data.

To perform the tracking, a multi-particle tracking code developed by Hansen Zhao was used, which is publicly available on GitHub (<https://github.com/HansenZhao/Multi-Particle-Tracking>). This code is based on code developed by Daniel Blair and Eric Dufresne for single-particle tracking purposes.⁸ The particle tracking function takes in a total of 4 arguments in addition to the image data, with three of these affecting the resulting tracking measurements. The first is the expected diameter of the particles given in pixels, which generally should be set to be a few pixels larger than the observed particles for the most ideal results. The second is the cut-off intensity, which defines how bright a pixel has to be when compared to the brightest pixel in the image for it to not get ignored during the particle tracking. Any pixels under the cut-off intensity are not included when the particles are tracked. The cut-off intensity is given as a fraction between 0 and 1. The last argument is the memory of the tracking, which is a numerical value defining how many frames a particle can be gone for before it is counted as a new particle.

With this particle tracking code in combination with the *msd_analyzer* class, a MATLAB script was written to utilise them together, both tracking and performing MSD analysis on the data. The *msd_analyzer* class⁶¹ was also used to perform drift correction on all MSD curves. The code was set to perform a velocity based correction, isolating and removing velocity caused from drift from the particle trajectories. Documentation and tutorials for the various functions, including drift correction, found in the "msd_analyser" class is available online (https://tinevez.github.io/msd_analyzer/). A copy of the final MATLAB script used for the particle tracking and MSD analysis is given in Appendix B. An overview of the data obtained for each image series analysed is given below in Figure 3

Table 3: An overview of the data obtained from the particle tracking, including a brief description for each one.

Output	Notes
Trajectories	Returns the trajectories for all particles
MSD curves	Returns a single plot including the MSD curves for all trajectories
Drift-corrected MSD curves	Returns a single plot including all drift corrected MSD curves
Curve fitting data	Returns data for a log-log curve fit performed on each MSD curve, both raw and drift-corrected.

2.2.1.4 Overview of particle tracking protocol

To give an overview of the entire particle tracking protocol, a simplified flowchart showing all the major steps involved in the process is given in Figure 6.

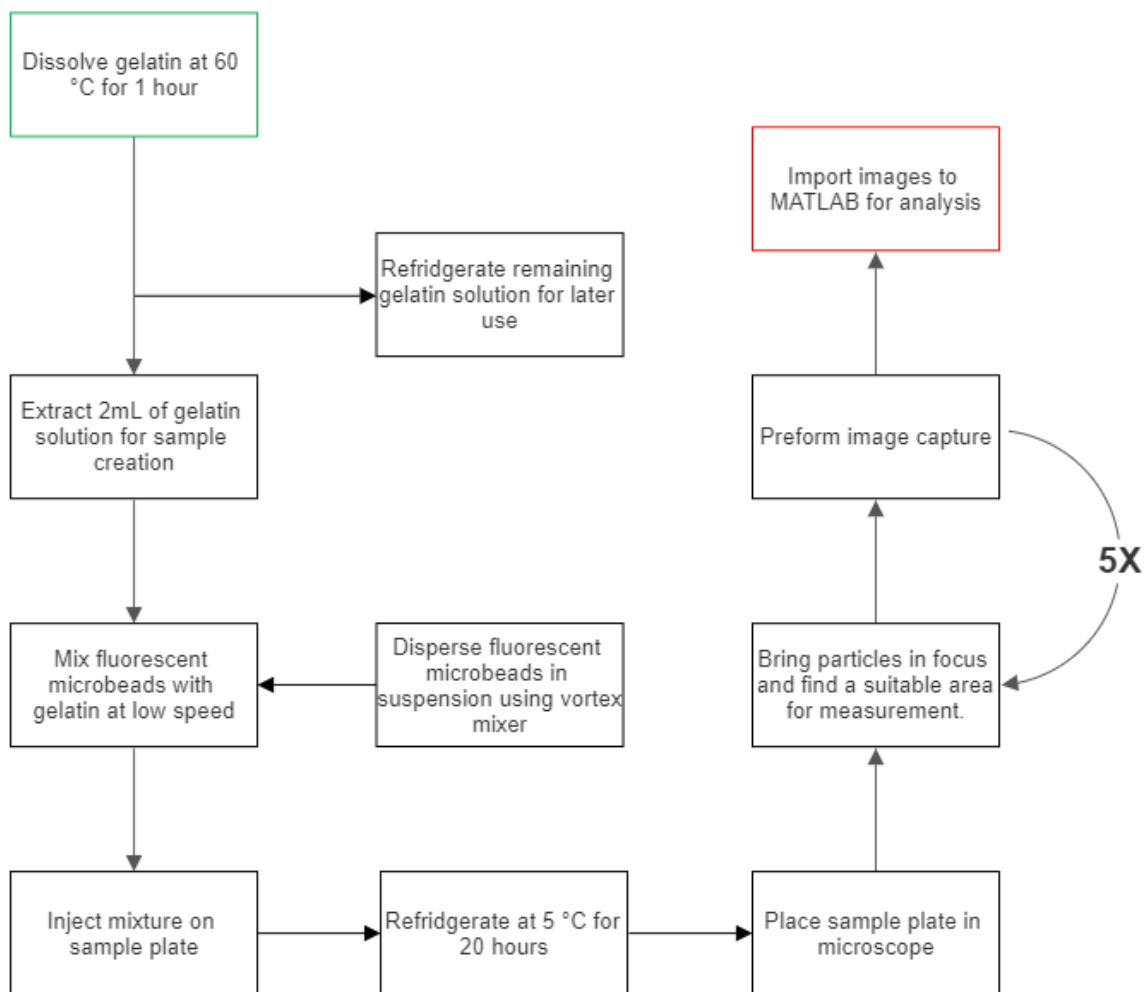


Figure 6: A flowchart summarising all major steps involved in the particle tracking protocol. The starting point is marked with green, while the final step is marked with red.

2.2.2 Release from gels in aqueous environment

2.2.2.1 Introduction

The objective of these experiments was to measure the release of tartrazine and blue dextran from gelatin gels over time without necessarily dissolving them, comparing gels made from pure mammalian gelatin, to gels containing equal parts mammalian and cold-water fish gelatin. The release from gels in aqueous environments was tested with the use of a SOTAX AT7 smart dissolution tester. The unit is comprised of 7 separate glass vessels in which dissolution tests may be performed, all of which sit in a water bath chamber for temperature control. Each vessel comes with a metal rod which can be raised and lowered from it, on which a mesh basket or a paddle may be connected. The metal rods are all connected to a motor, which allows for them to rotate at a constant speed. The general idea is that the vessels keep a solvent inside separate from the water bath, while the metal rod either provides stirring with a paddle, or keeps a sample, or solute suspended in the solvent with the mesh basket. Each vessel also contains a small sample tube, which can be used to manually extract samples from the solvent. For the experiments in this thesis, the baskets were used to hold the gelatin samples in the vessels. To measure the release over time, a UV-1600PC spectrophotometer was used to find the concentration of blue dextran and tartrazine in the extracted solvent samples, and plotting these values to visualise the release from the gels over time.

2.2.2.2 Determination of standard curves

To be able to find the concentrations of blue dextran and tartrazine in the medium surrounding the gels, it was necessary to establish a set of standard curves for each of the two compounds. To begin, the ideal absorbance wavelengths for each of the two compounds had to be found in order to maximise the absorbance gained from them. For this purpose, samples containing tartrazine and blue dextran were tested separately via wavelength scans, measuring their absorbance in the range of 300 to 800 nm. The samples were diluted until their absorbance peaks showed a maximum absorbance below 1, as anything above 1 would lay outside the linear absorbance range. For this reason, it is also generally desirable to keep the absorbance at around 0.8-0.9 as a maximum. Doing these dilutions also served as a basis for determining which concentrations to utilise for the standard curves.

The absorbance spectrum for a solution of 21 $\mu\text{g}/\text{ml}$ tartrazine is given in Figure 7. The absorbance spectrum indicates an absorbance peak for tartrazine between 425 and 427 nm. From this, it was decided that 425 nm would be used to measure the absorbance of tartrazine in the experiment samples. The absorbance spectrum for a solution of 1 mg/ml of blue dextran is given in Figure 8, which indicates an absorbance peak between 618 to 620 nm for blue dextran. From this absorbance spectrum, it was decided that 620 nm would be used to measure the absorbance of blue dextran in the experiment samples. Looking at the absorbance spectrum for blue dextran, it also shows an increasing absorbance at wavelengths below 475 nm. Given that the absorbance peak of tartrazine was found to be in the range of 425-427 nm, it shows that the absorbance of the two compounds would overlap if mixed, For this reason, blue dextran and tartrazine were tested in separate gels for all experiments.

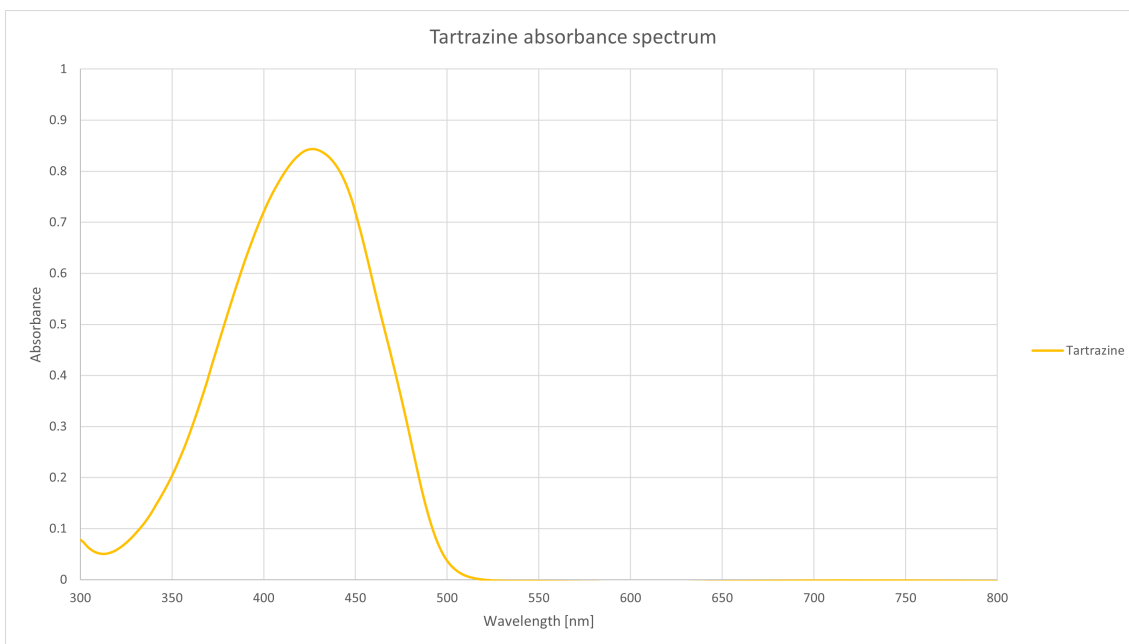


Figure 7: Absorbance spectrum for tartrazine, with the absorbance plotted against the wavelengths between 300 and 800 nm. The peak of the absorbance curve was deemed to lay around 425-427 nm.

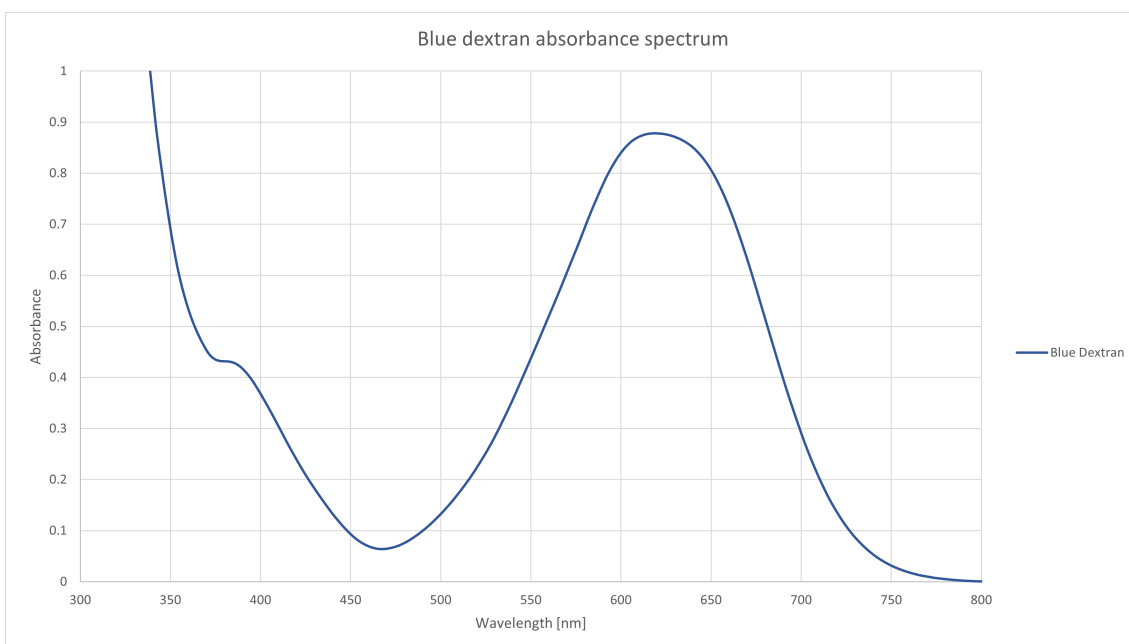


Figure 8: Absorbance spectrum for blue dextran, with the absorbance plotted against the wavelengths between 300 and 800 nm. The peak of the absorbance curve was deemed to lay around 618-620 nm.

With the peak absorbance wavelengths for each of the two compounds known, the standard curves for tartrazine and blue dextran were developed. From measuring the peak absorbance wavelengths, it was found that a concentration of approximately $21 \mu\text{g/ml}$ tartrazine gave an absorbance close to 0.85. It was determined from this that a concentration of $22 \mu\text{g/ml}$ tartrazine would serve as the highest point on the standard curve, as it would allow for a more simple dilution series than

21 $\mu\text{g}/\text{ml}$. Using this concentration as a starting point, a dilution series of tartrazine was made and measured at 425 nm to provide a standard curve for tartrazine. The resulting standard curve is shown in Figure 9, alongside the coefficient of determination and the equation for the standard curve. The equation for the standard curve of tartrazine is also presented below in Equation 2.

$$C = 24.632 \cdot A + 0.1106 \quad (2)$$

Here, C represents the concentration in the sample, while A represents the absorbance.

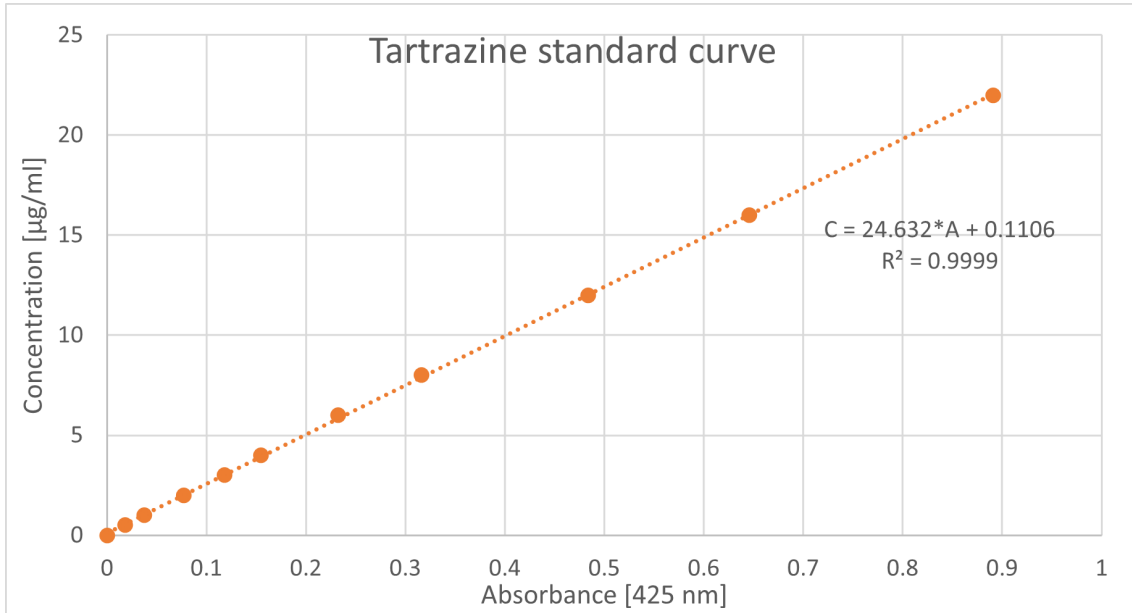


Figure 9: Standard curve found for tartrazine at a wavelength of 425 nm, The coefficient of determination and the equation for the curve fit is given below the curve. The absorbance for a dilution series of tartrazine starting at 22 $\mu\text{g}/\text{ml}$ was used to create the standard curve.

From measuring the peak absorbance wavelengths, it was found that a concentration of 1 mg/ml of blue dextran gave an absorbance of around 0.85. To get a more simple dilution series, a concentration of 1.12 mg/ml of blue dextran was used as the starting point of the dilution series. Utilising this, the standard curve for the absorbance of blue dextran at 620 nm was found. The resulting standard curve is shown in Figure 10, alongside the coefficient of determination and the equation for the standard curve. The equation for the standard curve of blue dextran is also presented below in Equation 3.

$$C = 1.1753 \cdot A + 0.0009 \quad (3)$$

In this equation, C represents the concentration of the sample, while A represents the absorbance.

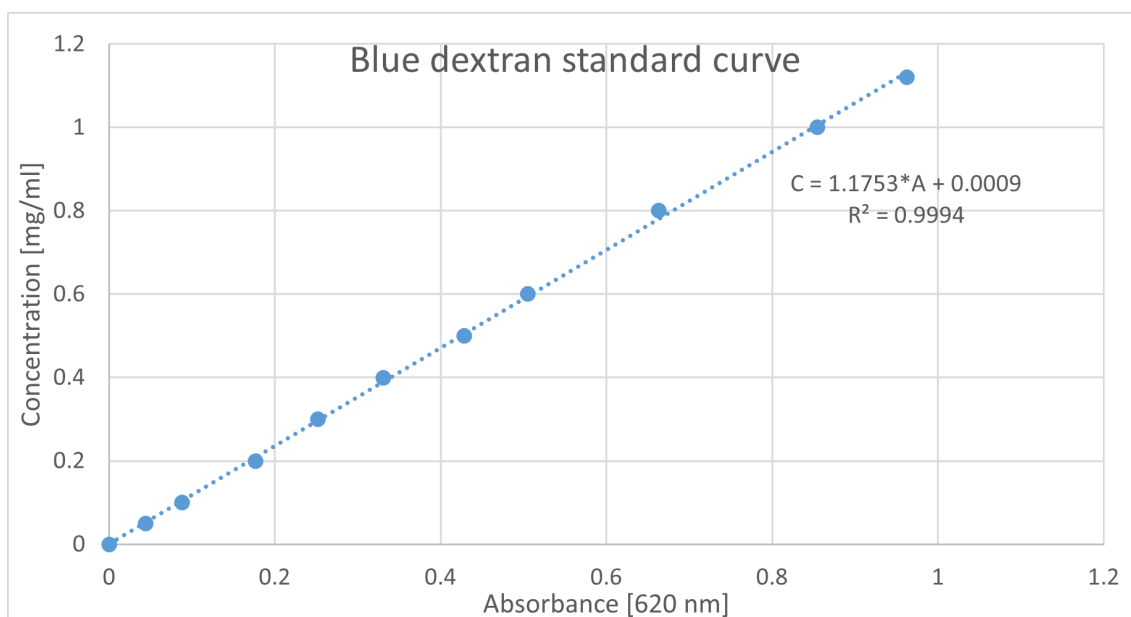


Figure 10: Standard curve found for blue dextran at a wavelength of 620 nm, The coefficient of determination and the equation for the curve fit is given below the curve. The absorbance for a dilution series of blue dextran starting at 1.12 mg/ml was used to create the standard curve.

With these standard curves known, they were also used to determine the ideal concentrations of blue dextran and tartrazine which had to be added to the created samples.

2.2.2.3 Sample preparation

The preparation of the samples started with dissolving the necessary gelatin for them. The gelatin and water was measured on a scale to an accuracy of 0.01 grams to create gelatin mixtures of an 18 w% total concentration. In the case of gels containing both cold-water fish gelatin and mammalian gelatin, the dry gelatin was mixed before dissolving them. To dissolve the gelatin, it was placed in a water bath at 60 °C for 1 hour with continuous stirring via a magnetic stirrer. Two parallels were made for each gel, one each for testing tartrazine and blue dextran, since these had to be tested separately. Both parallels were made using 5 grams of water, and 0.9 grams of gelatin for all cases.

While the gelatin was dissolving, the necessary amounts of blue dextran and tartrazine were measured out on a scale to an accuracy of 0.1 mg. To determine the necessary amounts, the volume of solvent, or more accurately liquid medium had to be taken in account. The way that the amounts were determined was by calculating the amounts necessary to provide a set concentration in the liquid medium, which were 22 $\mu\text{g/ml}$ for tartrazine and 1.0 mg/ml for blue dextran, as these would both give an absorbance of around 0.8-0.9. The amount of liquid medium used was decided to be 400 mL, as anything less would not fully submerge the samples. This meant that a total of 8.8 milligrams of tartrazine had to be added to the tartrazine gel. For blue dextran, this meant that a total of 400.0 mg had to be added to the blue dextran gel.

After measuring out the tartrazine and blue dextran, they were added to each their gelatin solutions. They were then dissolved and dispersed in the gels via magnetic stirrers, stirring for a total of 30 minutes to ensure proper mixing. To ensure that both gel parallels were of an equal surface area, they were both gelled in 5 mL gelatin moulds, which had been coated in !!!! oil to ensure that the gelatin did not stick to them. These gels were then allowed to gel for a total of 20 hours before analysis, at which point they were allowed to come up to room temperature for approximately 30 minutes before the start of the experiment. The gels were then placed in metal baskets, which were placed in the dissolution unit to be lowered in separate, but identical liquid mediums.

2.2.2.4 Protocol for release measurements

Prior to the start of the experiments, the liquid medium, which was deionized water, was measured and filled into the vessels in which the gels were going to be submerged. To each vessel, a total of 400 mL of deionized water was added. The liquid medium was allowed to sit for 2 hours in the vessel to allow for the temperature in the system to stabilise, and for the liquid medium to come up to the desired temperature for the experiments. In the case of the experiments in this thesis, the liquid medium was kept at room temperature, which was monitored to remain stable at 20 °C.

After this, and after the gel samples had been prepared and placed in the metal baskets, the baskets were then attached to the rotor arms. Each arm was set to spin at 75 rounds per minute to provide gentle agitation to the system, allowing for the released compounds to disperse more quickly in the solvent without risking the gels getting damaged from the centrifugal force. The samples were then lowered in the liquid medium, at which point a timer was started. Samples were taken from the solvent with increasing time gaps, with samples taken more often in the first 4 hours of the experiments. The specific time points of the measurements varied between experiments, but were kept the same between the tartrazine and blue dextran parallels. The gels containing pure mammalian gelatin were measured for a total of 48 hours, while the gels containing equal parts of mammalian and cold-water fish gelatin were tested for 46.5 hours. The reason why the time points of the measurements, as well as the experimental duration was not kept the same was due to it not being deemed a priority. The goal was to study the overall rate and behaviour of the release, thus the specific time points at which measurements were conducted was not deemed a large priority, so long as the frequency of the measurements was kept relatively similar.

After the samples were taken, they were immediately tested in a UV-1600PC spectrophotometer, the same as was used to find the standard curves, to determine the concentration of tartrazine and blue dextran. The concentration of tartrazine and blue dextran in each sample was found by utilizing the established standard curves, presented in Figure 9 and 10, respectively. These values were then plotted together to provide a visualisation of the release of both tartrazine and blue dextran from the gels over time.

2.2.2.5 Overview of release measurement protocol

To give an overview of the protocol used for the release measurements, a simple flowchart showing the major steps involved in the process is given in Figure 11.

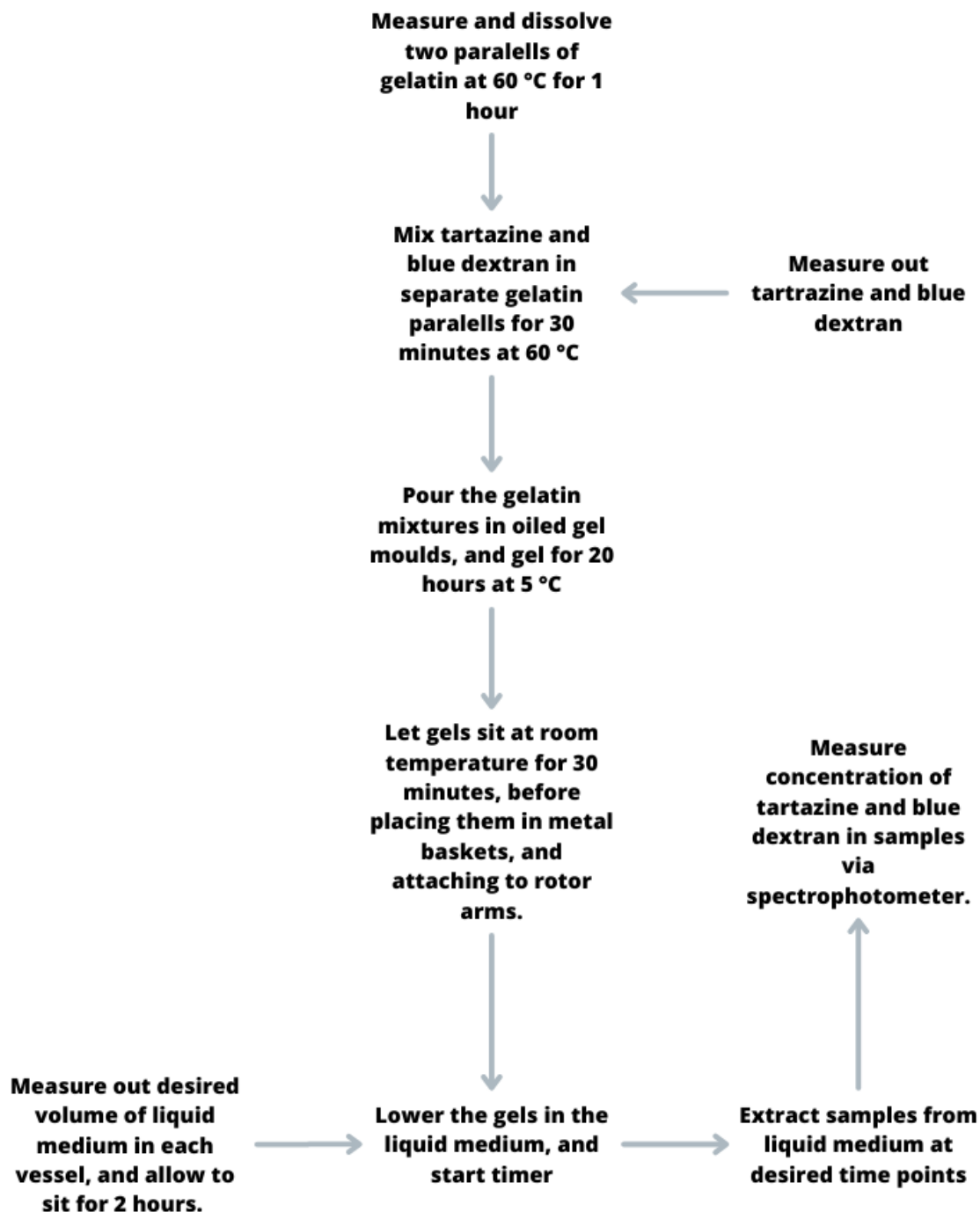


Figure 11: A flowchart summarising all major steps involved in the release measurement protocol. Volumes and weights used are not specified.

2.2.3 Fluorescence recovery after photobleaching

2.2.3.1 Introduction

Fluorescence recovery after photobleaching (FRAP) was used to study the diffusion properties in the matrix of gelatin emulsions containing equal parts cold-water fish gelatin and mammalian gelatin. The goal was to study whether or not the gel matrices of the emulsions would be significantly different from those in regular gels. To do this, the FRAP experiments were carried out on control gels as well, to provide a point of reference. A Leica SP8 confocal microscope was utilised for the FRAP analysis, using a white light laser at 496 nm for both imaging and bleaching. The laser was set to 100% power during bleaching. The following settings were used for the microscope:

- Power, 496 nm gate: **25%**
- Image format: **512x512**
- Speed: **400, bidirectional**
- Zoom factor: **5x**
- Image size: **93 μm x 93 μm**
- Pixel size: **182 nm x 182 nm**
- Optical section: **1.705 μm**
- Pixel Dwell Time: **1.2 μs**
- Frame rate: **1.54/s**
- PMT range: **505-560 nm**

Using these settings, the FRAP measurements were performed on a circular region of interest with a radius of 7000 nm. A total of 5 separate FRAP measurements were performed in each gel parallel.

2.2.3.2 Sample preparation

To prepare the samples used for the FRAP experiments, a 100 mL stock gelatin solution was created, containing 9 w% each of cold-water fish gelatin and mammalian gelatin to a total gelatin concentration of 18 w%. This was done by dissolving 9 grams each of the two gelatin types in 100 mL of pure water, dissolving at 60 °C for 1 hour under constant stirring.

To create the gelatin emulsions, 16 grams of this stock solution was measured out. This was mixed with 16 mg of 70 kDa Fluorescein isothiocyanate (FITC) –dextran using a magnetic stirrer, to a concentration of 1 mg/g FITC-dextran to gelatin solution. This was then mixed with 4 grams of corn oil to give a 20% oil mixture. All measurements were conducted on a scale with an accuracy up to 0.01 grams, with the exception of FITC-dextran which was measured to an accuracy of 0.1 mg. The oil-gelatin mixture was then allowed to sit for 30 minutes in a 60 °C water bath to heat the oil before emulsification was carried out. To make the emulsions, an IKA T 10 Basic Ultra Turrax homogenizer was used. The homogenizer had a numbered wheel from 1 to 6 to set the speed of it, with a speed of 4.5 used to make the emulsions. After the oil-gelatin mixtures were heated, they were emulsified by the homogenizer for exactly 3 minutes. Directly after the emulsification process, the emulsions were degassed in a vacuum degassing chamber to remove air bubbles. Control gels were also created directly from the stock solution, made by mixing 10 grams of the gelatin solution with 10 mg of FITC-dextran. A total of 2 parallels were made for both the emulsions and controls, resulting in 4 separate samples.

To plate the samples for analysis, 6 channel μ -slides were used (μ -Slide VI^{0.4}, Ibidi). These slides had a volume of 30 μL . Using syringes, the gelatin emulsions and controls were transferred to the channels. The wells in which the samples were filled were then sealed off using a thick layer of

parafilm. The reason why this was done was to protect the samples from air, and more importantly to reduce the amount of drift in the samples, as not plugging the wells was observed to lead to some drift of the oil droplets. The μ -slides were then covered with aluminium foil, and allowed to gel for 20 hours at 5 °C.

2.2.3.3 Protocol for measurements and analysis

To preform the FRAP analysis, the samples were placed in the microscope, and allowed to sit for 30 minutes to come up to room temperature. The FRAP analysis was then carried out using the settings specified in Section 2.2.3.1. The region of interest (ROI) was moved to maximise its distance from the oil droplets when measuring. All measurements were carried out with 5 pre-bleach frames, 3 bleaching frames and 100 post-bleach frames. With an iteration time of 0.648 seconds, this equalled a total of 3.240 seconds measured pre-bleach, 1.944 seconds of bleaching, and 64.800 seconds measured post-bleach. This gave a total duration of 69.984 seconds per measurement. For each individual sample, measurements of the passive bleaching from the scanning was also measured. This was done by simply scanning a new ROI in the gel for the same duration as the FRAP measurements, but without bleaching the ROI. All measurements were preformed at room temperature, with no temperature control. The resulting data was exported as CSV files.

After the data was gathered, it was analysed using EasyFRAP-web (<https://easyfrap.vynet.upatras.gr>), a web-based tool for FRAP data analysis.³⁶ The tool requires the user to input the bleach-recovery data, as well as the passive bleaching and background fluorescence intensity for each sample. The bleach-recovery data and passive bleaching were both measured as mentioned above. The background fluorescence intensity was set to zero for all samples, as FITC-dextran was the only contributor to the fluorescence intensity. This was checked by also measuring a gelatin sample containing no FITC-dextran, which gave zero fluorescence intensity. EasyFRAP-web takes this data, and returns the normalised bleach-recovery curves. The tool also preforms a curve fitting for each bleach-recovery curve, returning the R^2 , halftime of recovery $T_{1/2}$ and mobile fraction for each one. Using the halftime of recovery, the diffusion coefficient is then calculated with the use of the Axelrod equation, which is presented in Equation 1. Using these diffusion coefficients, the results from the emulsions and control gels can be compared, and used to evaluate whether there is a significant difference in their gel matrices.

2.2.3.4 Overview of fluorescence recovery after photobleaching protocol

To give an overview of the protocol used for the FRAP measurements, a simple flowchart showing the major steps involved in the process is given in Figure 12.

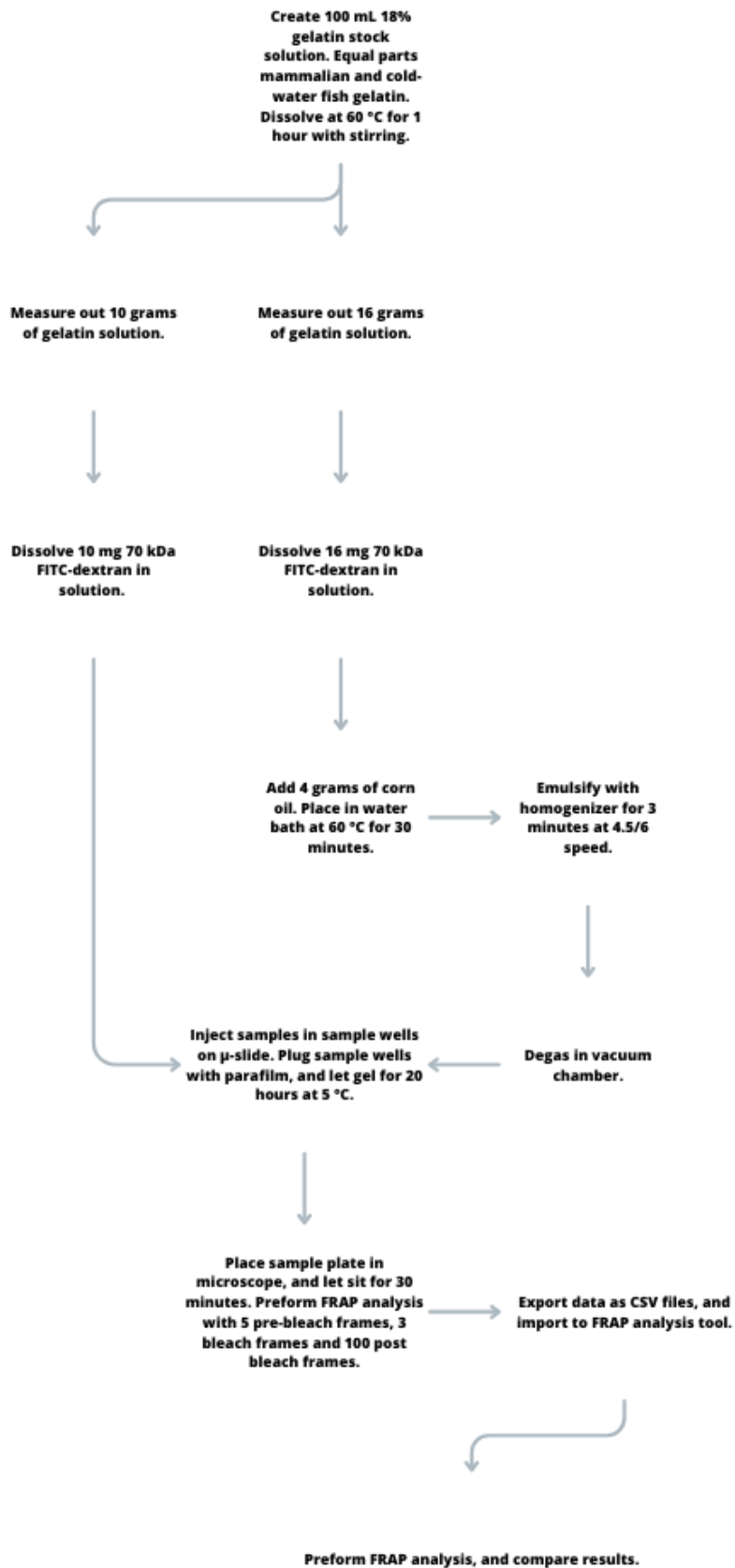


Figure 12: A flowchart summarising all major steps involved in the FRAP measurement protocol.

3 Results discussion

3.1 Particle tracking

3.1.1 Particle tracking at Tokyo University of Marine Science and Technology

As part of a 5 week stay at the Tokyo University of Marine Science and Technology various samples were tested via the use of particle tracking. Utilising a temperature controlled stage, the tracking was performed in samples containing pure cold-water fish skin gelatin, pure porcine gelatin and in a mixture of equal parts of both. All samples were of a 18 w% total gelatin concentration, and data was collected at 5 and 20 °C for all samples. The reason why these temperatures were chosen was to observe the gels at a state where all of them should remain solid, that being 5 °C, and at a state where cold-water fish gelatin should melt, that being 20 °C.²¹ The gels were allowed to gel at 5 °C for 20 hours before the analysis was conducted. This was done to allow the gels to form more robust networks before analysis, in the hopes that it would create a more clear separation between the different gel types. Gelatin is known to have a gel strength that continuously increases with time, however the change is far more drastic during the first few hours. After 4-10 hours, the change appears to generally slow down in most cases for mammalian gelatin, which suggests that a gelling time of 20 hours should be sufficient to provide a strong gel, particularly considering the high gelatin concentration used.^{5,21} The long gelling time was also desirable for the purpose of comparison, as previous experiments utilizing fluorescence recovery after photobleaching (FRAP) were performed on gels which had been rested for similar durations.³⁷

The particle tracking measurement was repeated a total of 5 times per sample to minimise the impact of possible random disturbances during the measurements. The cut-off intensity was adjusted for each individual measurement in order to eliminate any particles that were out of focus, and to eliminate any background noise from distant particles. To begin with, the samples were first analysed at 5 °C, where all samples should in theory be solid. The temperature of the stage was set before the samples were placed on to ensure minimal heating of the samples. The samples were moved from the refrigerator and to the stage utilizing a thermos container, which was cooled to 5 °C to keep the temperature of the sample constant during transport. After setting the samples on the stage, they were allowed to rest for a total of 30 minutes to ensure that the temperature was stable. When analysing the samples at 20 °C, where cold-water fish gelatin should in theory melt, they were allowed to rest for 1 hour to ensure that the sample was evenly heated and stable before analysis.

The samples containing pure cold-water fish skin gelatin were tested first, with an example of the resulting Mean Squared Displacement (MSD) curves given in Figure 13. The curves appear to have varying starting MSD, however they appear to have similar slopes. The curves appear to start relatively flat and then slope upwards with time. Looking at the yellow reference line at the top of the figure, it is also clear that the slope near the end is larger than 1. This would then indicate superdiffusive behaviour, something that is highly unlikely in such a system. Brownian motion should give a slope of around 1, meaning that even if the gelatin had remained completely dissolved in the medium, the curves should not have a higher slope than this. Seeing as the cold-water fish gelatin should be able to gel at 5 °C, the MSD curves should likely have a slope lower than this. A higher slope would indicate active transport, or some sort of additional energy affecting the particles, facilitating their motion. This could be caused by several different things, including active transport from microorganisms,⁴⁵ directional movement of gel matrix^{58,65} or simply some drift of the sample or objective.

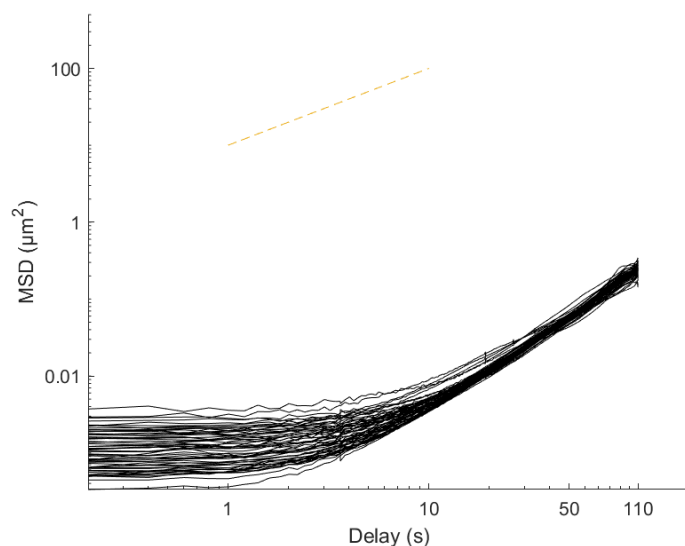
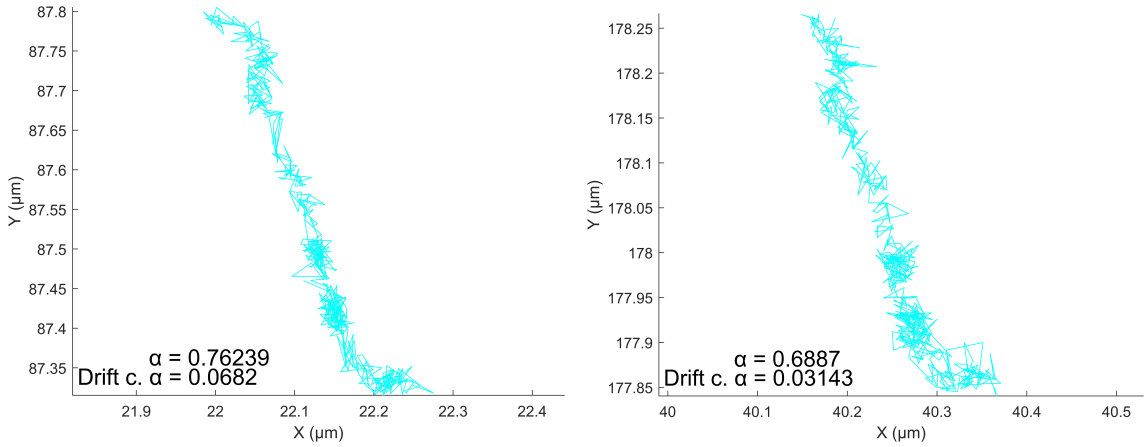


Figure 13: Mean Squared Displacement curve for cold-water fish gelatin at 5°C, tracking a total of 58 individual particles for 110 seconds. A linear reference line with a slope of 1 is included at the top of the figure.

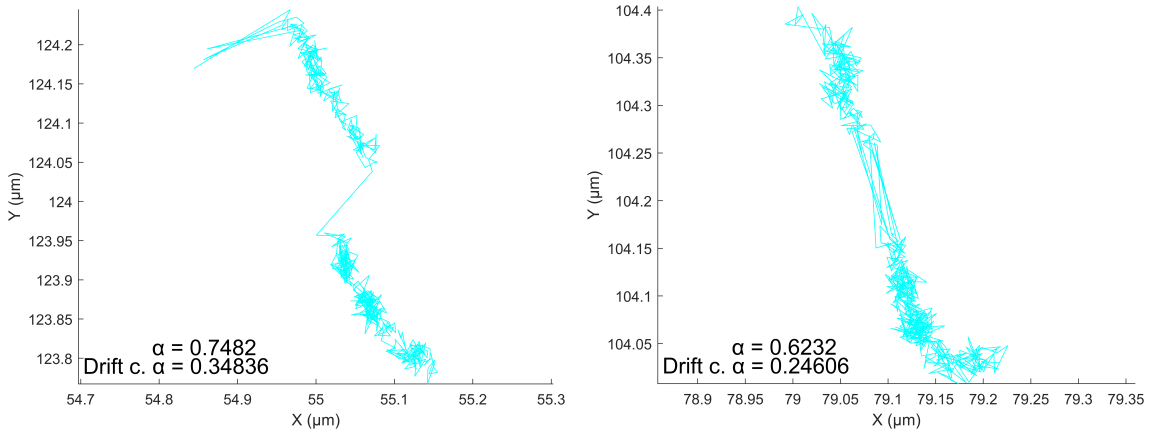
Active cellular transport could in theory cause some increased movement of the particles, but this is unlikely in these systems given that no microbial organisms were added. While there is a high possibility that some microbes from the equipment did end up in the final sample, it is unlikely that these would have multiplied sufficiently given the low temperature which the samples were kept at. In addition, the particles used were 1 micron in diameter, which would be too large for most common microbes to transport across their membrane.³⁸ In addition there has been research regarding the antimicrobial properties of gelatin and collagen which has indicated that gelatin may have certain antimicrobial properties, though the composition and conditions likely play a large role. While this is not definitive proof, it does strengthen the notion that microbial activity was not a major source of the high movement observed.³⁰ At the same time, it is hard to say if directional movement of the gel matrix did occur, though this would generally require some driving force. Given that the temperature was kept stable, a temperature gradient does not appear to be a likely driving force. The samples were also sealed off in the sample plates, which should also have eliminated the possibility of air pressure or flow affecting the gels. It may be possible that there were some capillary forces that might have caused the directional movement, though it is difficult to confirm or deny this.

The most likely explanation in this case seems to be drift, as the microscope itself was susceptible to vibrations and environmental disturbances which may have caused some drift of the sample. More accurately, the movement observed is likely caused by a drift in the focus or image, which could be due to minor movements in the stage, sample plate or lens amongst other things. This is further corroborated by the curves themselves all being highly similar in shape, which would indicate that all particles are moving in a similar way, not just some of them. Examining the curves closer seems to show the same as well. Figure 14 shows 4 of the tracks found for the particles in cold-water fish gelatin, all of which appear to follow a similar path. There are clear differences in the way the particles move over short periods, which does imply that there is something causing the particles to move differently from one another, indicating that there is diffusive motion happening. For more information about different types of movement a particle can show, see Section 1.4. Despite this, the overall paths appear to be quite similar for all tracked particles. All tracks seem to move downwards and to the right with a similar speed and direction, something that is typical when drift occurs. There appears to be something driving all particles in the same direction, and drift appears to be the logical explanation. While the exact reason for the drift is unknown, there is clearly some force that is causing every particle to drift the same. In other words, the fact that they all appear to move the same way indicates that the whole matrix is moving, not just the particles, though it is clear that the particles are moving around due to diffusion as well. It is also worth noting

that these measurements were conducted in Japan, a country in which earthquakes are relatively common. For this reason, buildings are also typically built to sway and dampen the effect of earthquakes, which naturally increases the risk ground movements affecting the measurements. While the smaller ground movements may not be possible for a human to notice, they might still cause enough of a disturbance to cause some drift when performing measurements at a microscopic level. To test if drift was a major source of the high slopes, the MSD curves were adjusted using the velocity drift correction mentioned in Section 2.2.1.3. The resulting curves are presented in Figure 15.



((a)) Two tracks showing no large jumps



((b)) Two tracks showing one or more large jumps in the middle

Figure 14: Four of the tracks found for 1 micron particles in pure cold-water fish gelatin with an 18 w% concentration. Tracking was performed at 5 °C for 110 seconds.

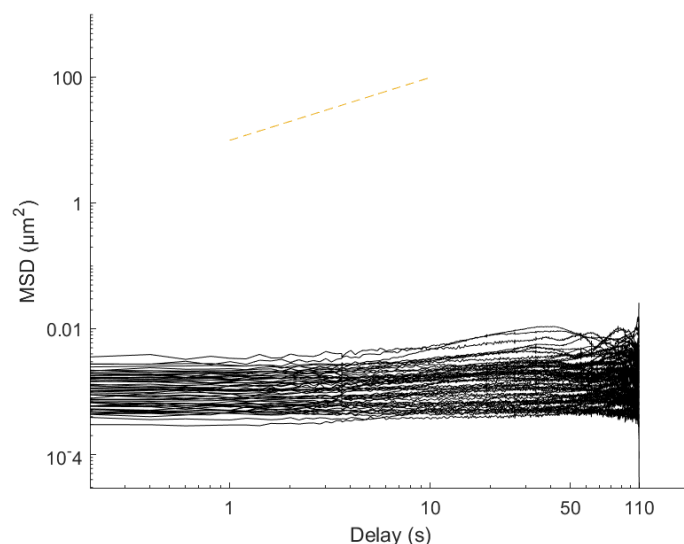


Figure 15: Drift corrected Mean Squared Displacement curve for cold-water fish gelatin at 5°C, tracking a total of 58 individual particles for 110 seconds. A linear reference line with a slope of 1 is included at the top of the figure.

All the curves in this case seem to be relatively flat across the entire duration of the measurement. This would indicate that the particles are highly constricted by the gel matrix, something that seems more likely in this system. The gel was stored at 5°C, which should be low enough for the chains to form triple helixes, and thus for a gelatin network to start forming. At the same time the gelatin was not allowed to heat up during the transport other than the brief periods in which it was transferred from the refrigerator and to the cooled container, and from the container to the cooled stage. This also minimises the probability of melting occurring, though given the small amount of gelatin used, there might still have been some melting even if minimal. Seeing as the melting temperature for cold-water fish gelatin is around 14-16 °C, it can be assumed that the brief moments of transport likely did not cause any major melting of the gel.²¹ None of the MSD curves seem to indicate strictly brownian motion either, which further supports this assumption.

Seeing as the gel would be expected to have a rather extensive structure after gelling for 20 hours, these curves seem much more reasonable. There seems to be some curves that sharply drop or rise near the end, which is likely due to some issues during the drift correction, or perhaps during the measurement itself. It is also possible that it simply is a result of how the MSD is calculated, as the number of data points making up the MSD value decreases with increasing lag time, which is noted as delay in the MSD plots here. The lag time quantifies the time between which the displacements making up the MSD value are measured, which naturally means that there will be fewer displacements making up the mSD for high lag times. This also means that any errors or deviations are more noticeable, as there is not as many values in the mean to cover up this deviation. The curves appear quite stable up to around 10 seconds, and for the most part even up to 50 seconds. The same results were seen across all the repetitions performed in the gel, which are presented in Appendix A. This seems to indicate that the drift correction is working well, or at the very least in a way that is consistent across different measurements. To compare the slopes of all the curves in each repetition together, a plot showing the slope α against the log-value of the MSD after 11 seconds is given in Figure 16. The reason why 11 seconds was chosen as the time was to avoid the apparent noise that seems to appear for later times, and because longer measurement times naturally leads to a higher possibility of disturbances affecting the results.

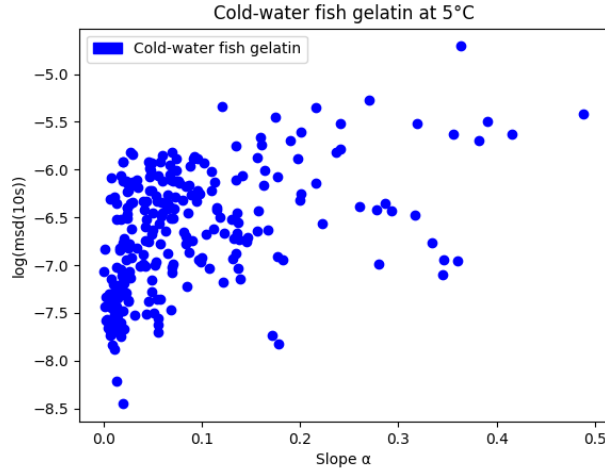


Figure 16: Slope α plotted against $\log(\text{MSD})$ for all tracked particles in cold-water fish skin gelatin at 5°C .

There does appear to be a relatively large spread in the slope values, however a vast majority of curves appear to have a slope somewhere between 0 and 0.1. While there are clearly still deviations, even the deviating points still show a sub-diffusive behaviour, having a slope lower than 1. It is difficult to say whether or not the deviations are a result of analytical error or if it is simply particles that have been less constricted, however looking at the tracked paths for the deviating curves would seem to imply the former. The curves that have significantly higher slopes all have distinctive regions where the particle appears to rapidly jump back and forth, which is likely caused by some error during the tracking of the particle. This can be seen in some of the tracks shown in Figure 14. The paths at the top of the figure both appear to have no large jumps, and thus also have relatively low α values at less than 0.1 once corrected for drift, which is seen on the bottom left of each track. On the other hand, the tracks shown on the bottom part of the figure appear to have these large jumps back and forth near the middle of the track. What these two curves have in common is the fact that they both exhibit higher α values once corrected for drift compared to the curves exhibiting no large jumps, which would indicate that these jumps are a major cause for the deviations observed.

Due to the fact that the tracking only measures the apparent centre of the particle, any variation in fluorescent intensity in the particle, such as if it is moving up or down relative to the lens can cause the tracking algorithm to adjust where it thinks the centre is between images. While the tracks do appear long, the length of the tracks in each case is still extremely low, appearing to lay between 0.5 and $0.8 \mu\text{m}$ in length. While it is difficult to tell their exact length, they do not appear to be longer than $1 \mu\text{m}$. This would mean that they are shorter than the diameter of the fluorescent beads, which should on average be around $1 \mu\text{m}$. This shows that while the jumps appear to be large, they are in practice only around $0.1 \mu\text{m}$. Each pixel in the image is approximately $0.27 \mu\text{m}$, which would mean that the observed jumps are shorter than 1 pixel. This would mean that even a slight deviation in focus can have significant effect on the observed path, thus making the system extremely sensitive to environmental disturbances. If just one pixel of the particle falls out of focus enough to be disregarded by the tracking code, it could be enough to cause jumps like these. If the intensity of said pixel lies extremely close to the cut-off intensity selected during tracking, it could cause it to be accepted in one image and disregarded in the next due to very minor shifts in the focus, thus causing such jumps. While it is difficult to test if this is what is causing these jumps, it does seem to be the most likely explanation.

It is not certain that this is the reason for the deviation in the slope α compared to the majority, however it does appear to be given the fact that each deviation has these noticeable jumps in their tracks. It could still be possible that certain particles were able to move further, perhaps due to moving between gaps in the matrix, which would also lead to a higher α value. If this was the case, then the paths would be expected to look more like beads on a string. This is due to the particle

moving in a constrained area, which would be the bead in this case, and then slipping between a gap in the structure, causing a significant jump in the path, which would be the string. The track in the bottom left of Figure 14 seems like a possible candidate for this, as it only shows one large jump in the very middle of the path. While this might just be coincidence, judging by the fact that it does appear to jump around at the top left of the track, it is not possible to say for sure. Thus it is difficult to say exactly what is causing the deviations, though it might be a mixture of these two factors.

Going back to Figure 16, there does also appear to be a significant difference in the MSD values even for the points that have similar slopes. While this might be partially caused by analytical errors during tracking, it is not unreasonable to have such differences. The slope value α is closely linked to how far the particle moves from the original coordinate. Since the mean squared displacement (MSD) value is a measure of the squared distance that a particle has moved from its original position, it means that for a particle to have a non-zero α value it has to be moving away from the original position. The faster the particle is moving away from the original position, the higher this slope will be. This means that the MSD value and the slope is naturally linked, as a steep slope would typically mean a higher MSD. This does however not mean that particles that are confined necessarily have to have a similar, or even low MSD value. The MSD value shows how far a particle is from the original position regardless of direction, which means that if a particle were to maintain a constant distance from the original position, it would still have a certain MSD even if the slope is zero. An extreme example of this would be spinning around with a ball tied to a rope. The starting position would be with the ball held against your chest as you are spinning. At some time the ball is then released, causing the MSD to jump to a certain value. This jump would then be the first measurement point, and so long as the length is kept constant, the MSD will remain constant for all following measurements. Increasing the length of the rope would increase the MSD, but it would still be constant, meaning a slope close to zero. This same effect can be obtained when a particle is moving around in a confined space. Seeing as the particle cannot move further away than to the edges of the confined space, it will keep bouncing around randomly for the duration of the measurement. This means that while the MSD will likely vary with time, it will not increase significantly so long as the confined space is small enough.

The MSD that is obtained from such a confined particle will then be a result of the size of the space, a larger space allowing for a higher MSD than a smaller one. This would explain why there is a noticeable spread in the MSD even for the particles which have similar α , simply because the space in which they are confined varies in size. Interestingly there appears to be a slight increase in α as the MSD increases, with the particles having high MSD values appearing to show a slightly higher α on average if the outliers are disregarded. This could also be explained by the fact that there simply is a higher chance for the distance from the starting position to appear to increase when the confined area becomes larger, especially over a short period of time which is the case here. It might simply be that the particle was measured close to the original position initially, and then measured further away for later time points. The chance for this will likely increase as the confined space gets larger, up until the space is so large that the particle can be measured for the entire duration without touching the edges. In that case the particle would show Brownian motion rather than confined motion, since it simply is not confined enough. If either the speed of the particle was to increase or the size of the confined space was to decrease, it would once again show confined motion. Taking this into consideration, it doesn't seem unreasonable that the MSD would vary in the way that is seen at the lower α values in Figure 16. To further strengthen this, the data can be compared to the findings for carrageenan in the study conducted by Lester C. Geonzon et al.²⁹ While carrageenan cannot be used as an analogue for gelatin, it can still be valuable to see what is observed for other gels under similar conditions. For pure κ -carrageenan at 5 ° C, a relatively similar spread can be seen around α -values 0.0-0.2. While there are not as many noticeable outliers in the data for carrageenan, it is also worth noting that there seems to be far fewer particles tracked, which would naturally decrease the chance of outliers. What is quite interesting about this comparison is the observed MSD values, as the spread in MSD values appears to closely resemble the spread noticed for cold-water fish gelatin. This helps to strengthen the notion that the spread is not simply caused by analytical errors, but is rather caused by the natural variation in the sizes of the confined areas that the particles move within. It does appear that cold-water fish gelatin was able to form a rigid gel network, however given

that the data for carrageenan was found for $0.1 \mu\text{m}$ spheres, it is hard to make a comparison with the κ -carrageenan. What this experiment does show is that cold-water fish gelatin is able to form a dense enough matrix to confine particles with a diameter of $1 \mu\text{m}$ or higher, though it is not possible to say if it could contain smaller particles or not.

Mammalian gelatin is known to form strong gels that can keep its structure at significantly higher temperatures than cold-water fish gelatin, and so a sample containing pure porcine gelatin was tested as a means of comparison. The goal with this was to have the data for both pure porcine and cold-water fish gelatin separately, so that the two could be compared to both one another and to mixtures containing both types. The sample was created in the same way as for the cold-water fish gelatin sample, gelling for 20 hours at 5°C . The data was processed in the same way as for the cold-water fish gelatin as well, using the same drift correction method which is described in Section 2.2.1.3. An example of the drift corrected MSD curves is given in Figure 17. The curves appear to behave similarly to those found for cold-water fish gelatin, being relatively flat with a sudden drop at the end. The curves also appear to have a small rise around 50 seconds, which was also seen to a more significant degree on the curves for cold-water fish gelatin. Seeing as porcine gelatin is known to have a melting point of around $33\text{--}34^\circ\text{C}$,²¹ it seems reasonable that it would be able to form a dense matrix at 5°C . In addition it is worth noting that $18 \text{ w}\%$ gelatin is a relatively high concentration of gelatin, and so the fact that the gel seems to restrict the particles lies in line with what would be expected.

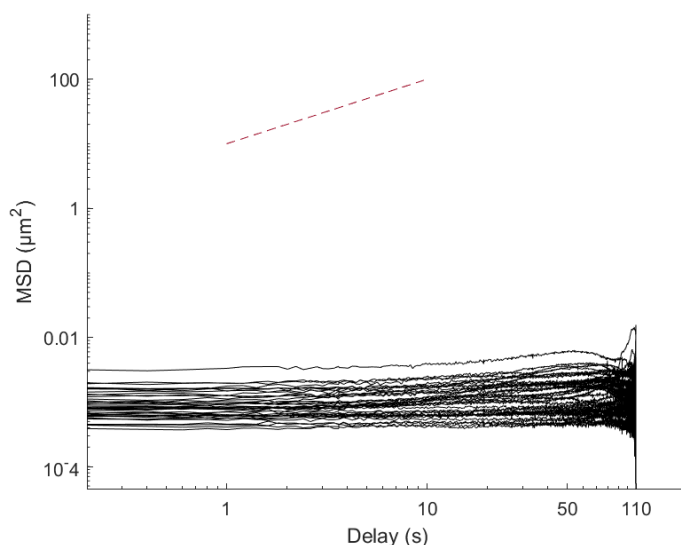


Figure 17: Drift corrected Mean Squared Displacement curves for porcine gelatin at 5°C , tracking a total of 41 individual particles for 110 seconds. A linear reference line with a slope of 1 is included at the top of the figure.

For comparison, these curves can be compared to what was found for warm-water fish gelatin by Yasuyuki Maki and Masahiko Annaka.⁴³ While mammalian and warm-water fish gelatin are not perfect analogues, they do have similar properties when it comes to strength and stability of their gels. The paper focuses on studying the gelation of warm-water fish gelatin, and includes data showing the average MSD curve over time as the gelling occurs. According to the data presented in the paper, the MSD curve appears to become mostly flat after 6 hours of gelling. This data is found for particles with a diameter of $0.6 \mu\text{m}$, which means that they are significantly smaller than those used in this thesis. Assuming that mammalian gelatin behaves the same, it seems highly reasonable that the $1 \mu\text{m}$ particles would have a flat MSD curve after 20 hours. The longer gelling time coupled with the larger particles should in theory only make it harder for particles to move, meaning that the flat curves are in line with what would be expected in this case. Comparing the curves found for porcine gelatin with those for cold-water fish gelatin also helps to strengthen the validity of the results for cold-water fish gelatin. Seeing as mammalian gelatin is well known to form strong gels, it is interesting to see that the cold-water fish gelatin is able to provide similar results at lower temperatures.

Plotting the MSD against the slope α for the porcine gelatin as well helps to show the similarity more clearly. Using the values at 11 seconds, this plot is shown in Figure 18. Looking at this figure, it is clear that the two gels are both confining the fluorescent particles in highly similar ways. The bulk of the particles appear to lay between α values of 0-0.1 in both cases, with a slightly lower average for the porcine gelatin judging by the spread. They both appear to show similar MSD values as well, with the bulk of the particles laying between $\log(\text{MSD})$ values of -0.6 and -0.8. The largest difference between the two seems to be the number and severity of the outliers, as porcine gelatin appears to have fewer and less extreme outliers. The most severe of the outliers seems to have an α value between 0.25 and 0.30, while the cold-water fish gelatin has several outliers with higher values than this. While it is impossible to say for certain why this is the case, there could be several explanations. One possibility is that it simply is random, either caused by issues during analysis or image capture. Numerous factors such as the amount of drift, focus stability and the clarity of the particles may have played some role.

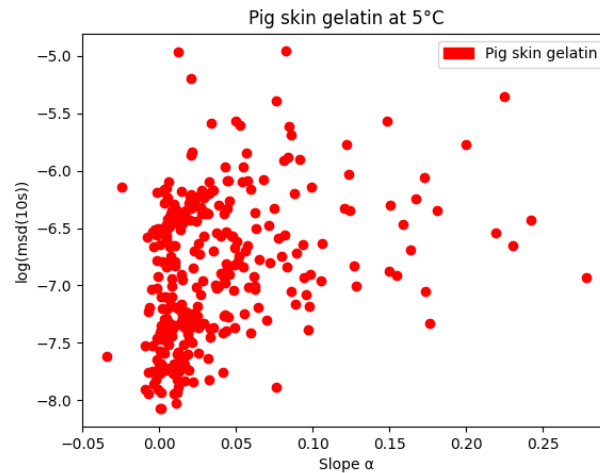


Figure 18: Slope α plotted against $\log(\text{MSD})$ for all tracked particles in porcine gelatin at 5°C.

Looking at a few of the tracks found, which are presented in Figure 19, it is clear that there is less drift happening. While the cause is unknown, this is likely part of the reason why there are fewer outliers for porcine gelatin. The tracks do appear to move a shorter distance than those presented in Figure 14, showing more circular or star shaped regions which are typical for confined particles. It could be that the particles simply are less restricted in the cold-water fish gelatin due to the matrices having large enough gaps for the particles to move between confined areas, though it seems unlikely given that the paths do not show any indication that this was happening. At the same time, this would also likely have been more clearly reflected in the α values if it was the case, as the jumps would have caused a noticeable increase in MSD. Judging by the fact that the drift corrected MSD- and α -values appear to be highly similar, it seems more plausible that the difference was simply caused by external factors causing more drift in the case of the cold-water fish gelatin. Looking at the tracks again, some of them also appear to exhibit the same jumps that were seen in the tracks for cold-water fish gelatin. The tracks containing a large amount of these jumps also appear to show higher α values than the ones without, which helps to strengthen the idea that they are a major cause for the apparent outliers.

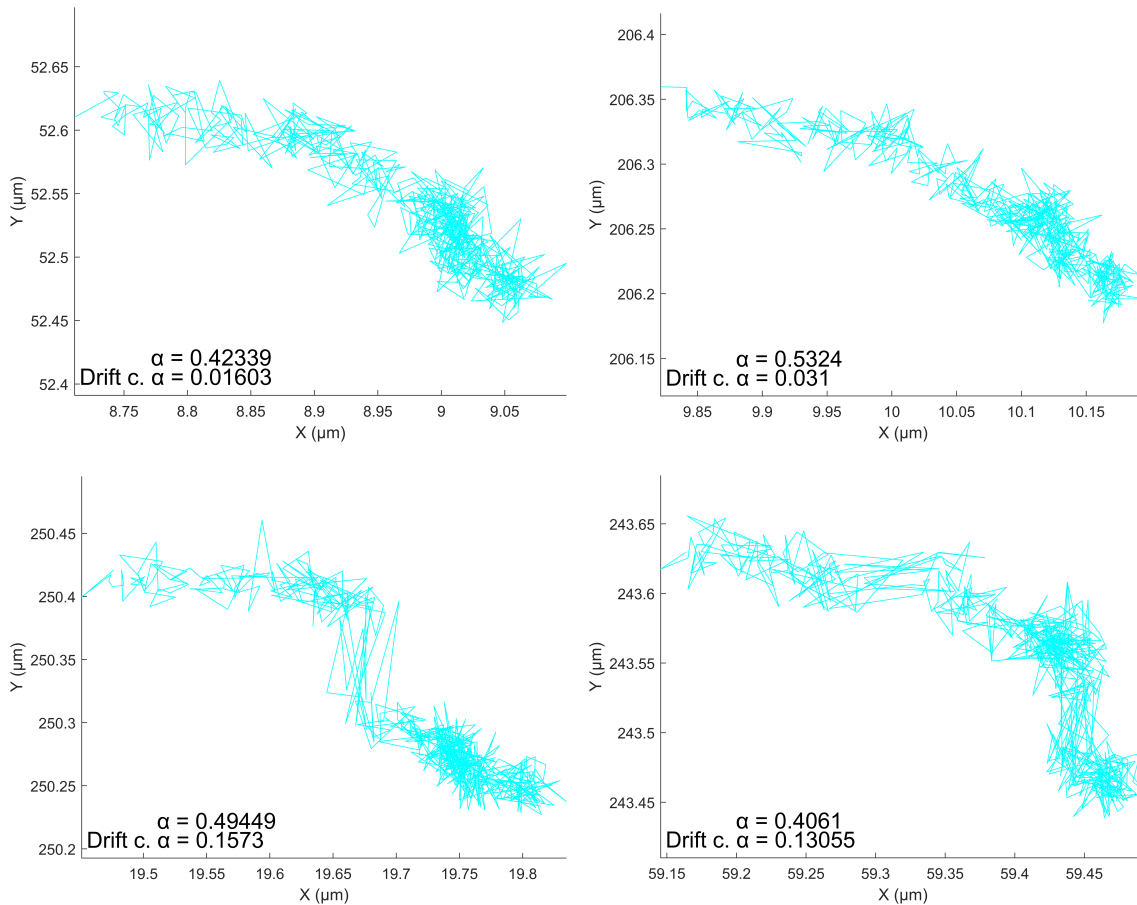


Figure 19: Four of the tracks found for 1 micron particles in pure porcine gelatin with an 18 w% concentration. Tracking was performed at 5 °C for 110 seconds.

The causes for the jumps are unknown, but it is likely to be a mixture of factors like discussed earlier. One possibility is that particles that lay closer to the edge of the focus depth may have caused more of the apparent jumps, as any drift either towards or away from the lens could have caused the edges of the particles to shift in and out of focus. Seeing as there was no way to guarantee exactly how in or out of focus every particle was, this could have varied heavily between measurements, causing some of the more significant outliers that are observed. Regarding the drift, there is also no guarantee that the drift was constant for all measurements. Due to the fact that the drift likely was caused by external factors, it is impossible to say how these may have varied between measurements. Measurements took place over several hours for just one sample, and so the chances that the drift varied between samples are significant. It is important that this is taken in account when evaluating these results, as there are simply many potential external factors that may have caused random errors. For example it is not possible to predict or counteract drift caused by vibrations in the ground, but the fact that the results appear to give a clear pattern in spite of this is an indication that the results are still good.

Like previously discussed there might also be a small chance that the gaps in the matrix for cold-water fish gelatin were large enough for some particles to move through them, which might not have been the case for porcine gelatin. While there is currently no specific data regarding the sizes of the gaps in gelatin matrices, it seems reasonable to assume that porcine gelatin might give smaller gaps due to the stronger gelling properties. The gelatin concentration being 18 w% may also have played a role in decreasing the observable differences between the gel types, as it is a relatively high concentration. Increasing the concentration of gelatin does in turn increase the density of the gelatin matrix, which has been shown via the use of electron microscopes, like R. Moučka et al. have done for bovine gelatin.⁴⁷ The images clearly show a significant decrease in the pore sizes

as the gelatin concentration increases, with a large amount of pores appearing to be around $1 \mu\text{m}$ in diameter even at a 10 % concentration. Considering the fact that the properties of bovine and porcine gelatin are near identical, the pore sizes being small enough to contain the particles in an 18 w% gel appears reasonable. Despite cold-water fish gelatin creating weaker gels, the high concentration likely played a role in making the matrix dense enough to confine the particles. The pore sizes being larger seems probable, however the concentration might have helped make them small enough to contain the particles. If the concentration was lowered, it would be reasonable to assume that the observed differences might have been higher as well. Seeing as the particles used in this experiment were relatively large at $1 \mu\text{m}$, it could be that they were too large to observe any difference. If smaller particles were used, it might have been possible to observe a larger difference between the two gel types. Taking both smaller particles and a lower concentration would then make it even more probable to observe differences, making it easier to distinguish the two gelatin types in regards of their barrier properties. Regardless of this, the data suggests that for particles of $1 \mu\text{m}$ or higher there is little difference between the barrier properties of porcine and cold-water fish gelatin at 5°C .

After both the porcine and cold-water fish gelatin were separately tested, a mixture of equal parts of both types was created for the purpose of seeing how the mixture behaves under similar conditions. The mixture was created by adding equal volumetric parts of the dissolved gelatins, utilizing the same solutions which were used to create the samples previously tested, which was done to help eliminate possible differences that might occur during the weighing and dissolving of the gelatin. After this mixture was created, the sample was prepared utilizing the same procedure as for the other samples. The drift corrected MSD curves found for the particles in the mixture are presented in Figure 20, which appear highly similar to the curves found for the pure gelatins.

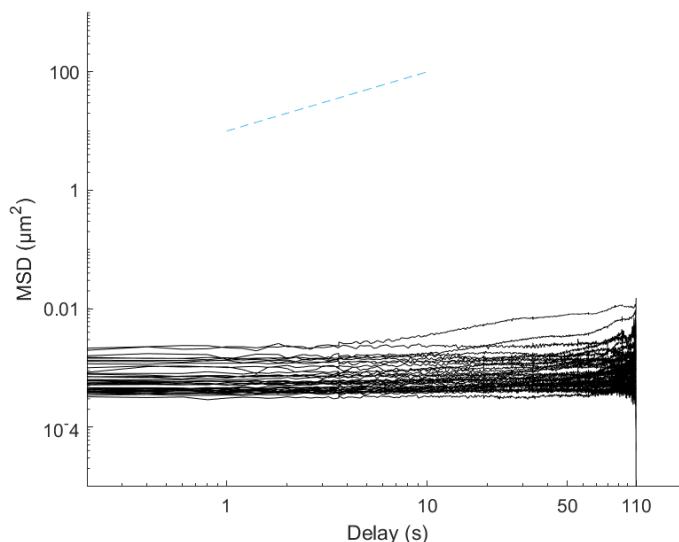


Figure 20: Drift corrected Mean Squared Displacement curves for mixtures of equal part porcine and cold-water fish gelatin 5°C , tracking a total of 40 individual particles for 110 seconds. A linear reference line with a slope of 1 is included at the top of the figure.

Considering the fact that the MSD curves for porcine and cold-water fish gelatin were highly similar, it seems reasonable that the mixture would have similar curves as well. Whether the gels created a mixed system or not is not possible to say in this case, as even if they were separate, it would be difficult to distinguish between particles found in the porcine regions to the ones in the cold-water fish regions. This means that that it is difficult to draw any conclusions from this data in regards to how the gelatin types interact other than the fact that they do not seem to react in a way that noticeably increases the pore sizes in their respective matrices. In other words, they gelatin types do not appear to interact in a way that disrupts or hinders the creation of their gel matrices. At the very least, the gelatin matrix in the mixture seems to be comparable to the matrices found in the pure gelatins. Plotting the MSD values against the slopes α like what was

done for the other samples also helps to illustrate the similarities, and this is shown in Figure 22. The distribution appears to resemble what was found for the porcine and cold-water fish gelatin, with a majority of the curves having an α between 0 and 0.1. The MSD values also seem to be similar, with most particles having a $\log(\text{MSD})$ value between -6 and -8. There are clearly outliers in regards to both axes, however they appear to be similar to the ones found for the other samples as well, being no more noticeably prevalent or significant. The most notable difference from the pure samples is that the particles appear to be more concentrated at lower MSD-values. While the distribution in both cold-water fish gelatin and porcine gelatin appeared to be relatively even, the mixture seems to show a higher density at MSD values below -7. This would seem to indicate that the particles on average are more tightly confined than for the pure samples, having less space to move around in. It is difficult to say what might have caused this difference, as it could simply be random. Considering the fact that the amount of particles as well as the focus on the particles varied between measurements, it is not unlikely that the distribution might have been caused by chance. It could for example be that the focus was kept more even between measurements in the mixture, thus creating less of a variation due to this. It could also be caused by which particles were tracked, as it could be that the particles that were tracked in the mixture just happened to be the ones that were most confined. Another possibility could also be that there was less disturbance and drift occurring during the measurements in the mixtures, however this is difficult to say. Looking at some of the tracks found for the mixture, which are shown in Figure 21, this does not appear to be the case.

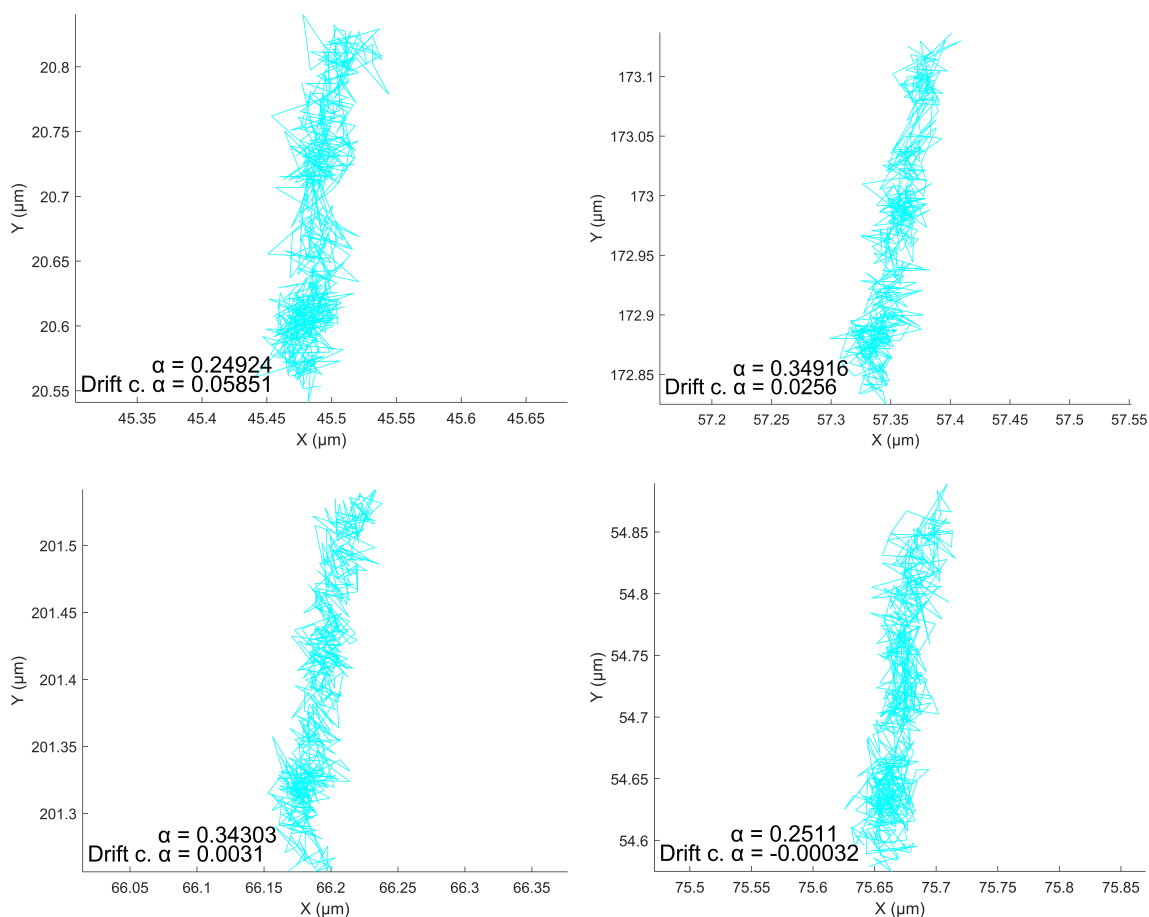


Figure 21: Four of the tracks found for 1 micron particles in in a mixture of equal parts porcine and cold-water fish gelatin with an 18 w% total concentration. Tracking was performed at 5 °C for 110 seconds.

While the tracks are seemingly shorter than the ones found in cold-water fish gelatin which are shown in Figure 14, they do not appear significantly shorter than the tracks found in porcine gelatin, shown in Figure 19. They appear to be somewhat shorter on average, however the difference seems to be minimal. Given that drift is suspected to play a large role in the length of the tracks, this difference in length is not of major concern. While the argument can be made that there was less drift, the minimal difference between the porcine gelatin and the mixture in terms of the length and shape of their tracks suggests it is not a major factor regardless. Seeing as the way that the gelatin types interact during gelling is still highly unknown, there is a small possibility that something might have occurred during the gelling process to create a more dense matrix. This does however not seem likely when taking in consideration previous findings in similar mixtures using fluorescence recovery after photobleaching (FRAP). What is seen when measuring the diffusion in mixtures of porcine and cold-water fish gelatin is that they generally have a higher diffusion coefficient than a pure porcine gel of the same concentration.³⁷ This suggests that substituting a part of the porcine gelatin with cold-water fish gelatin increases the ability for molecules to move within the matrix, in turn suggesting that the matrix is then less dense. Taking in account the fact that the gelatin types on their own behaved extremely similar to one another in terms of confining the particles as well, it seems unlikely that the mixture would somehow constrict the particles more than either of the pure samples.

It is also worth noting that the gelatin types are made from the same amino acids, just at varying compositions. Both types gel in the same way, that being by the creation of junction zones between amino acid chains, with hydroxyproline in particular being a major driving force for the creation of the junction zones. If both gel in the same way and have the same amino acids, it does not seem likely that mixing them would increase the matrix density. If both types of gelatin form gels that are comparable to one another, then mixing should in theory lead to a product similar to the pure gelatin types unless there is some unknown interaction between their chains. Even if they do create a completely mixed system with both gel types fully mixed together without any separate regions, this should in theory not lead to a more dense matrix so long as the junction zones are still formed in the same way.

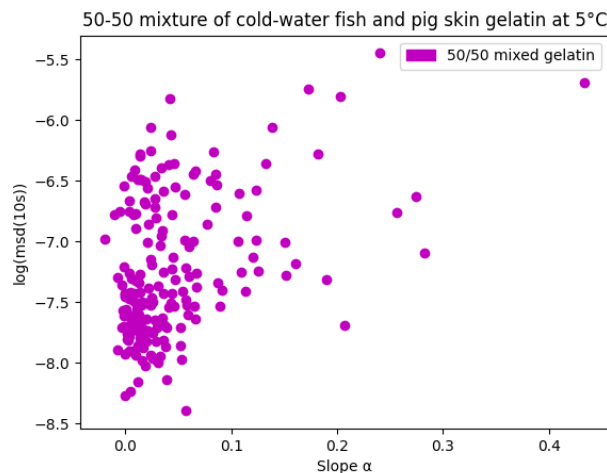


Figure 22: Slope α plotted against $\log(\text{MSD})$ for all tracked particles in a mixture of equal parts cold-water fish gelatin and porcine gelatin at 5°C .

To further show the similarity between all three samples, their α -values are all plotted together against their respective $\log(\text{MSD})$ values after 11 seconds in Figure 23. This figure combines the previously shown plots for each separate sample together, showing how similar their results were. The majority of the particles in each sample all appear to concentrate around the same area in regards to both axes. Like previously discussed, this shows how similar the results were to one another. There does not appear to be any major differences between the three samples in terms of how the particles were confined, which was in part expected due to the temperature being at 5°C .

This cold temperature coupled with the long gelling time allowed for both gel types to form rigid matrices, in turn making them both able to effectively confine the $1\ \mu\text{m}$ particles. Other than some minor differences which have been thoroughly explored already, it is clear that the behaviour in this specific case is highly similar between all samples. Considering the fact that both pure samples were shown to give similar results, the mixture doing the same also seems reasonable. While these results were somewhat expected, they serve as a control and comparison for the behaviour at higher temperatures.

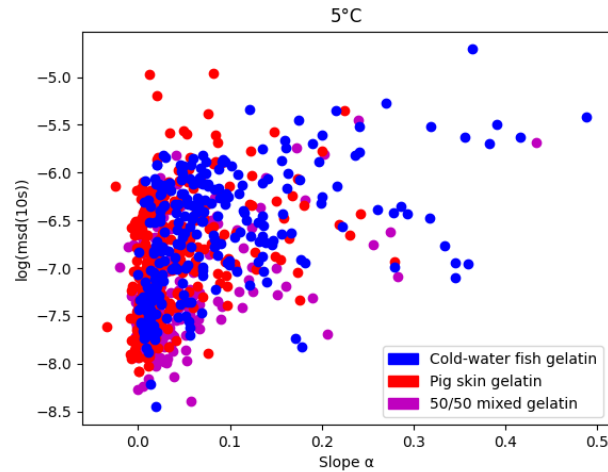


Figure 23: Slope α plotted against $\log(\text{MSD})$ for all tracked particles in porcine gelatin, cold-water fish gelatin and a mixture of equal parts cold-water fish gelatin and porcine gelatin at 5°C .

At 5°C the cold-water fish gelatin was expected to remain as a rigid gel, however at temperatures above 8°C it should in theory melt.²¹ For this reason, all of the samples were also tested at a temperature of 20°C . This temperature was selected as it would in theory be more than high enough to cause a melting of the cold-water fish gel, while still allowing for the porcine gel to remain solid due to it having a melting temperature around 33°C .²¹ All procedures and protocols were followed in the same way as for 5°C , utilizing the same samples as well to eliminate as many potential error sources as possible. This means that while the sample remained the exact same between temperatures, it also meant that any errors such as scratches on the objective glass or clumping of the gelatin or particles would also be carried over. It is difficult to say if any errors like this significantly effected results, however given the fact that the results at 5°C seemed to lie in line with expectations, it does not appear to be the case. The MSD curves for the first parallel in each sample are presented in Figure 24, which shows MSD curves that appear to be highly similar to those observed at 5°C for the mixed and porcine gels.

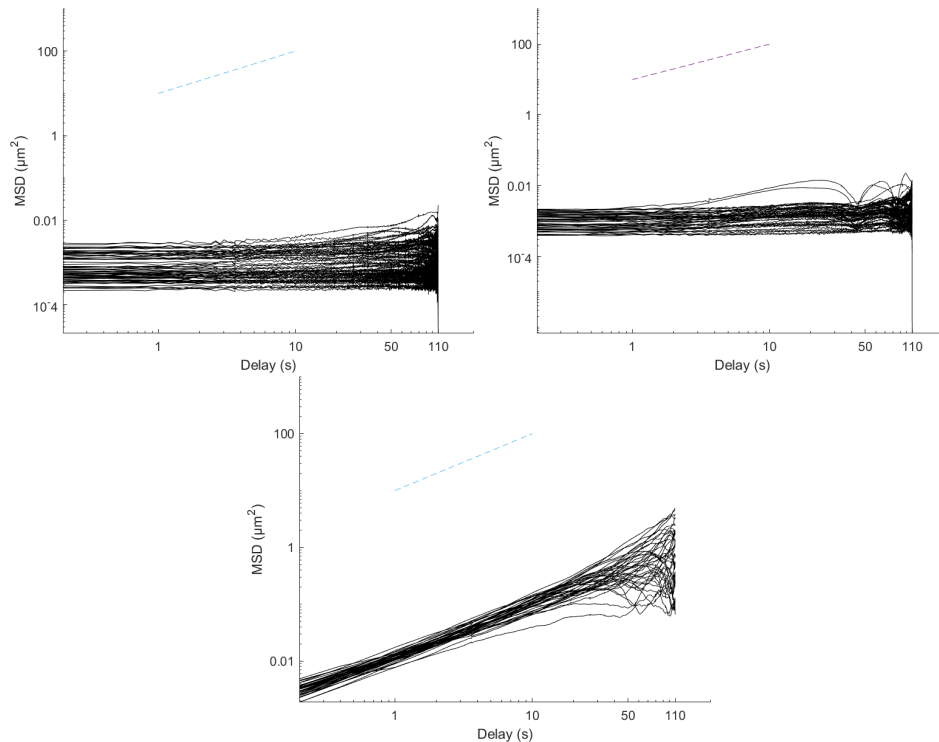


Figure 24: Drift corrected MSD curves for pure porcine gelatin (top left), a 50-50 mixture between porcine and cold-water fish gelatin (top right), and pure cold-water fish gelatin. All MSD curves were obtained at 20 °C.

The sample containing pure cold-water fish gelatin, which is shown on the bottom, has a significantly different curve compared to what was observed at 5 °C. It appears to linearly increase, and comparing it to the reference line at the top of the figure seems to indicate that the slope is close to 1. This would suggest that the gel had melted, thus allowing the particles to exhibit Brownian motion instead of confined motion like what is seen in the other gels. This lies in line with expectations, as cold-water fish gelatin should melt above approximately 8 °C like previously mentioned. Given the fact that all curves appear to follow the same linear trend, it suggests that the gel had enough time to completely melt before the measurement was taken. The MSD curves found for the porcine gel, which is shown on the left hand side of the figure, appear to be largely similar to the ones found at the lower temperature. They still seem to be largely flat, and with MSD values comparable to those seen at the lower temperature. This would indicate that the gel did not melt or get significantly altered by the increase temperature, which was expected due to the higher melting temperature. These two plots neatly illustrate the two possible extremes that could happen in such systems. The porcine gelatin shows the MSD curves for particles that are completely confined in a matrix, while the cold-water fish gelatin shows the MSD curves for particles that are allowed to move freely without any restriction. This then leaves the mixed system containing equal parts of both gelatin types, which appears to still show results that are highly similar to those in pure porcine gelatin. Despite the mixture containing 50% cold-water fish gelatin, there is no indication that any melting occurred judging by the curves, nor that there was any increased separation in the observed behaviour for the particles. They still appear to behave similar to what was observed at 5 °C, and to what is observed for porcine gelatin as well.

To examine the differences further, the MSD values after 11 seconds for all particles were plotted against their respective slope values α in Figure 25. The figure shows the resulting points for all three samples, and all 5 repetitions. As could be seen from the MSD curves, there is a clear separation between the porcine and cold-water fish gelatin at 20 °C. The distribution in the porcine gelatin appears to be nearly identical to the one observed at 5 °C in regards to both axes. The majority of the points are still concentrated between $\log(\text{MSD})$ values of -6 and -8, and between α values of 0 and 0.2.

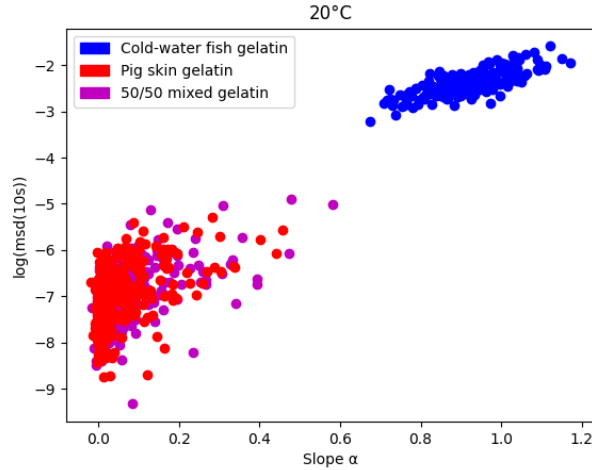


Figure 25: Slope α plotted against $\log(\text{MSD})$ for all tracked particles in porcine gelatin, cold-water fish gelatin and a mixture of equal parts cold-water fish gelatin and porcine gelatin at 20°C.

The particles seem to have a slightly higher average α compared to those seen in Figure 23 for porcine gelatin, though the difference appears to be relatively small. The reason for the slight increase could simply be due to increased drift or less effective drift correction, however there is a chance that the difference is also a result of some weaker bonds in the matrix disappearing due to the increased temperature. It is difficult to say what causes the increase, though considering how large the difference is between the particles in the porcine and cold-water fish gelatin, it is not a significant issue. The main reason for the analysis of the pure samples was to establish a framework to which the mixed samples could be compared, so as long as the difference between them is clear, it should not affect the end conclusion.

Interestingly, the distribution in the cold-water fish gelatin is much more flat than what is seen at lower temperatures, which is likely a result of the lack of restriction. The distribution along the y-axis is in large part due to the size of the area in which the particles are contained, and so when the particles are given less restrictions, it makes sense that this distribution would flatten out. As the particles are defined by Brownian motion, their MSD values are simply a result of their random movement through the sample, which should be similar for all particles so long as there is no facilitated movement taking place. At the same time it is also clear that their MSD values are much higher, which is a result of there being no matrix to restrict how far they can move, thus making it so that they can move further from their reference position. The particles also appear to have a larger, and more even spread in terms of their slopes α . While they appear to be centred close to 1 on average, most of the particles lay either above or below this value. The particles with lower values could be caused by several different factors, though it might also be random. There is a possibility that the particles may have collided with something, or even one another, which could have caused the particles to bounce back towards the direction which they came from. There was also still a significant amount of dissolved gelatin in the sample which may have slowed down or hindered the particles to some extent. Another plausible explanation would be the drift correction causing some errors, which would also help to explain the curves which have slopes higher than 1. Like discussed in a previous section, a slope of 1 is highly unlikely given the conditions. There is no reason to believe that there would be any sort of active transport occurring for the particles, and so it is likely that the spread in α values is caused by some issues during the data analysis. It is also worth noting that Brownian motion giving a slope equal to 1 is a statistical average, not a strict rule.

The drift correction does give better results than the raw MSD curves, however there is no way to guarantee that it perfectly removes any and all drift from the tracks, nor that it does not remove some part of the track which is not caused by drift. This means that while the drift correction

might give more accurate results, it is unlikely that the results are perfect given the limitations. The motion of the particles is something that is highly random and hard to predict, and with so many particles there is a real chance that some of their motion might have been marked as drift by the software, or that their random motion may have masked drift in certain regions. While it is difficult to say how good or bad the drift correction worked in each scenario, it is likely that some part of the spread and the outliers are caused by the limitations of the drift correction code.

Regardless of the large spread along the x-axis, the data seems to be highly concentrated in a single area. More importantly, the data seems to be consistent between parallels, and clearly distinguishable from the data for pure porcine gelatin. Looking at Figure 25 once more, what is interesting is that the data points for the mixed gel seem to correspond to the ones in the pure porcine gel. While there does seem to be a slightly larger portion of outliers which could be the result of many different factors like previously discussed, the most important thing to note is that the behaviour seems to be highly shifted towards the porcine gelatin. Despite cold-water fish gelatin making up half of the total gelatin content in the sample, the results do not reflect this. In regards to confining 1 μm particles, it seems that there is no distinguishable difference between the pure porcine gel and the mixed gel. At the same time there also does not seem to be any separation in the data like what would be expected if the two different gelatin types experienced phase separation. In other words, it does not seem that the gels separate, but rather that they bind together to create a combined matrix. If there was phase separation, there should also have been more of a spread or split in the data points found in the mixed system. If the gel did contain regions rich in cold-water fish gelatin, it would be expected that at least some particles in the mixed gel would exhibit behaviour closer to what is seen in pure cold-water fish gelatin. This would in turn be highly visible in the MSD data considering just how different the data from porcine gelatin and cold-water fish gelatin looks.

To help strengthen the notion that there was no phase separation, this data can be compared to what was found by Lester C. Geonzon et al, where they utilised particle tracking in mixtures of κ -carrageenan and λ -carrageenan.²⁹ What they found is that the samples containing the pure carrageenan types gave distinctive regions much like what was seen for the gelatin types when plotting them in the same way. For pure κ -carrageenan the points are concentrated in a narrow spot between 0 and 0.2 on the x-axis, with a larger spread across the y-axis just like the porcine gelatin. The λ -carrageenan on the other hand gave points that concentrated close to 1 on the x-axis, with a relatively flat and wide spread just like what is seen for cold-water fish gelatin. While it is important to note that the carrageenan was tested at 5 °C, it is interesting to see just how similar their behavior is to the gelatin types. The major difference between the gelatin and the carrageenan seems to come when they are mixed, as the carrageenan types seem to show phase separation. This can be seen by the way the points distribute in the mixtures, as they seem to spread out between the two regions where the points for the pure samples concentrated. Rather than exhibiting behaviour more similar to one type of carrageenan, the system seems to behave like both at the same time, hence why they suspect the phase separation. The mixed gelatin types do not show any behaviour like this, rather expressing an even, singular behaviour which is close to that of pure porcine gelatin. Due to this, it seems highly unlikely that there was any phase separation that occurred.

These results seem to show that it is possible to substitute as much as 50% of mammalian gelatin in a sample with cold-water fish gelatin without significantly affecting the diffusion properties. It cannot be said for certain if this would be the case for smaller particles as well, but it does seem to be the case for particles that are at least 1 μm in diameter. What this means is that despite cold-water fish gelatin being unable to gel and form a matrix at room temperature alone, it seems to be able to form a matrix when it is mixed with a mammalian gelatin. It does not appear to just get trapped by the gel matrix formed by the mammalian gelatin, but rather it seems to actively provide additional strength to the gel. If it simply got bound to the mammalian gelatin matrix without providing any strength, it would likely have been more visible in the particle tracking data, as the matrix would in that case be significantly less dense. While this cannot be said for certain, the fact that the particle tracking data for the mixture is almost identical to the data for pure porcine gelatin seems to point towards the cold-water fish gelatin actively strengthening the gel.

3.1.2 Particle tracking conducted at the Norwegian University of Science and Technology

Due to the limited stay at the Tokyo University of Marine Science and Technology, only the mixture containing a total of 50% each of both porcine and cold-water fish gelatin was tested apart from the pure gels of both types. Due to the results previously discussed however, a further testing of mixed gels was desirable. The main purpose of further testing was to see if lower fractions of mammalian gelatin would provide similar results, mainly a behaviour that is closer to that of pure porcine gelatin than to cold-water fish gelatin. The idea was to see if a mixture containing only 10% porcine gelatin would give similar results, with the other 90% of the sample being cold-water fish gelatin. The issue with this idea was that all previous measurements would have to be repeated as well, due to the fact that different equipment would have to be used to capture images of the gels.

For the image capturing, a new microscope setup was used. To keep results as consistent as possible, a mercury lamp was utilised to illuminate the sample in the new setup as well, using a 40x zoom lens to keep the level of magnification the same too. The largest difference between the two microscope setups was the resolution of the resulting images, as the images captured using the new microscope were 2752 x 2208 pixels compared to 1360 x 1024 pixels in the other setup. This meant that the new images would have over 4 times as many pixels as the older ones, allowing for a higher level of precision when tracking the movement of the particles. This increased precision became clear when plotting the MSD curves. An example of the MSD curves found for pure porcine gelatin is shown in Figure 26, where the drift corrected curves are shown on the right hand side of the figure.

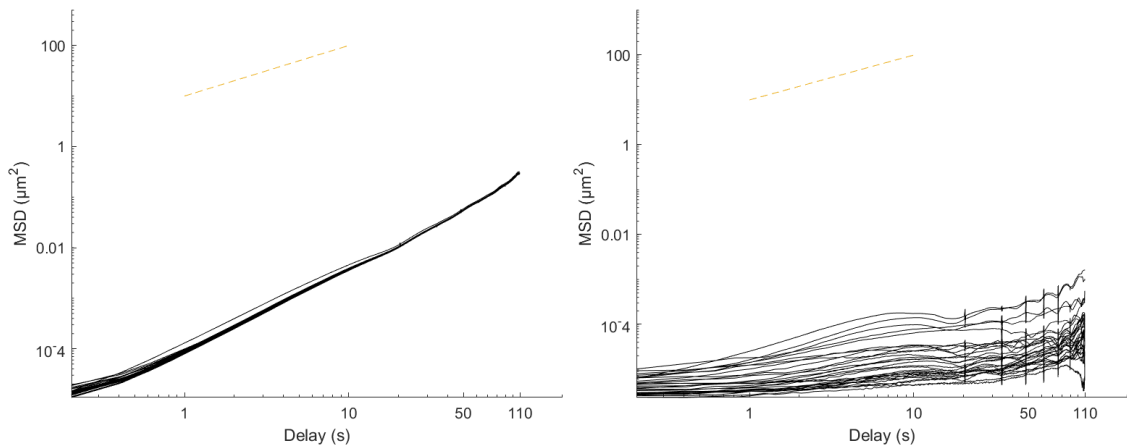


Figure 26: MSD curves for particles tracked in an 18 w% solution of porcine gelatin at room temperature. The solution was allowed to gel for 20 hours at 5 °C before analysis. The curves on the left side represent the raw MSD curves, with the drift corrected curves shown on the right.

When comparing these to the curves obtained using the other microscope setup at 20 °C, presented in Figure 24, it is clear that the starting MSD is significantly lower in the new curves. While the exact reason for this difference is not known, it would seem likely that it is a result of the increased pixel density in the images. The MSD which the line starts at is the first measured MSD value, meaning the distance that the particle travelled from the original position. In other words, it is the distance that the particle moved between the first two captured images, where the first image gives the original positions for each particle. Due to this, an increased resolution would likely have some effect on the starting MSD, as the tracking is then able to more accurately depict the finer movements of the particle. While this does seem beneficial, it does also open the analysis up to being more susceptible to disturbances and drift.

Looking at the drift corrected MSD curves presented in Figure 26 they do seem to curve upwards more than what was observed in the ones seen in Figure 24, but at the same time they also have

significantly lower MSD values on average. This means that while the MSD does increase more significantly relative to the starting value, the overall displacement is generally much lower for the measurements in the new setup. In other words, the particles appear to move less relative to the starting position for the older results, even though they move significantly less in the newer measurements. This is likely in large part due to the increased resolution that was previously mentioned, which does make the tracking more accurate. The issues with these results is largely that the slope α is based on the relative change in MSD, thus meaning that the increased noise in the MSD curves affects the obtained slope significantly. Due to the curves having such low MSD values, any disturbance or uncertainty is amplified significantly, meaning they will affect the end result to a higher degree. This is likely part of the reason why the MSD curves appear to be more noisy and uneven, as the drift and tracking issues are further amplified when compared to the previous measurements. Despite this, the curves do appear to remain relatively similar in shape, and with a slope that is clearly lower than the reference line at the top of the figure for the most part. Similar results were seen for further repetitions as well, which are presented in Appendix A. Looking at the raw MSD data which is presented at the left hand side of Figure 26 also helps to illustrate how significant the drift was. All the curves appear highly similar, and with a steep slope. This is a solid indication that there is significant drift happening, as the individual behaviour of each particle is almost completely overshadowed by the drift, which is what is likely causing them to be so similar. Comparing them to the raw MSD values for the previous measurements in porcine gelatin, such as those shown in Figure 27, it is clear that the amount of drift is not particularly higher than what was seen previously, however the impact likely is. It is also worth noting here that the code used for performing the particle tracking and MSD analysis was created and tested using data obtained at TUMSAT, meaning that it might simply not work as well with this new setup.

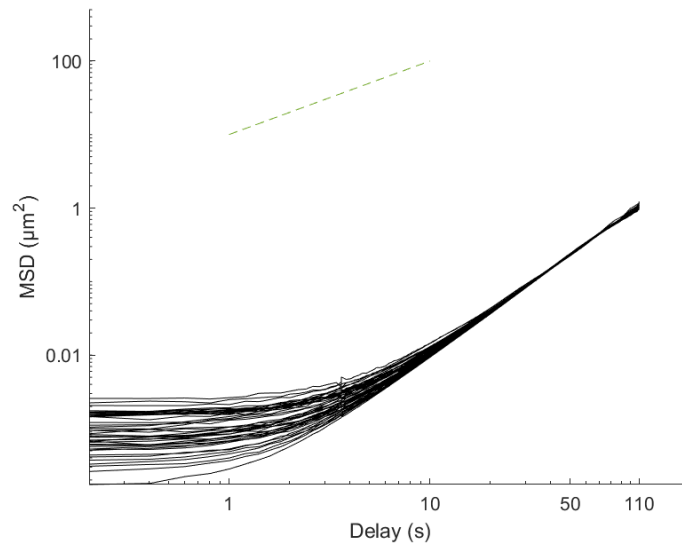


Figure 27: Mean Squared Displacement curve for porcine gelatin at 20°C, tracking a total of 46 individual particles for 110 seconds. A linear reference line with a slope of 1 is included at the top of the figure.

For the measurements shown in that figure it is clear that they experience a high level of drift, ending up with a higher MSD at the end than for the new measurements. Despite this, the curves still appear to be more distinguishable and flat early on, something that cannot be said for the newer measurements. The curves obtained from the newer measurements appear almost completely linear at the start, which is likely in large part due to the amount of drift relative to the low starting point. The fact that the curves start so low means that the drift does affect the initial slope of the curve more significantly, which is likely what is seen in this case. When these curves are then corrected for drift, the software will likely still do a similar job, however all of the flaws and imperfections are far more noticeable due to the non-drift related motion being much lower. In other words when the particles show more movement outside of the drift, it is

easier for the software to distinguish and isolate this movement from the drift. While it is also highly likely that other factors discussed previously, such as the particles falling out of focus, or the intensity cut-off causing some particles to "flicker" between images, it seems more likely that the increased resolution plays a large role in creating the more noticeable differences seen between the curves in Figure 26. Similar curves were also seen for mixtures containing 50% each of porcine and cold-water fish gelatin, as shown in Figure 28, where the raw MSD curves are shown on the left, and the drift corrected curves are shown to the right.

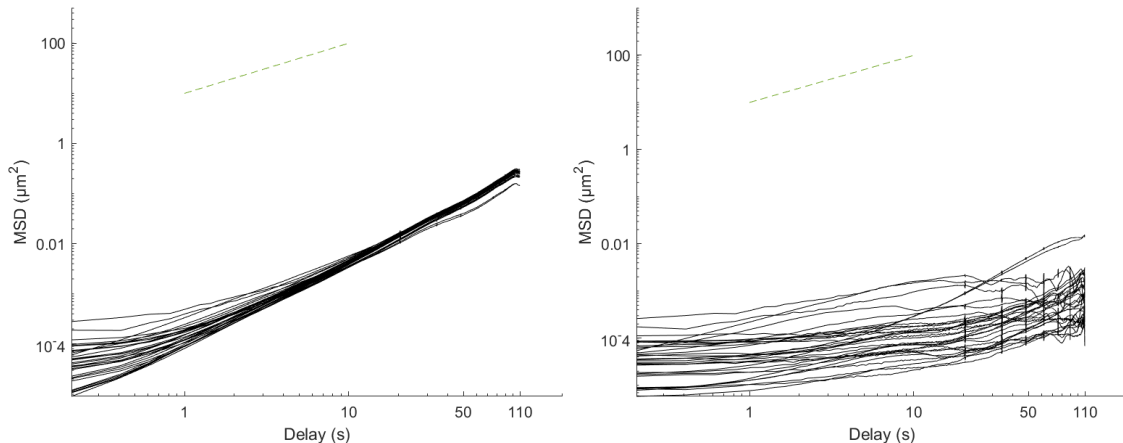


Figure 28: MSD curves for particles tracked in a mixture of equal parts porcine and cold-water fish gelatin with a total gelatin concentration of 18 w%, measured at room temperature. The solution was allowed to gel for 20 hours at 5 °C before analysis. The curves on the left side represent the raw MSD curves, with the drift corrected curves shown on the right.

Interestingly there does seem to be a larger spread in the starting MSD, which could be caused by various different factors such as an increased size of the confined areas due to addition of cold-water fish gelatin, which would allow particles to move more. It is also possible that the differences are caused by issues in the tracking as well, something that has been thoroughly explored in the previous section. The most interesting thing about these curves is that they neatly illustrate how large of a difference the starting position of the curve makes. It is clear that the particles experience similar drift, as can be seen by how the curves all assimilate for later time points, however the curves that start higher have a noticeably more flat shape at the start. This does help to show how large of an impact the starting MSD makes on the overall shape of the curve. Regardless of this, the drift corrected curves appear to be similarly noisy and variable in shape. To help illustrate the variation between curves, all slopes α for both the mixture and the pure porcine gelatin are plotted against their $\log(\text{MSD})$ values at 11 seconds, which is shown in Figure 29. It is clear that the variation in their slopes is significantly higher than for the previous measurements, which can be seen in Figure 25.

While the previous measurements gave α values between 0 and 0.2 for the most part, the newer measurements show a spread over the entire area between 0 and 1. This does suggest that the new data is of a lower certainty, as there is no clear reason why the variation should be that much higher. Given the fact that the gelling conditions and time was kept the same for the new samples, it is highly unlikely that the larger spread comes from a significant difference in the gel matrix, particularly considering that the porcine gelatin should not be melting at room temperature. The porcine gelatin used in both cases also came from the same provider, meaning that there should have been minimal difference in their properties. While the spread along the x-axis is significantly higher, the spread along the y-axis seems to be relatively comparable in size. The major difference in the $\log(\text{MSD})$ values as compared to the previous measurements is their value, as the new data shows a lower overall $\log(\text{MSD})$ for most points. This is likely due to what has been discussed previously, mainly that the increased resolution caused a more accurate and fine tracking, causing

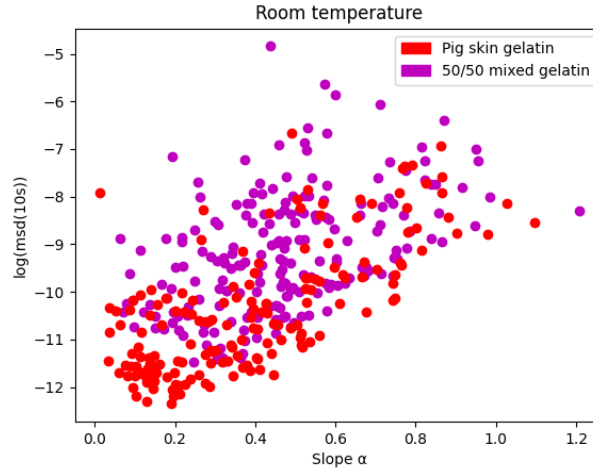


Figure 29: The slope α plotted against the $\log(\text{MSD})$ values for all tracked particles in porcine gelatin and a mixture of equal parts cold-water fish gelatin and porcine gelatin. The figure consists of data compiled from 5 separate measurements in each sample. The measurements were conducted at room temperature.

a generally lower amount of observed displacement. While the results are not ideal or comparable to the previous measurements, they do appear to give relatively similar spreads for both the mixed gelatin and the porcine gelatin, which is what would be expected given what has been seen previously.

Due to the fact that the code used to analyse the data was created and optimised for the system used at TUMSAT, it is important to be careful when interpreting the results. Given the large and even spread seen in Figure 29, it is therefore difficult to draw conclusions from it. What can be said is that the particles clearly appear to be quite highly constricted given how low many of the α -values are, and that the total mobility, seen on the y-axis, remains low across all measurements both for these results, and the ones obtained at TUMSAT. While these new results are relatively noisy, they still might be able to give some good information on the behaviour relative to pure cold-water fish gelatin. Looking at the MSD curves for cold-water fish gelatin shown in Figure 30, it would seem that they are significantly less affected by the drift. This can be seen by the fact that there appears to be nearly no visual difference between the raw and drift corrected curves, which would indicate that the Brownian motion is masking the drift, as there is no reason to believe that the drift would not be present.

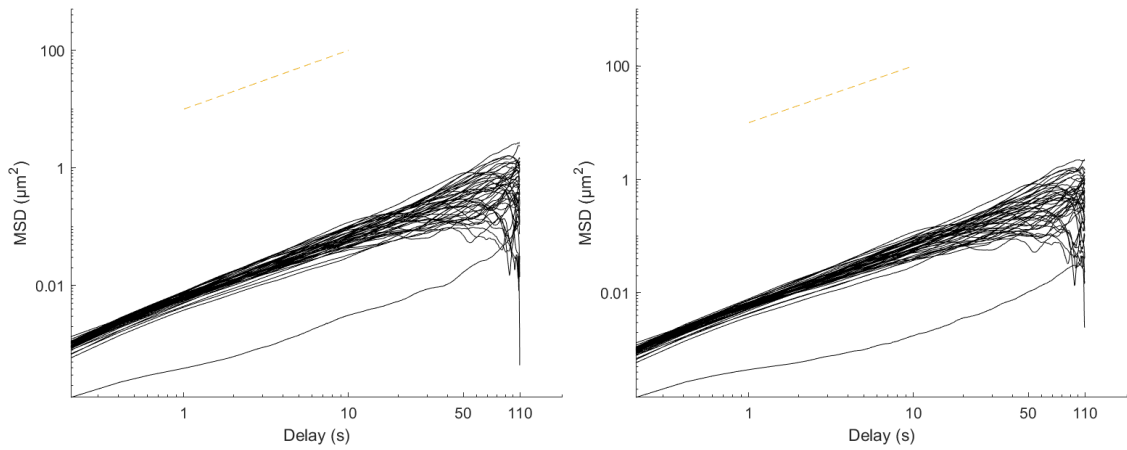


Figure 30: MSD curves for particles tracked in an 18 w% solution of cold-water fish gelatin at room temperature. The solution was allowed to gel for 20 hours at 5 °C before analysis. The curves on the left side represent the raw MSD curves, with the drift corrected curves shown on the right.

While there is a chance that there was less drift occurring during these measurements, the fact that there seems to be nearly none would suggest that there is some masking going on. While it is not possible to say what exactly caused the masking, one possible explanation could be that the increased mobility of the particle simply caused the drift to be less noticeable. As the observed particle is moving freely instead of in a confined space, it will naturally give a higher MSD on average, which would cause any drift to be less noticeable. Simply put, the drift could be less noticeable due to the fact that it is significantly smaller relative to the motion of the particle when compared to the particles in the other samples. Looking at the curves, they also seem to have a slope that is close to 1, which is what would be expected for the sample given that cold-water fish gelatin should melt at room temperature. So while the lower amount of drift does appear to be strange, the results themselves seem to lay in line with expectations. Plotting their slopes α against their $\log(\text{MSD})$ values helps to further illustrate this, which is shown in Figure 31 together with the values for the other two samples as well.

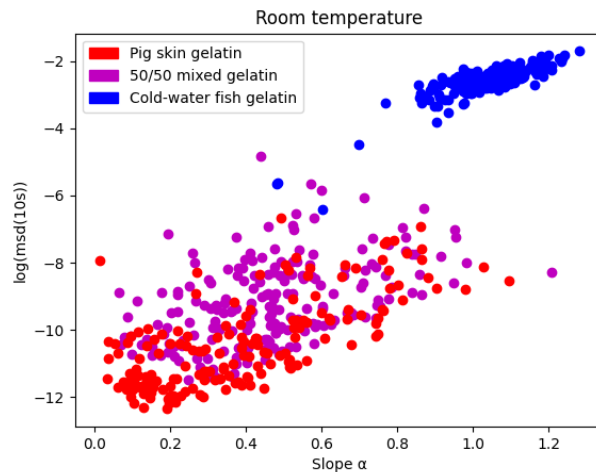


Figure 31: Slope α plotted against $\log(\text{MSD})$ for all tracked particles in porcine gelatin, cold-water fish gelatin and a mixture of equal parts cold-water fish gelatin and porcine gelatin. The figure consists of data compiled from 5 separate measurements in each sample. The measurements were conducted at room temperature.

Looking at these, it becomes increasingly clear that the results obtained for pure cold-water fish gelatin are highly similar to the ones found previously, as seen in Figure 25. Both the shape and spread of the values appears to be highly similar for both, with the only significant difference being that the new values appear to be slightly shifted towards a higher α . While this is not ideal, the shift appears to be relatively small, and is likely not indicative of any facilitated motion. In theory all points should have an α close to 1 in the case of a fully liquid system, however this is only a theoretical ideal. In reality there are far too many factors affecting the particles for them to all give the exact same curves, thus a spread is to be expected. The size and shape of the spread highly depends on the accuracy of the measurements. While a slope higher than 1 is indicative of some sort of facilitated motion, the fact that they are so close to 1 does suggest that it is more than likely a result of either analytical errors or drift, which has already been thoroughly explored. As stated in the previous section, the fact that a portion of the points have an α higher than 1 is not a big issue, as the main point with the plot is to see the difference between the porcine and cold-water fish gels, which is still present. Despite the significant increase in the spread for the porcine gelatin results, it is still clearly distinguishable from the cold-water fish gelatin. On top of this, the fact that the 50-50 mixture also shows the a similar spread as the porcine gelatin only further illustrates that the results are sufficiently accurate enough to show whether the behaviour of a gel is closer to porcine or cold-water fish gelatin. Despite the clearly lower quality of the results, they should therefore be able to show which gelatin dominates in terms of diffusion in a mixture of the two.

While the data presented so far in this section has been a repeat of the data obtained and discussed previously, the reason for the repeat was to have a set of data to compare a new sample to, that being a mixture containing 90 % cold-water fish gelatin and 10 % porcine gelatin. The goal with this was to see if the diffusion properties would still be similar to pure porcine gelatin, even with such a low fraction of it in the mixture. The sample was prepared utilizing the same stock solutions used for the previous samples, and some examples of the obtained MSD curves are presented in Figure 32.

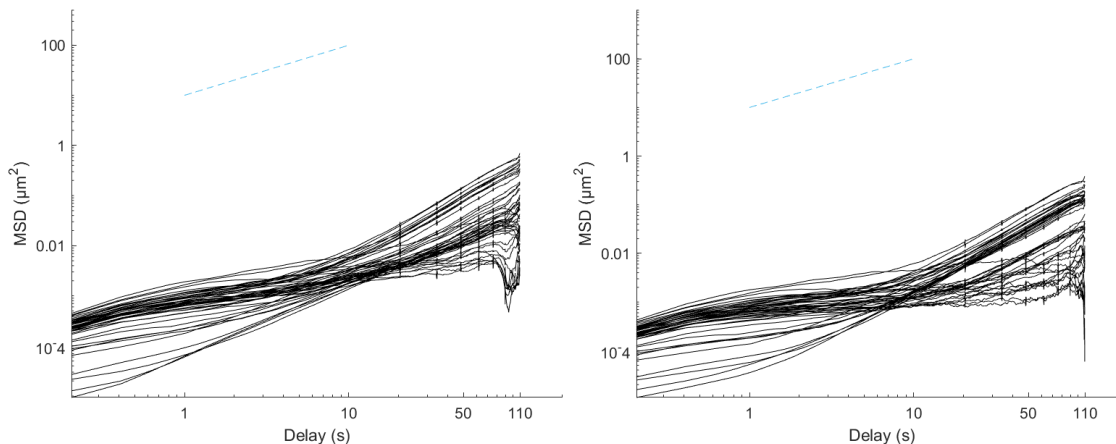


Figure 32: MSD curves for particles tracked in a mixture of 10% porcine and 90% cold-water fish gelatin by weight, with a total gelatin concentration of 18 w%. All measurements were performed at room temperature. The solution was allowed to gel for 20 hours at 5 °C before analysis. The curves on the left side represent the raw MSD curves, with the drift corrected curves shown on the right.

What appears most noticeable about these curves is the apparent difference between the curves. It appears as if a portion of the curves rise at a faster rate, ending with a significantly higher MSD than the other, more flat curves. While this could indicate some variation in the gel matrix, it does not seem likely that the steeper curves are a result of the gel matrix melting. One indication that this is not the case would be the shape of the curves. While some do seem to gain a steep curve after some time, they all appear to be relatively flat at the beginning. As has been seen previously, this is not indicative of a molten gel, where the curve would be significantly more linear. Even the

curves that start lower and seem to be more linear do still have a clear bend to them, indicating that the high slope is more likely to be a result of some analytical error. While the exact reason for the observed rise cannot be explain, it is likely to be a combination of drift and tracking issues. One other possibility could also be issues with the imaging, as it was observed that the image appeared to be slightly distorted near the edges for some of the measurements in these samples. The cause was determined to be that the immersion oil that connected the sample and the lens seemed to dry out, causing the contact surface between the oil and sample plate to shrink. This in turn created some distortions near the edges of the image as the amount of oil gradually decreased. It was first observed before the mixture containing 90% cold-water fish gelatin was tested. While it was corrected before measuring by adding more immersion oil, it does pose a possible source of error for several of the observed outliers seen previously as well. While these reasons are purely speculative, the suspicion of these curves being faulty does increase when comparing them to the curves obtained during the following repetitions. The curves for one of the following repetitions are given in Figure ??, which appear to show a significantly more similar shape between curves. Unlike the curves seen in the other repetition, these do not seem to show any significant split in behaviour. While there is still a seemingly high variation in the starting MSD, they do appear to show a similar shape and slope, and a similar behaviour for higher time values.

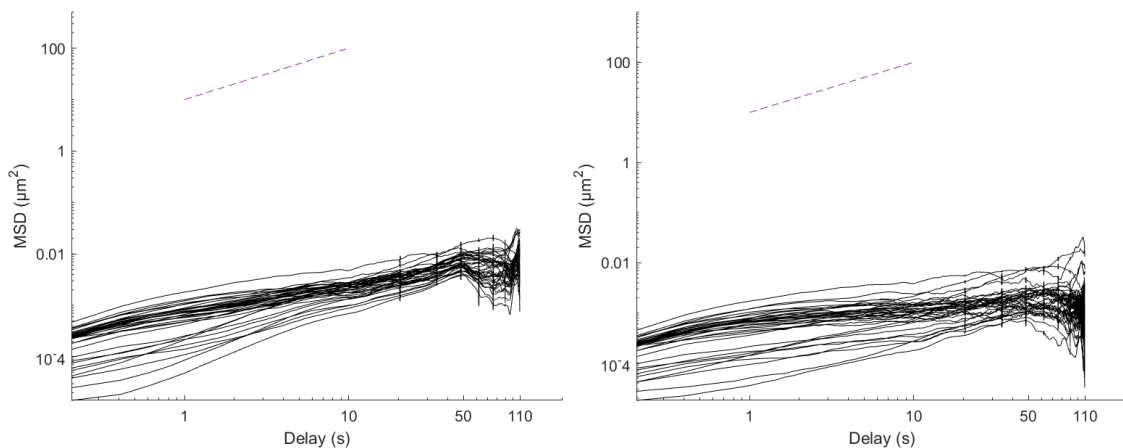


Figure 33: MSD curves for particles tracked in a mixture of 10% porcine and 90% cold-water fish gelatin by weight, with a total gelatin concentration of 18 w%. All measurements were performed at room temperature. The solution was allowed to gel for 20 hours at 5 °C before analysis. The curves on the left side represent the raw MSD curves, with the drift corrected curves shown on the right.

What is interesting to note, as was seen for the other curves as well, is the fact that the starting MSD values seem to be higher than for the samples containing more porcine gelatin. They do also appear to be significantly less noisy, which is likely correlated to the higher starting values, which has been discussed previously. Interestingly they do also appear to be relatively flat in shape, which indicates that the gel behaviour is more closely resembling porcine gelatin than cold-water fish gelatin at room temperature. This is more clearly seen when the slopes α are plotted against their $\log(\text{MSD})$ values together with the data from the other samples which has been shown previously. This is shown in Figure 34, which shows that the mixture consisting of only 10% porcine gelatin, represented by the cyan points, gives results that more closely resembles those seen in pure porcine gelatin. There is an obvious difference between them, mainly that the points appear to be less spread out for the mixture. The most likely explanation for this is that the higher starting MSD values made the noise which was observed in the porcine gelatin less noticeable. It is clear that the MSD values in the mixture containing 10% porcine gelatin are higher on average, more closely resembling the MSD values observed for the data obtained using the other setup at at TUMSAT at 20 °C, which is repeated below in Figure 35. This becomes even more apparent when plotting this data together with the newer data obtained at NTNU, which is done in Figure 36. Here it is clear that the shape and distribution of the data for the mixtures containing 10% porcine gelatin is much more similar to the data obtained at TUMSAT, while the data for the

50% mixture and pure porcine gelatin is significantly different from these. The results for the pure cold-water fish gelatin seem relatively similar for both data sets.

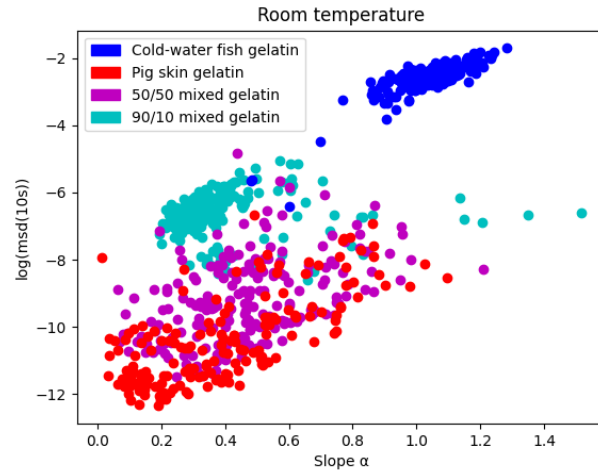


Figure 34: Slope α plotted against $\log(\text{MSD})$ for all tracked particles in porcine gelatin, cold-water fish gelatin and mixtures containing 50% and 10% porcine gelatin mixed with 50% and 90% cold-water fish gelatin, respectively. All samples had a total gelatin concentration of 18 w%. The figure consists of data compiled from 5 separate measurements in each sample. The measurements were conducted at room temperature.

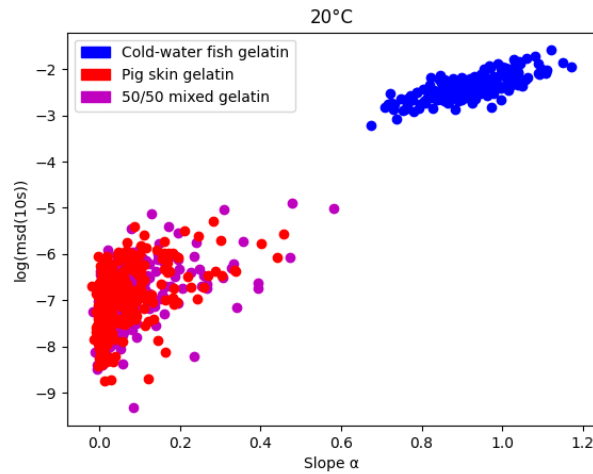


Figure 35: A copy of Figure 25: Slope α plotted against $\log(\text{MSD})$ for all tracked particles in porcine gelatin, cold-water fish gelatin and a mixture of equal parts cold-water fish gelatin and porcine gelatin at 20 °C.

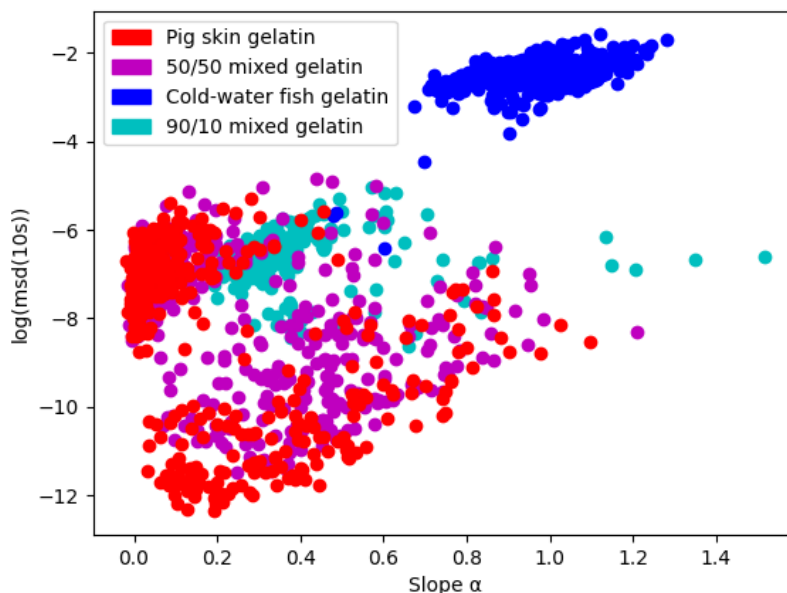


Figure 36: Slope α plotted against $\log(\text{MSD})$ for all measurements preformed at TUMSAT and NTNU. The figure contains data for porcine gelatin, cold-water fish gelatin and mixtures containing 50% and 10% porcine gelatin mixed with 50% and 90% cold-water fish gelatin, respectively.

What is interesting is that this does somewhat seem to confirm the suspicion that the lower MSD values did create more noise in the resulting MSD slopes. Considering the fact that all factors were kept the same across all the analysed samples, there is no clear reason why the spread for the 10% porcine gel mixture should be so much lower in Figure 34 otherwise. If the spread was purely a result of issues with particle tracking, the same kind of spread should also in theory have been seen for this sample. Considering the fact that the samples with MSD values higher than those seen for porcine gelatin in Figure 34 have a significantly smaller spread, it does appear likely that the low MSD values are part of the reason for the increased spread. Moving on, the higher MSD values do indicate that the particles have more room to move around in than for the other samples containing higher concentrations of porcine gelatin. There does almost seem to be a sort of gradient, with the data from the pure porcine gelatin being concentrated at the lower left of the figure, the data from the 50% porcine gelatin mixture being slightly higher and shifted to the right on average, and finally the data for the 10% porcine gelatin sample laying even higher and somewhat more to the right as well. It seems to indicate that the gelatin matrix is growing weaker with the higher amount of cold-water fish gelatin, however the behaviour is still highly different from that of pure cold-water fish gelatin. Even with 90% of the gelatin matrix consisting of cold-water fish gelatin, the behaviour still is remarkably similar to pure porcine gelatin. This would seem to indicate that in terms of particles $1 \mu\text{m}$ in diameter or larger, there is little difference in their ability to diffuse through these matrices. While there does appear to be some differences in the size and density of the matrices judging by the observed MSD values, the diffusion remains highly constricted even for mixtures containing just 10% porcine gelatin.

This is highly interesting, as it does seem to suggest that very little mammalian gelatin is needed to significantly alter the gelling properties, as well as the temperature stability of cold-water fish gelatin. Just 10% mammalian gelatin seems to be enough to make cold-water fish gelatin stable at room temperature, when it normally would melt at just 8°C . While it is difficult to say exactly how stable the mixtures were, the fact that they show the ability to restrict the $1 \mu\text{m}$ particles does indicate that there is at the very least some sort of gelatin matrix present. Looking back at the similar tests preformed in carrageenan mixtures by Lester C. Geonzon et al,²⁹ it also becomes increasingly clear that the gelatin mixtures do create a fully mixed system. If the cold-water fish gelatin did not somehow interact with the porcine gelatin, there is an extremely low possibility that the results would be as uniform as they appear to be, as one would then expect to see more

of a split in the observed behaviour such as what was seen for carrageenan. The fact that adding just 10% mammalian gelatin seems to be able to provide such a drastic difference in behaviour compared to pure cold-water fish gelatin is intriguing, as it could potentially open up for a wider range of use cases for cold-water fish gelatin. Being able to easily stabilise and make cold-water fish gelatin more viable as a gelling agent does appear to be possible with the addition of just a small portion of mammalian gelatin, however there is still a need to further explore other properties of these mixtures to fully determine their viability. The mechanics behind how such a small amount of porcine gelatin is able to induce gelling in the mixtures is also not known, something that could be highly interesting to study to better understand what is going on in these systems. One possible explanation could be that the mammalian gelatin is acting as a sort of crystallisation nucleus for the system, inducing the gelling of the cold-water fish gelatin in that way. While this is purely speculative, it could potentially be something worth investigating.

Seeing as dosing cold-water fish gelatin with just a small part of porcine gelatin can give it desirable properties, it could possibly mean that such mixtures could see commercial use. There are also other possible methods for improving the gelling properties of fish gelatin, such as the addition of gellan which was tested by T. Petcharat et al, which has also shown positive results.⁴⁹ This does reveal that the addition of mammalian gelatin is only one of possibly many methods to potentially make cold-water fish gelatin more usable in the industry, however it does have the unique advantage of its simplicity. If the other properties of these mixtures such as the thermal stability and the gel strength also see similar behaviour to that of the diffusion properties, it could be possible to subsidise parts of existing gelatin products with cold-water fish gelatin without significant drawbacks. If gelatin is the main gelling component of the system, then in theory it could be possible to simply replace a large portion of it with cold-water fish gelatin without drawback. In addition it also could be possible to add cold-water fish gelatin as a way to add gel strength, without necessarily replacing the existing gelatin. The fact that cold-water fish gelatin did appear to most likely provide some strength to the gel when mixed with porcine gelatin, it seems likely that it could be added to a mammalian gel to provide some strength and density to the gel matrix. All of this could mean new potential uses for the enormous amounts of fish waste that is produced by the fishing industry, particularly considering the fact that collagen makes up a large portion of the waste. The ever growing market demand for fish does pose issues in regards to waste, both economically and environmentally. The marine collagen market is already growing significantly, and providing more potential uses for the fish waste via gelatin may help to further this growth.¹⁸ Providing more viable and economically beneficial uses for the fish waste is a potential way to help decrease the amount of waste that is produced, and the use of cold-water fish gelatin as a substituent or even addition to products traditionally containing mammalian gelatin might just be such a use case. While it may not be able to fully replace mammalian gelatin, it can potentially replace a large portion of it, seemingly without many of the issues that would come with using pure cold-water fish gelatin. Instead of importing large amounts of mammalian gelatin, a company may be able to utilise cold-water fish gelatin if the price and shipping costs of it is beneficial, and thus cutting down on the amount of mammalian gelatin which has to be imported. While it is not possible to say if this could be viable, it does pose an opportunity in the cases where it might be. Considering the fact that the fish gelatin market is so small compared to the market for mammalian gelatin could mean that the lower competition and demand could be used as an advantage in terms of both availability and prices.³³

3.2 Release from gelatin in an aqueous environment

To further explore and characterise the diffusion properties of mixtures of cold-water fish gelatin and mammalian gelatin, tests were carried out on these gels utilising a dissolution unit. Instead of measuring dissolution however, the apparatus was used to measure the release of compounds from the gels and to an aqueous phase. While the particle tracking mainly focused on the diffusion within the gelatin matrix, the purpose of these tests was to examine if the diffusion out of the gels would show a similar behaviour. The tests were performed by measuring the release of coloured compounds from the gels to an aqueous phase or solvent, with the concentration of these compounds in the solvent being tested via spectrophotometry. In this case the solvent used was pure water, and the tests were carried out at room temperature. The reason for this choice was mainly to study the rate of diffusion out of the gels while minimising the degradation and dissolving of the matrix, as it was the diffusive properties that were desirable to examine. The water was selected to serve as a solvent as it should in theory not dissolve the gel matrix without heating, thus meaning it acted more as a liquid phase rather than a solvent for the gel. The temperature was also selected for the same purpose, as it should in theory not be sufficient to denature or melt the porcine gelatin. Despite the conditions not being conducive to a dissolution of the gel, it can't be completely ruled out as a factor. This means that while the main source of release seems likely to be diffusion, the release referred to here encompasses both the dissolution and diffusion.

For these tests, tartrazine and blue dextran were chosen due to their significantly different molecular sizes. Tartrazine is a small coloured compound which is commonly used for food colouring, and has a molar mass of just 534.4 g/mol.²⁷ This is in contrast with the blue dextran used, which should have had an average molecular weight of 2 000 000 g/mol, meaning that there is a large gap in size between the two coloured compounds. This in theory would provide differing results as well, as the tartrazine would be expected to diffuse out faster than the blue dextran due to its small size. This is due to the fact that the smaller size would allow it to more easily diffuse through the gel matrix, allowing it to diffuse out into the solvent at a faster rate. Studying the diffusion of both large and small molecules out of the gel matrix would make it possible to see if the behavioural differences between the mixed gels and pure mammalian gels would be different depending on the size of the molecule studied. It is important to note that the blue dextran used in the experiment possibly was somewhat degraded, as it had been sitting unused for several years beforehand. This means that the average molecular weight could have been somewhat lower than what it was stated to be by the provider, though it should still have been significantly larger than the tartrazine. This does mean that the data provided for blue dextran can't without doubt be said to be valid for the given molecular weight of 2 000 000 g/mol, though it should still serve as a representative for molecules of a significantly larger size than tartrazine.

One thing that should also be noted is that the tartrazine and blue dextran were tested in separate gels, the reason for which was that their absorbance wavelengths gave some overlap. This is something that was thoroughly explored in the materials and methods section, the main point being that the two compounds can't be accurately measured via spectrophotometry when mixed. This does pose some potential sources of error, as there is a possibility that there were some variation between the matrices that held the tartrazine and blue dextran. This could potentially have caused some differences in their diffusion behaviour, however given the fact that the gels were created from the same stock solution, there should have been minimal differences between the matrices. The gels were also created at the same time using gelatin moulds of the same size, meaning that the volume of the gel also should have been relatively even across all tests. This means that in terms of the gelatin portion of the gels, there were likely minimal differences, however the major difference between them came from the amounts of blue dextran and tartrazine added. Due to the fact that the absorbance of blue dextran was much lower relative to the concentration when compared to tartrazine, there had to be significantly higher amounts of blue dextran added to provide similar absorbance levels between the two. The amounts added were calculated to provide a maximum possible absorbance close to the highest points on their standard curves, which are shown in Section 2.2.2. The resulting equations representing the standard curves for tartrazine and blue dextran are given in Equation 4 and Equation 5, respectively. The C represents the concentration in the sample, while A represents the absorbance of the sample. The absorbance

wavelengths are given to the right of the equations.

$$C = 24.6322 \frac{\mu\text{g}}{\text{ml}} \cdot A + 0.1106 \frac{\mu\text{g}}{\text{ml}} \quad [\lambda = 425\text{nm}] \quad (4)$$

$$C = 1.1753 \frac{\text{mg}}{\text{ml}} \cdot A + 0.0009 \frac{\text{mg}}{\text{ml}} \quad [\lambda = 620\text{nm}] \quad (5)$$

Using these standard curve equations, it's possible to see that for tartrazine to give an absorbance of 0.9, a concentration of 22.2796 $\mu\text{g}/\text{mol}$ is needed. In comparison, to obtain the same absorbance with blue dextran, a concentration of 1.0587 mg/mol is needed. This means that over 40 times more blue dextran is needed to obtain a similar absorbance, something that could potentially affect the gel. Given the relatively low amount of tartrazine, it seems unlikely that it would have had a significant effect on the resulting gel. While the reactivity between gelatin and tartrazine is unknown, however considering that the tartrazine molecules are highly water soluble at 20-25 $^{\circ}\text{C}$,²⁷ it seems likely that it would be dissolved in the water fraction of the gel. The low amount of tartrazine coupled with the high solubility does then seem to suggest that it likely didn't affect the resulting gel significantly, however the same is more difficult to say for blue dextran. The fact that there was so much blue dextran present in the gel does pose questions as to whether or not that might have affected the formation of the gel matrix, though it is difficult to deny or confirm this. Dextran and gelatin do generally not interact naturally, typically requiring cross-linkers to achieve a mixed network.²⁴ This means that the dextran likely shouldn't interact with the gelatin, though this can't be said for certain. The higher amounts of blue dextran relative to tartrazine would mean that any interaction with the gelatin would have had a more severe effect on the resulting gel matrix. While these potential source of error are purely speculative, they should be kept in mind when evaluating the results.

3.2.1 Pure porcine gelatin

To serve as a basis and a point of comparison, gels containing pure porcine gelatin were created. These gels were made to a total concentration of 18 w% gelatin. The gels were then poured in moulds and placed in a refrigerator at 5 $^{\circ}\text{C}$ approximately 20 hours before the start of the experiment, giving them the same gelling time and concentration used for the particle tracking gels. This means that the gels should have in theory been highly similar to the porcine gels used in the particle tracking experiments, however as discussed the addition of tartrazine and blue dextran might have had some effect on the properties of the gel. At the same time the gels made were also larger in volume, which might have also had some effect on the gelling process. What this means is that the porcine gels created likely were highly similar to the ones used in the particle tracking, and considering the low mobility observed in those experiments, it would be reasonable to assume similarly slow diffusion rates for at least the large blue dextran molecules. After placing the gels in the sample holders for the dissolution unit, they were also allowed to heat up to room temperature, the same as was done for the particle tracking samples. In addition the water bath used for temperature control and the solvent water was allowed to sit for 24 hours before analysis to allow the stabilisation of the temperature, which was observed to remain stable at approximately 20 $^{\circ}\text{C}$ for the duration of the experiment. All of these factors would suggest that the temperature likely wasn't a major source of error, which is particularly important considering how temperature fluctuations possibly could affect the gelatin. The melting temperature for gelatin was not of a big concern however, due to the fact that it should be over 30 $^{\circ}\text{C}$,²¹ If the gel by some error was heated or cooled by a few degrees during the experiment, there is no way to say how this could have affected the results. Though there is a possibility that the temperature might have fluctuated during the nights when the system wasn't observed regularly, there is nothing to suggest that this was the case.

The resulting concentration of tartrazine and blue dextran in the solvent water over time is given in Figure 38 and 37, respectively. One thing that does stand out about these two figures are how relatively similar they appear to be. There are clear differences in the curves, though the overall behaviour does seem to be consistent between the two, mainly that they follow a mostly linear and slow rise.

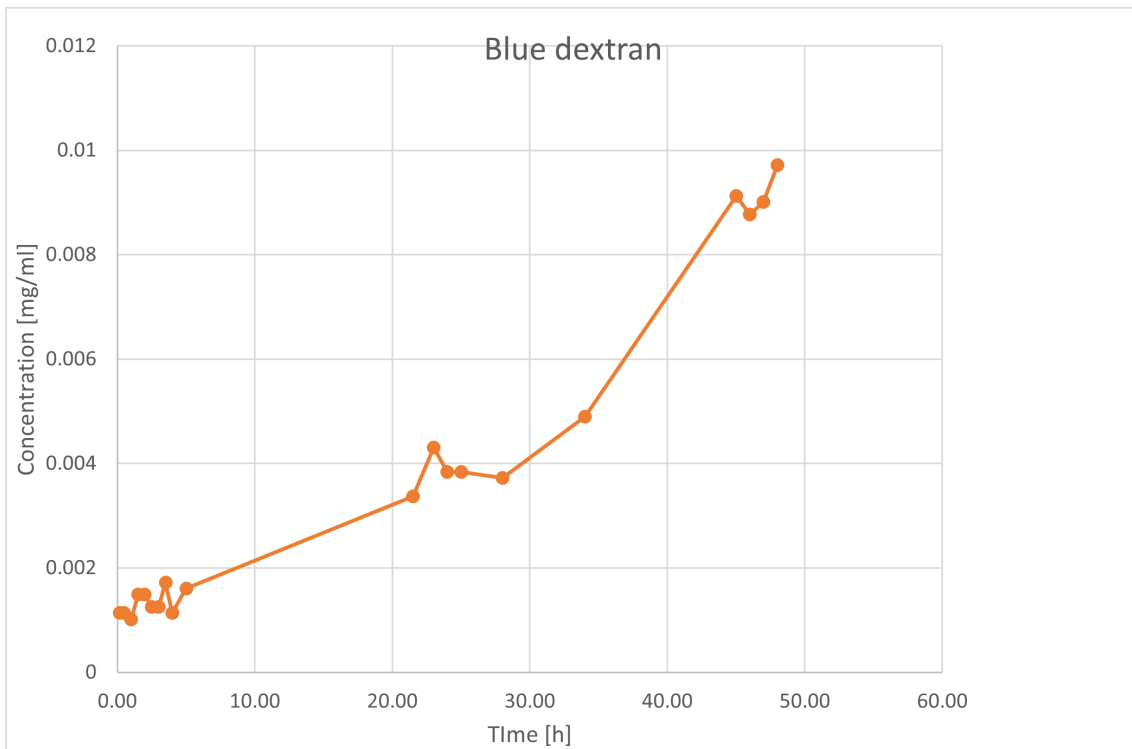


Figure 37: Concentration of blue dextran over time in liquid medium kept at room temperature. Each point corresponds to a measurement, with the final measurement taken after 48 hours.

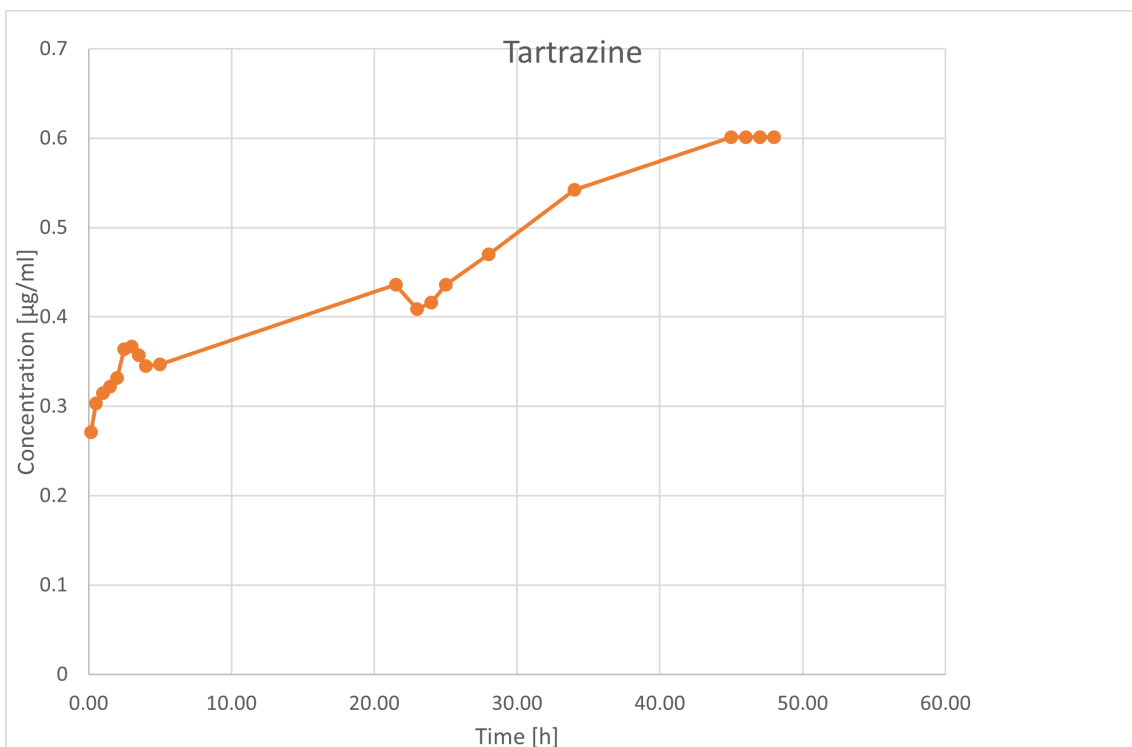


Figure 38: Concentration of Tartrazine over time in liquid medium kept at room temperature. Each point corresponds to a measurement, with the final measurement taken after 48 hours.

Starting at the left, they both seem to be relatively noisy and unstable before the large gap between 10 and 20 hours. The reason for this noise could be several factors, but it is most likely in part due to the system stabilising after the initial addition of the gels. When the gels were lowered in the solvent, any of the coloured compounds that might have been at the surface of the gels would have been quickly released. This quick release, coupled with the fact that there was not any heavy stirring in the solvents apart from the gentle spinning of the sample holder means that the system might have needed some time for the released compounds to properly disperse. It is also worth noting that the observed concentrations were extremely low, meaning that any small disturbances or errors such as dust or contaminants in the samples would have been highly noticeable. Regardless of the noise at the beginning, the rest of the curves do appear somewhat better. Both curves see a slow linear rise leading up to the 21 hour mark, before they both spike in opposite directions. The blue dextran curve seems to spike up, while the tartrazine curve spikes downwards. Given that this is only in one point, it seems likely that it is simply caused by some disturbance or error. Following the spike it appears that both curves obtain a slightly higher slope, rising at a faster pace than they did previously. The sudden increase in their slopes could simply also be due to inaccuracies during the measurements, however the swelling of the gels might have played some role. The main reason for this suspicion is that the gels were observed to swell after they were submerged in the solvent. The gels were observed to swell to the point where they filled the entire holding container they were submerged in, meaning that they they swelled to the point of getting restricted by the container. Interestingly the gels were seen to reach that point at around the 24 hour mark, which does somewhat seem to line up with the relative increase of slope in the curves. To briefly explain why this could have been a cause, it has to do with the influx of water to the gel. As the gels are swelling rather fast, water is diffusing inside the gel at a fast pace as well, something which could have hindered the diffusion of molecules out to some extent. As the gels then reach the edges of the container they can no longer continue the swelling, which would then have lead to a less restricted diffusion out of the gels. This is purely speculative, however the times do appear to line up quite well, This could mean that these two things are possibly related, but this cannot be confirmed. Whatever the reason for the steeper curves might be, they both appear to start flattening out leading up to the 48 hour mark.

All of these small details seem interesting at first glance, and they could possibly have several explanations as has been discussed, but the most important thing which has not yet been touched on is just how low the diffusion out of the gels was. All of what has been discussed so far has been regarding the shape of the curves taken at face value, and without considering just how insignificant those small details and variations in the curves are. When looking at the concentrations shown on the y-axis of the figures, it's clear that even after 48 hours, the amounts of concentrations of the coloured compounds present in the solvent are not even close to the amounts added to the gels. The gels were melted completely in the solvent after the final measurement was taken, measuring the maximum possible concentrations that could have been achieved. When plotting this data next to the previously shown curves, it illustrates just how little ended up diffusing out of the gels. This is shown in Figure 39 for blue dextran, and Figure 40 for tartrazine. The dotted green line at the top of the figure represents the average value observed after melting the gel at 40 °C for 40 minutes, measuring every 10 minutes for a total of 30 minutes to ensure the value obtained was stable. The concentration was measured after 30 and 35 minutes as well, however it was observed to still be increasing at those points, thus they were not included in the average. The plotted data from these measurements is given in Appendix C.

The orange lines in Figures 40 and 39 represent the data from the 48 hour release tests, which was shown in Figure 37 and 38. Looking at these figures, the data which was previously shown appears close to completely flat and smooth. All of the details and spikes previously discussed are not visible, the reason being that the measured concentrations were so small. While the downwards spike seen in the tartrazine curve does look significant when zoomed in, the spike accounts for less than 1% of the maximum possible concentration. When comparing to the maximum values, it does seem that more tartrazine was released. Taking the final measurement from the tartrazine curve and dividing it by the maximum possible concentration, it shows that only around 3.39% of the tartrazine added to the gel ended up diffusing out. In comparison, the same calculation shows that just 1.27% of the blue dextran diffused out over the same time period. While this does show that the portion of tartrazine that diffused out was over twice as high as the blue dextran,

it's still an incredibly low amount. The observation that the blue dextran seemed to be restrained by the gel matrix to a higher degree does lay in line with expectations given the size differences, though the tartrazine being highly constricted as well is more surprising. Given the small size of the tartrazine molecules, it seems reasonable to believe they would be able to diffuse out of the gel with relative ease.

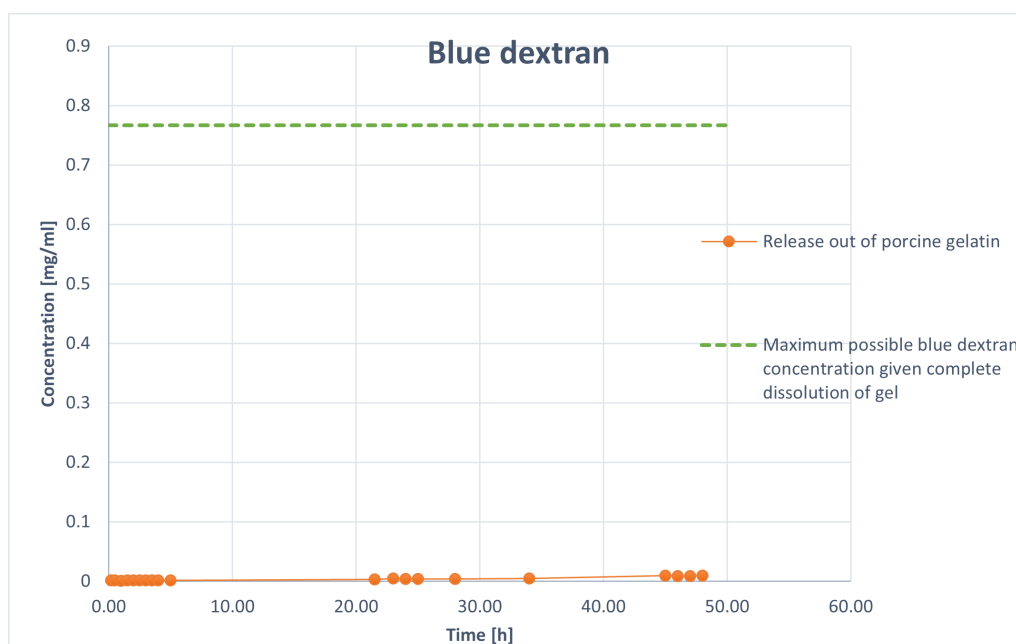


Figure 39: Concentration of blue dextran over time in liquid medium kept at room temperature. Each point corresponds to a measurement, with the final measurement taken after 48 hours. The average measured concentration after complete melting of the gel matrix is given as a dotted line.

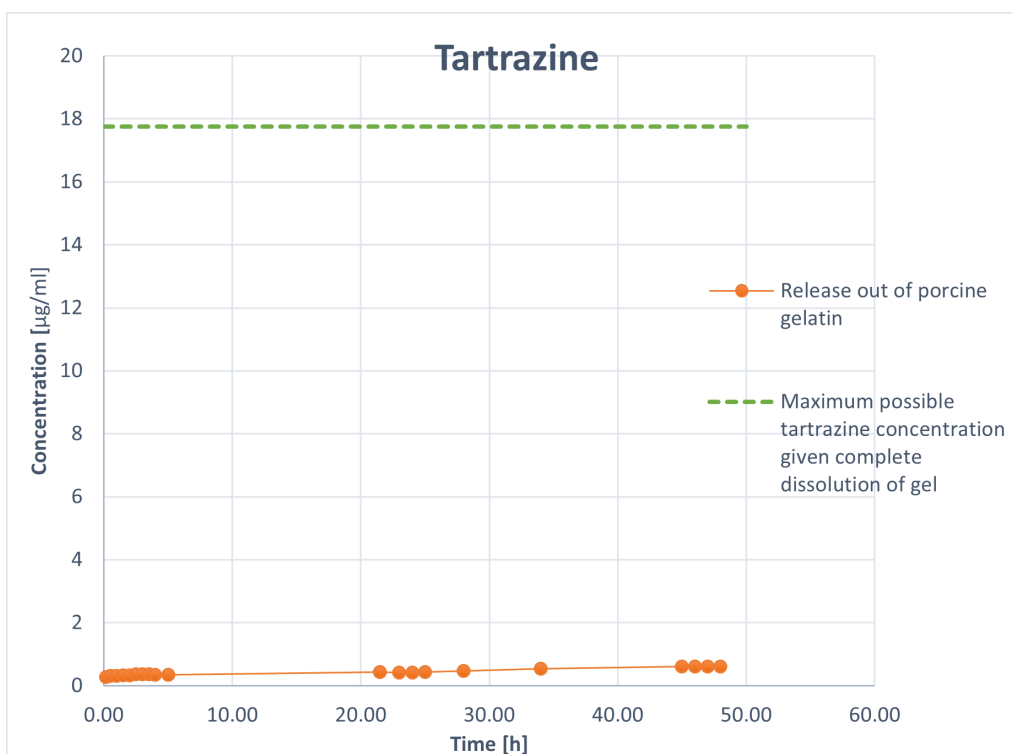


Figure 40: Concentration of Tartrazine over time in liquid medium kept at room temperature. Each point corresponds to a measurement, with the final measurement taken after 48 hours. The average measured concentration after complete melting of the gel matrix is given as a dotted line.

Previous experiments have shown larger molecules such as 70 kDa FITC-dextran to be able to diffuse through gel matrices of similar concentrations relatively quickly.³⁷ Though those experiments focus on the internal diffusion in the matrix, the diffusion out of the gel is still linked to this, as the molecules do have to internally diffuse out to the borders of the matrix before they can diffuse out of it. This would suggest that while the tartrazine likely could diffuse out faster, there is something hindering this. In general, gelatin is known to have a low dissolution rate, which has been studied previously by A. Duconseille et al.²³ What they discuss is that there are several reasons for the low rate of dissolution in gelatin, however the two major contributors are chain length and the amount of cross-links between the chains. When it comes to the cross-links, factors such as gelling temperature, time and even humidity plays a role. In this case, both temperature and gelling time were selected to give a high amount of cross-linking, or in other words a high gel strength. The chain length for the porcine gelatin used is not known, but it does seem like it was high enough to give a strong and flexible gel. In other words, the porcine gels used in these experiments were made to have a high strength, which would explain why the release from them is so low. It is also important to note that the temperature used was only around 21 °C, which is well below the melting temperature of gelatin. The solvent used was also just pure de-ionized water, which should not break down the matrix of the gel. Dissolution experiments are typically carried out using factors that destabilise and break down the gels, which was not the case here. The solvent and temperature were selected as to specifically not break down the gels, as the main idea was not to study how they dissolve, but rather how the molecules diffuse out of the matrices. As described in the paper by A. Duconseille et al, dissolution of gelatin is usually carried out by melting the gel. When using pure water at room temperature as the solvent, there isn't anything to cause such a melting to happen.

The fact that gelatin already has a low dissolution rate coupled with the mild dissolution factors used means that the slow release of tartrazine and blue dextran out of the gels make more sense. As described in that paper, the first step of the dissolution is the swelling of the gel, something that took nearly 24 hours to finish in these experiments. With the swelling stage alone taking such

a long time, it doesn't seem surprising that the release out of the gels also happened very slowly. If the gels naturally swell up in aqueous environments, it could also be that the diffusion out of the gel was hindered by the influx of water. The low diffusion of tartrazine is more surprising than the blue dextran, given that tartrazine is a relatively small molecule. Even with a gel concentration of 18 w%, it seems somewhat strange that it would be able to hold the tartrazine in that well. This could imply that there is some interaction between the gel matrix and the tartrazine which is keeping it from diffusing out, as it would explain how the gel matrix is able to restrict such small molecules. While this does seem like a possibility, it is difficult to say if this did happen, as it would require further investigation.

To summarise, the low diffusion rates out of the gel are likely coupled with many of the reasons for the low dissolution rate that gelatin gels exhibit. Seeing as the solvent was just water at room temperature, there was nothing to drive the dissolution of the gelatin, which meant that only the diffusive properties of the gels were driving the release of tartrazine and blue dextran from the matrices. While it should still have been possible for at least the tartrazine to diffuse out of the matrix, the slow rate of diffusion would seem to suggest that the gel matrix somehow managed to confine these molecules even with their size being so small. It's not possible to say if they were highly confined within the gel as well, though previous experiments have shown that similar gels are not able to fully restrict 70kDa FITC-dextran, which suggests that the diffusion out of the gel is somewhat more restricted than the internal diffusion. This could imply some interaction between tartrazine and the gelatin matrix. It could be possible that the influx of water into the gel as it swells could have been hindering the molecules from diffusing out like mentioned, but it doesn't explain why the rate of diffusion still remained low even after the swelling finished. While it is hard to say exactly what the reason for the low diffusion out of the gels is, the behaviour itself is still highly interesting. What can be said for certain is that when placing the porcine gels in water at room temperature, both the tartrazine and blue dextran exhibit low rates of diffusion out of the gel matrices. This speaks to the stability and strength of these gels, as even after 48 hours under the same conditions, molecules as small as tartrazine still remained confined in the gel for the most part. The stability and strength of porcine gelatin gels is something that's already been well documented in the past, even by the particle tracking experiments previously shown in section 3.1, and these findings do serve as a good basis for comparison when testing gels containing cold-water fish gelatin.

3.2.2 Gel containing equal parts pig skin and cold-water fish skin gelatin

To explore the stability of gels containing both porcine and cold-water fish skin gelatin, gels containing equal parts of both gelatin types were tested. The conditions and methods used for creating the gels were the same as those used for the porcine gels, including the gelling conditions and the total gelatin concentration in the gels. This was done to allow for comparison between the mixtures and the pure porcine gels, similar to what was done in the particle tracking experiments. To preface the results, it should be mentioned that the only notable difference between the experimental procedures for the mixed and pure samples is the amount and frequency of the measurements. For the mixed gels, samples were taken more frequently for the first 5 hours when compared to the porcine gels. Samples for later times were taken at slightly different time points, though the general scattering of the measurements across the experimental duration were similar. The experiments were also stopped at 46.5 hours instead of 48 hours due to time constraints. While these differences could play a small effect on the results, the overall behaviour and conclusions drawn from the results should not be significantly affected by these small changes. The most significant change is likely the shorter experimental duration, though given that it was only 1.5 hours shorter, it should not have had a large effect other than a slightly lower total release of the tartrazine and blue dextran than it would otherwise have had. The concentration of blue dextran and tartrazine in the solvents over time is presented in Figure 41 and 42, respectively.

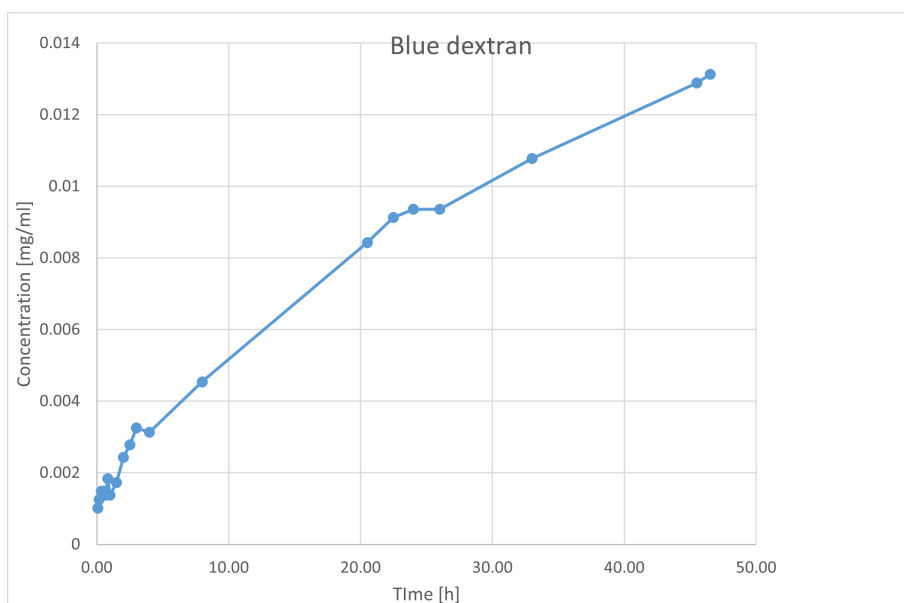


Figure 41: Concentration of blue dextran over time in liquid medium surrounding a mixed gel containing equal parts porcine and cold-water fish gelatin at room temperature. Each point corresponds to a measurement, with the final measurement taken after 46.5 hours.

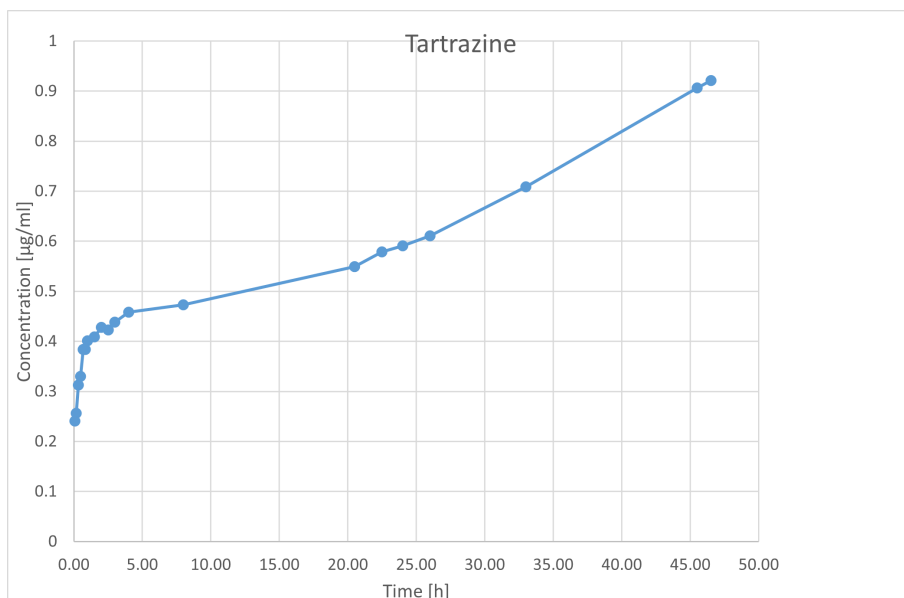


Figure 42: Concentration of Tartrazine over time in liquid medium surrounding a mixed gel containing equal parts porcine and cold-water fish gelatin at room temperature. Each point corresponds to a measurement, with the final measurement taken after 46.5 hours.

The most noticeable thing about these curves is the similarity between them, as both seem to follow a mostly linear pattern. Tartrazine seems to rise quite sharply at first, which is most likely caused by the tartrazine in the surface of the gel getting released. After around 4 hours it seems to flatten out more, following a slow and mostly linear rise. It could be said that it appears to show an exponential rise for later time points, though it's hard to tell with the given data. Blue dextran on the other hand seems to be fairly linear across the entire duration. There is more noise near the beginning, though as discussed for the mammalian gels, it's most likely due to the system stabilising. The curve does also seem to stall briefly around the 24 hour mark, which could in part be due to it being raised from the solvent to perform evaluations on the swelling briefly. While it was only out for approximately 30 seconds, it could have caused some delay in the diffusion still. The fact that the curve seems to continue normally after the stall does also support this idea, suggesting the stalling wasn't simply an error, like what was seen in the mammalian gels when they spiked.

All of this does seem quite interesting, but when they are compared to the maximum possible concentration in the solvent, it's clear that the amounts released were extremely small. As was done for the mammalian gels, the mixed gels were melted at 40 °C for a total of 70 minutes, measuring at the concentrations after 40 minutes to get an average value for the maximum concentration possible in the solvent. This then gives an approximation of the maximum possible concentration achievable in the system. These maximum values for both blue dextran and tartrazine are plotted alongside their respective curves in Figure 43 and 44, respectively.

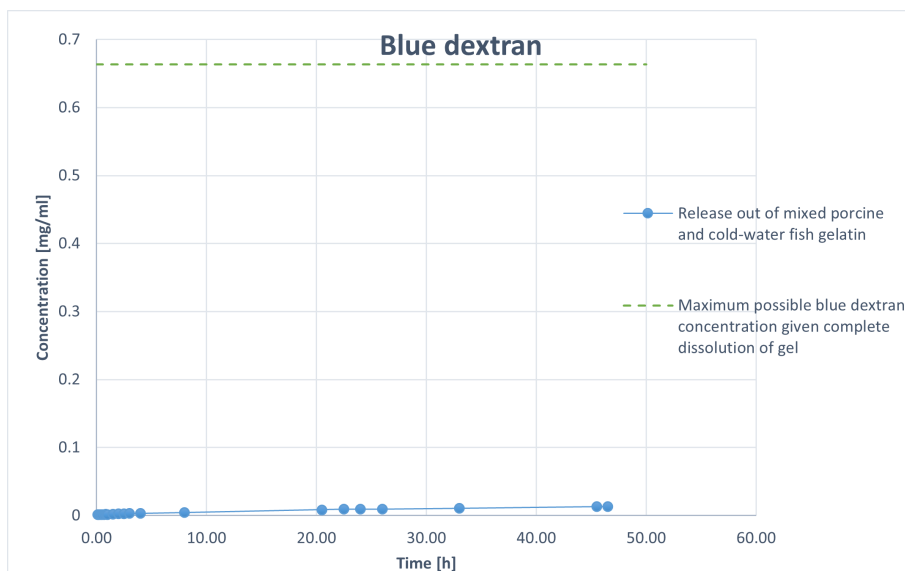


Figure 43: Concentration of blue dextran over time in liquid medium kept at room temperature. Each point corresponds to a measurement, with the final measurement taken after 46.5 hours. The average measured concentration after complete melting of the gel matrix is given as a dotted line.

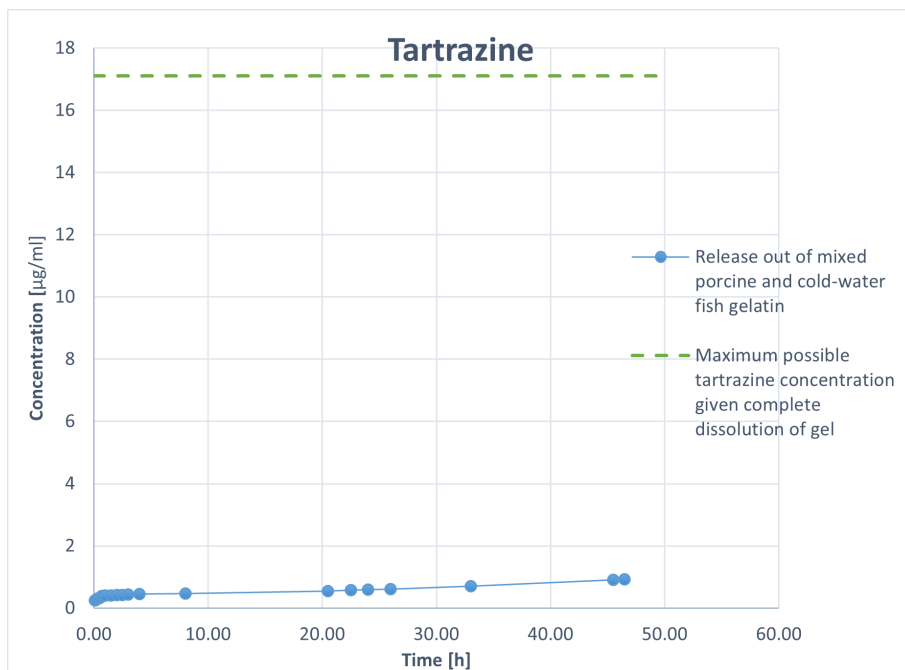


Figure 44: Concentration of Tartrazine over time in liquid medium kept at room temperature. Each point corresponds to a measurement, with the final measurement taken after 46.4 hours. The average measured concentration after complete melting of the gel matrix is given as a dotted line.

It becomes clear that all of the small variations and details discussed above are close to indistinguishable in these new figures, mainly because very little of the two compounds ended up diffusing out of the gels. Both curves appear almost completely linear when plotted alongside their maximum, with the curve for blue dextran appearing almost flat. Tartrazine does seem to show a somewhat more significant rise, though when comparing to the maximum, only around 5.38% of

the tartrazine ended up diffusing out from the gel after 46.5 hours. Over the same period of time, only 1.98% of the blue dextran ended up diffusing out from the gel. What this means is that the gels appeared to confine both tartrazine and blue dextran effectively at room temperature, seeing a very slow rate of diffusion. This is highly interesting considering that half of the gel matrix was comprised of cold-water fish gelatin, which should have melted at this temperature. The fact that both tartrazine and blue dextran remained in the gel also suggests that the cold-water fish gelatin did not melt. If melting had occurred it would be highly unlikely that the matrices could have confined them to such a high degree, as it would most likely have caused a general weakening in the gel matrix, and for any cold-water fish gelatin in the surface of the gel to dissolve. If 50% of the matrix had melted, it seems unlikely that only around 5% of the tartrazine would have ended up getting released even if most of that melted matrix might have not been in the surface of the gel sample. This suggests that the porcine and cold-water fish gels most likely interact to form a mixed network rather than form individual domains, the same exact thing that was also seen when performing particle tracking in the same mixtures. If they didn't, then the cold-water fish gelatin domains would have melted at this temperature, which was 20 °C, and most likely caused a significantly more noticeable release. Simply put, the behaviour doesn't seem to suggest that the cold-water fish gelatin is separate from the porcine gelatin, but that it instead interacts with it to form a shared network. While these results alone cannot confirm this, it becomes increasingly more plausible when they are compared with the results from the pure porcine gels.

3.2.3 Comparison and interpretation of results

On their own, the results from the porcine and mixed gels do show that they both appear relatively stable under the conditions used. Both seem to show a highly similar behaviour in that regard, as both give mostly linear curves, and a low overall release of both tartrazine and blue dextran from the gels. The similarities become more apparent when the data for both experiments is plotted together. The curves depicting the concentration over time for blue dextran in both gels is presented in Figure 45, with the same thing shown for Tartrazine in Figure 46.

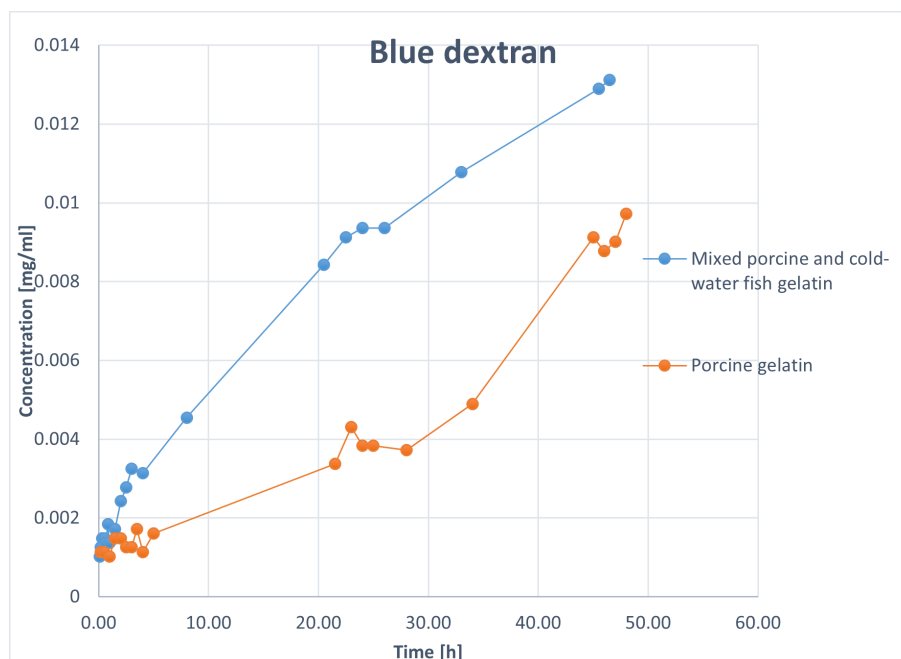


Figure 45: Concentration of blue dextran over time in solvent medium surrounding the mixed gel containing equal parts porcine and cold-water fish gelatin, and the pure porcine gel, measured at room temperature. Each point corresponds to one measurement.

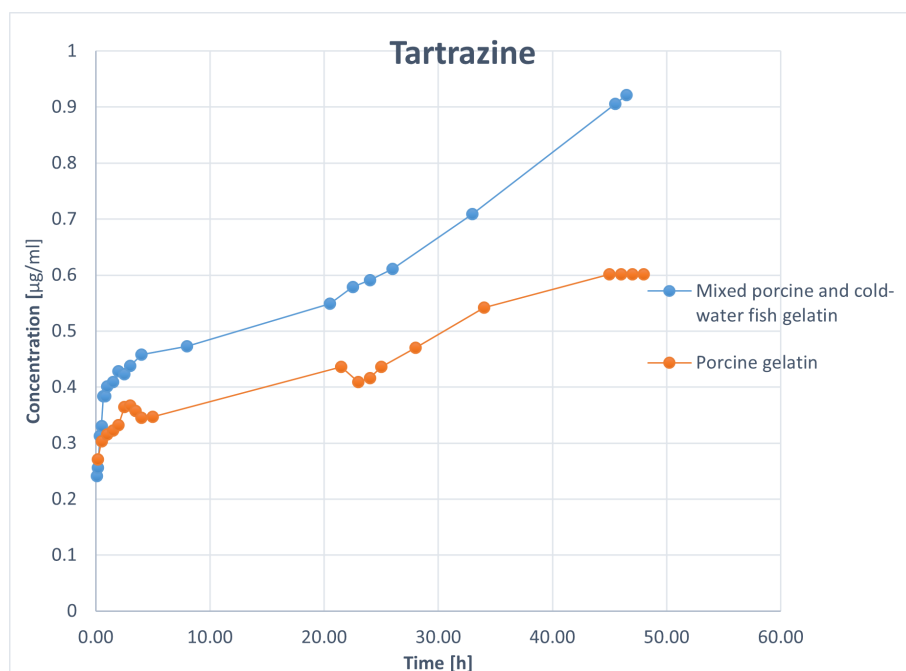


Figure 46: Concentration of Tartrazine over time in solvent medium surrounding the mixed gel containing equal parts porcine and cold-water fish gelatin, and the pure porcine gel, measured at room temperature. Each point corresponds to one measurement.

Looking at these figures, it's clear that while there was a higher amount of both tartrazine and blue dextran diffusing out of the mixed gels, the overall behaviour and rate of diffusion wasn't dissimilar to the porcine gels. When looking at the blue dextran curves they both seem to start at around the same concentration early on, with the mixed gel seemingly allowing for a slightly higher diffusion early on. What's interesting is that the diffusion rate appears to increase for porcine gelatin later on. Taking the last measurements in both cases, the mixed gel only released 0.71% more of the added blue dextran, which is not a huge difference. Similar things are seen for the tartrazine data, where the mixed gel appears to release more tartrazine early on. Despite this, the diffusion rate out of the porcine gel appears almost identical for later time points, up to around 34 hours where they diverge. The concentration of tartrazine in the medium surrounding the mixed gel seems to keep increasing linearly, while the concentration around the mammalian gel appears to stop increasing. What exactly causes this difference is hard to tell, as it's not clear whether it is simply an error in the measured concentrations, or if the tartrazine does in fact stop diffusing out of the porcine gel. Given that it's only observed near the end, it's hard to draw any conclusions on this given that it's unknown how the behaviour continues after this. Like discussed in section 3.2.1, it's possible that it's simply a temporary stall in the diffusion, but this again is not possible to say for sure. It doesn't seem likely that the diffusion would simply stop permanently, as there is no reason to believe that the gel should start suddenly completely confining the tartrazine within the matrix. It's also not possible to say whether the same would also happen for the mixed gel given enough time. Whether it is caused by a decrease in diffusion, or it is an error, the end result is still incredibly close to that of the mixed gel. Comparing the end values to the maximum possible concentrations for each of the two gels, it shows that the mixed gel only released 2% more of the tartrazine in the gel. While this difference is noticeable it's still a relatively low change considering that half of the gel matrix is replaced with cold-water fish gelatin, which should on its own melt at room temperature.

The fact that the diffusion rates of both blue dextran and tartrazine out of the gels are still incredibly low for the mixed gels is a good indication that the cold-water fish gelatin isn't melting. Like discussed in the previous section, if this was the case then it would likely be far more noticeable. If half of the gel matrix were to melt and dissolve, it seems unlikely that the diffusion rate of something as small as tartrazine would be affected to such a low degree. Seeing as both the

tartrazine and blue dextran was dispersed evenly in the gels, if the cold-water fish gelatin were to melt and dissolve, any tartrazine or blue dextran trapped within would also be released. Unless the porcine gelatin somehow concentrated in the outer layers of the gel to keep the cold-water fish gelatin trapped, which there is no reason why it should have, melting seems highly unlikely. Simply put, the highly similar results for the mixed and porcine gels indicate that cold-water fish gelatin must somehow mix and incorporate with the porcine gelatin. This is exactly what was concluded from the particle tracking as well, presented in section 3.1. What was seen there was that all the particles appeared to diffuse at a highly similar rate, indicating a homogeneous matrix. At the same time, it also showed that there were minimal differences between the 50-50 mixed gel and the pure porcine gels in terms of how they confined the $1\mu\text{m}$ particles. All of this does seem to fall in line with the results seen here as well. Just as there were minimal differences between the gels in the particle tracking, there are also minimal differences here, even for smaller molecules such as tartrazine. The fact that only 2% more tartrazine released when replacing half the porcine gelatin with cold-water fish gelatin is highly interesting, as it indicates that the cold-water fish gelatin is able to not only integrate with the porcine gel, but also provide a similar amount of strength and structure as the porcine gelatin it replaces. If pure cold-water fish gelatin was tested it would simply melt and diffuse nearly instantly, meaning that it would provide a 100% release of the added tartrazine and blue dextran. When considering this, the fact that having as much as 50% cold-water fish in the gel only gives 2% higher release than a pure porcine gelatin shows just how minimal of a difference the cold-water fish gelatin makes. Being able to replace that much of the porcine gel with something that alone would simply melt, and still see differences that small goes to show how interesting their interaction truly is.

Both of these experiments seem to point in this exact direction, something that further strengthens their validity. Being able to show similar and mutually supportive results using two completely different methods is incredibly intriguing, as this helps to decrease the chance of their individual findings being faulty. In terms of both internal and external diffusion, it seems that adding porcine gelatin to cold-water fish gelatin gives results that are close to those seen for pure porcine gelatin of the same total concentration. While there does still appear to be differences, the behaviour is without a doubt much more similar to porcine gelatin than cold-water fish gelatin. It also fits with what has been observed previously using FRAP measurements, that being an overall small increase in diffusion for gels containing both cold-water fish gelatin and mammalian gelatin compared to pure mammalian gelatin.³⁷ While mixed gels do seem to give higher diffusion in general, the data seems to imply that this increase is relatively small, meaning that the barrier properties are not heavily impacted by the presence of cold-water fish gelatin.

3.3 Emulsion tests

To further test the properties of mixtures containing mammalian and cold-water fish gelatin, their emulsification properties were also desirable to study. Experiments conducted by another master's student Kristian Sylliåsen (personal communication) had shown that when used for oil emulsions, these mixtures appeared to exhibit lower droplet sizes on average when compared to pure mammalian gels. These results seemed to indicate a relative increase in the emulsifying properties when utilizing cold-water fish gelatin in the gel, causing a theory that the cold-water fish gelatin may have been more surface active than the mammalian gelatin. If this was the case, it seems reasonable to suspect that the cold-water fish gelatin would also to a higher degree concentrate around the oil droplets. This would then cause a shift in the relative concentration of mammalian to cold-water fish gelatin in the matrix, meaning a relative enrichment in cold-water fish gelatin at the oil interface and a relative depletion of cold-water fish gelatin in the rest of the matrix. A simplified illustration of this theory is shown in Figure 47, showing that as the oil is added, the overall composition of the matrix changes. If this did happen, the total concentration of gelatin would not change, just the distribution of each of the two gelatin types.

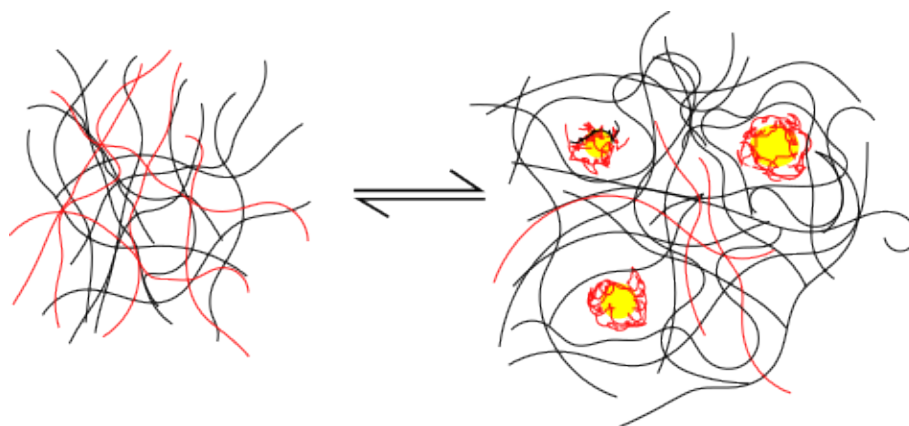


Figure 47: Suggested distribution of cold-water fish gelatin and mammalian gelatin in oil emulsions. The black lines represent mammalian gelatin, the red lines represent cold-water fish gelatin and the yellow circles represent oil droplets. Pure gel is shown on the left, while the emulsion is shown on the right.

This proposed theory did seem highly interesting, however there was no proof to show whether or not the cold-water fish gelatin did concentrate around the oil droplets like suggested. Previous experiments conducted on mixtures of mammalian and cold-water fish gelatin using Fluorescence recovery after photobleaching (FRAP) have shown a difference between pure mammalian gels and gels containing part cold-water fish gelatin in regards to their diffusive properties, and thus FRAP could in theory also possibly show if there was a difference in the gel matrices. The idea was to preform FRAP tests on oil emulsions created using gels containing both cold-water fish gelatin, and comparing this to some control gels consisting of the same gel base. The fluorescent molecules used was 70 kDa Fluorescein Isothiocyanate(FITC)-Dextran, the same as were used for the previous experiments as well. Both the controls and the emulsions were created at the same time from the same gel solution as to ensure that the relative amount of cold-water fish gelatin to mammalian gelatin in the samples remained as similar as possible. This was done by creating one stock solution containing 50% each of the two gel types, and using a scale to measure out the appropriate amount of gelatin for the emulsions. This means that the relative amounts of cold-water fish gelatin and porcine gelatin should have been relatively constant across all samples, and so the only key difference between them in theory would be the emulsification process. Any observable difference would thus likely be linked to the emulsification process, excluding any environmental differences during analysis and possible disturbances. While there is a possibility some disturbances such as contamination of the sample or objective did occur, precautions were taken to ensure these were minimal, though the ability to control for factors such as vibrations and temperature were limited.

It is also highly possible that there were oil droplets directly above or below the bleached region during the FRAP analysis that may have disturbed the measurement by hindering the diffusion of FITC-dextran, however no such cases were observed when analysing the recordings. It can't be ruled out as a possibility, though it doesn't appear to have been a major cause of error.

What seems more likely to possibly have caused some error would be drift, as the oil droplets were observed to heavily drift when the samples were initially placed under the microscope. Most of the oil droplets were observed to drift in the same direction, and at a similar velocity. This alone would seem to suggest a drift of the focal area similar to what was seen in the particle tracking rather than a drift in the sample itself, however not all oil droplets were observed to drift. The drift also appeared to only draw the particles away from the injection well, regardless of how the sample was rotated. When looking at the samples over time, several droplets were also observed to stand still, or move at a slower pace when compared to the rest. This is illustrated in Figure 48, where the displacement of the oil droplets over 50 seconds is shown.

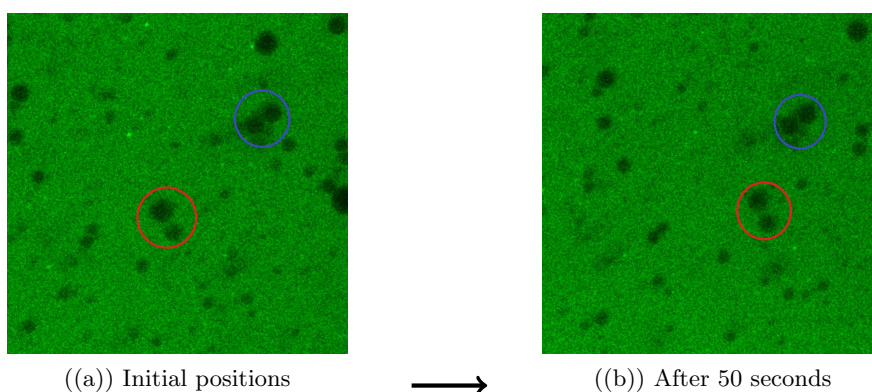


Figure 48: Images captured at 0 and 50 seconds during a fluorescence recovery after photobleaching experiment in a gelatin-oil emulsion. The black areas are the oil droplets. The red and blue circles show the positions of the same two sets of oil droplets at both time points.

The red circles mark two droplets that exhibit drift, while the blue circles mark droplets that exhibit no drift. It's clear that there is something causing the droplets to drift, however the fact that not all of them do would suggest that the drift was at least in part due to some force pushing or pulling on the droplets. Whatever the cause was, it did make it impossible for the FRAP analysis to be conducted. Several tests were conducted on the samples to deduce the source of the drift, including cooling the sample via a cooling element, utilizing agar in place of gelatin and using fluorescent micro-beads in place of the oil. All of these tests appeared to show little to no difference in the drift, but what did make a large difference was sealing the wells of the sample plate. Previous experiments, including the ones previously referenced as a basis for these experiments were all conducted with the wells kept open. There was parafilm placed on top of the wells to prevent drying during the gelling process, however it was not kept air tight. By taking parafilm and using it as a plug to seal up the sample wells, the drift was observed to almost completely disappear. It's clear that sealing the wells did solve the issue, though the exact reason why isn't known. The most probable explanation would seem to be that there were capillary forces acting on the sample, which would have occurred for several reasons. It could be that the open wells caused the samples to start drying out, leading to a contraction of the gel matrix. It's also plausible that there was some tension in the gel from the way it was injected, being forced through a narrow channel while gelling quickly due to an increased rate of cooling. The exact mechanics as for how this tension would occur is difficult to say, though the injection method may possibly have had some effect. No matter what the reason as to why the drift disappeared when plugging the wells was, it did solve the issue in a way which allowed for the tests to continue. It is worth noting that this drift was difficult to observe without the presence of the oil droplets, which could be a possible source of error for previous FRAP data as well.³⁷ This could help to explain some of the apparent noise seen in those results, however it can't be said for certain how large of an error

it might have caused. Though this finding does to some extent pose a question to the validity of that data, it doesn't seem likely that it would change the overall conclusion. It might be a source of the noise, though the overall trends in the diffusion, as well as the differences between mixed and mammalian gels seem to be strong and clear. If nothing else, the fact that mixed gels show a overall higher diffusion coefficient for all cases still suggests that the diffusion rate does increase when the fraction of cold-water fish gelatin increases. If there was no difference between the diffusion in the gels containing cold-water fish gelatin and those not, it seems unlikely that the results would show such a clear and mostly uniform difference at each concentration. While the observation of drift might weaken the validity of the data to some degree, it's not clear that it would change the overall conclusion much, that being that the mixed gels give higher diffusion coefficients.

Utilising this, the emulsions and controls were tested via FRAP analysis. The data was analysed by the use of online tool easyFRAP-web (<https://easyfrap.vmnnet.upatras.gr>).³⁶ Both the pure gelatin and the emulsion were tested using 2 parallels, each parallel measured a total of 5 times, This means that the average diffusion coefficients for both are a combination of 10 separate measurements, the purpose of which was to reduce the effect of any random errors. As seen in previous data,³⁷ there tends to be some variation even within the same sample, meaning that singular measurements alone might deviate enough to affect the conclusions. Gels create non-homogeneous matrices by nature, meaning that they aren't completely uniform and even on a microscopic level. The gels might appear to be so on a macroscopic level, however when zooming in such as in the case of a FRAP experiment, it seems reasonable to assume that there might be some observable variations. This is also one of the main reasons for running repetitions, as they allow for the possibility to determine an average over several points in the gel, giving a better representation of the gel as a whole. While the severity of the variations within the gels isn't known, it can be assumed that the repetitions at least in part helped to mitigate the effect of the variations.

The results obtained for the control gels are shown in Table 4, while the results for the emulsions are given in Table 5. The tables show the halftime of recovery, mobile fraction and diffusion coefficient for all repetitions. The average values are marked with yellow, and given at the bottom of tables. When looking at these average values, they appear to show a relatively small differences between the control and the emulsion. Considering the fact that the gels were created from the same gel solution, the lack of difference does point to the emulsions not making a significant difference in the matrices. Focusing on the diffusion coefficients, there is a difference of just 0.03 m²/s on average.

Table 4: The resulting halftime of recovery, mobile fraction and diffusion coefficients for all parallels and repetitions performed in the 18 w% control gelatin. The gelatin consisted of equal parts pig skin and cold-water fish skin gelatin by weight.

Sample	T _{1/2}	Mobile Fraction	R ²	D m ² /s
1.1	3.66	0.89	0.99	2.16
1.2	4.07	0.9	0.99	1.95
1.3	3.77	0.87	0.99	2.10
1.4	3.84	0.9	0.99	2.06
1.5	3.57	0.89	0.99	2.22
P1 Mean	3.78	0.89	0.99	2.10
2.1	3.9	0.92	0.99	2.03
2.2	3.68	0.89	0.99	2.15
2.3	3.62	0.92	0.99	2.19
2.4	3.86	0.9	0.99	2.05
2.5	3.96	0.92	0.99	2.00
P2 Mean	3.80	0.91	0.99	2.08
Average	3.79	0.90	0.99	2.09

Table 5: The resulting halftime of recovery, mobile fraction and diffusion coefficients for all parallels and repetitions performed in the 20% oil emulsion. The control solution was used as the base, adding oil to an end concentration of 20% by weight.

Sample	$T_{1/2}$	Mobile Fraction	R^2	$D \text{ m}^2/\text{s}$
1.1	3.61	0.9	0.99	2.19
1.2	3.73	0.89	0.99	2.12
1.3	4.14	0.9	0.99	1.91
1.4	3.52	0.91	0.99	2.25
1.5	3.42	0.89	0.99	2.32
P1 Mean	3.684	0.898	0.99	2.16
2.1	4.42	0.94	0.99	1.79
2.2	4.12	0.94	0.99	1.92
2.3	3.89	0.92	0.98	2.04
2.4	3.49	0.9	0.99	2.27
2.5	3.33	0.94	0.99	2.38
P2 Mean	3.85	0.928	0.988	2.08
Average	3.77	0.91	0.99	2.12

Looking at the amount of variation within just the parallels, it's difficult to argue that this difference is significant enough to show any trend. Looking at Table 4 as an example, the first and second repetitions in the first parallel have a difference of $0.21 \text{ m}^2/\text{s}$. Even when comparing the two repetitions closest to one another in that parallel, that being the third and fourth, they still have a difference of $0.04 \text{ m}^2/\text{s}$. In other words, the variations within each sample are significantly higher than the differences observed between the control and emulsion. It is worth noting that the two averages being so close to one another is likely in part due to coincidence, seeing as the variation between repetitions are so large. This is even more apparent when looking at the data from the emulsions in Table 5, which show even higher amounts of variation within each parallel. It is difficult to say what exactly may have caused the variation to be larger, as it could have several explanations. It could simply be a result of more noise due to the oil droplets impeding on, or blocking the bleached region in part. For example if an oil droplet was to lay directly under the observed region, it would likely occupy part of the area which would typically be bleached, thus reducing the amount of FITC-dextran which has to diffuse in to regain the pre-bleach intensity. This is a possibility due to the fact that a White Light Laser (WLL) was used for a bleaching, which performs a one-photon excitation. The issue with this type of excitation is that it will cause some bleaching below the region of interest, creating a cone-shaped bleaching area. The observed region is in contrast just a two-dimensional area, meaning that the bleaching underneath isn't observed or taken in account. This two-dimensional simplification is also the basis for the FRAP analysis, which only accounts for the diffusion in the observed 2D space.³ So while the bleaching happening below the region of interest isn't accounted for, it will still have some effect on the end result due to the fact that the whole bleached area has to be filled for the intensity to fully recover. If for example if the amount of bleaching below the region of interest suddenly decreased, the recovery of the intensity would likely be much faster. This is also why the oil droplets might have had some effect, like illustrated in Figure 49. The figure shows a simplified illustration of how the oil droplet might have interfered with the bleaching. The oil droplet occupying some of the area which would typically have been bleached would likely have some effect on the halftime of recovery, in theory decreasing it. This is however just speculative, as there is no way to prove or disprove whether this might have happened.

Regardless of what might have caused the seemingly high amount of variation within the emulsion measurements, it's still clear that the observed differences between the emulsions and controls are too low to prove that their matrices are significantly different. To summarise what's been discussed above; the fact that the variations in diffusion coefficients are so large within each sample, the small difference seen between the emulsion and control is not sufficient enough to prove that their matrices are different. This does at the same time also seem reasonable when considering what's

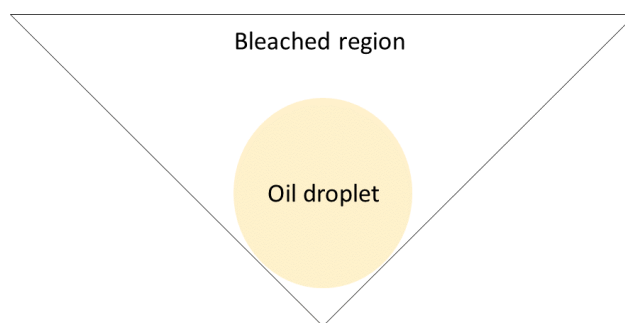


Figure 49: A simplified illustration showing how oil droplets under the region of interest (ROI) could interfere with the bleaching during a fluorescence recovery after photobleaching experiment. The flat side of the triangle represents the ROI.

been seen previously. Both the particle tracking tests and the tests performed in the dissolution unit have shown that the difference in diffusion between pure mammalian gelatin and the mixtures are minimal. Even when taking in account previous FRAP data,³⁷ it doesn't seem unreasonable to think that there wouldn't be an observable difference. When looking at the referenced FRAP data, it's clear that while there are differences between the gels with and without cold-water fish gelatin, the difference is still only appear to be somewhere around $0.2 \text{ m}^2/\text{s}$, even when comparing a 20 w% mammalian gel, to a gel containing 10 w% each of mammalian and cold-water fish gelatin. In other words the difference between a pure mammalian gel, and a 50-50 mixture with cold-water fish gelatin is not that high. Even if a large portion of the cold-water fish gelatin was to concentrate around the oil droplets, it seems likely that the change in diffusion wouldn't be that high. Even if all of the cold-water fish gelatin were to be drawn out of the gel matrix, which seems unreasonable to assume given that only 20% of the emulsion weight was oil, it doesn't seem like the diffusion coefficient would increase by much. Coupled with the seemingly high amount of variation within samples that was observed in the emulsions, the low difference between the controls and emulsions seems sensible.

In the end, the results were not able to provide any proof that the cold-water fish gelatin concentrated around the oil in the emulsions. Taking in account the low difference seen between mixed and mammalian gels in both the particle tracking and the tests performed in the dissolution unit, these findings do appear reasonable. Simply put, the previous experiments have shown that the differences in diffusion behaviour is small even when substituting a large portion of the mammalian gelatin with cold-water fish gelatin. Even if there was a difference in the relative amount of cold-water fish gelatin in the matrices of the emulsions compared to the controls, it seems that the diffusion behaviour might not get affected enough to be used as a means to prove this. It means that while the method didn't provide proof for the theory, it also can't be used as definitive proof against the theory. The data itself doesn't tell much, though it does strengthen the notion that the diffusion behaviour is relatively constant in gels containing both porcine and cold-water fish gelatin. Even across 4 separate samples, the diffusion coefficients remained extremely similar, showing just how stable and predictable these systems can be.

4 Conclusion

The results obtained from particle tracking and the release in an aqueous environment both seem to indicate the same thing, namely that the barrier properties of cold-water fish gelatin mixed with mammalian gelatin are remarkably close to those seen for pure mammalian gelatin. The particle tracking experiments suggest that gelatin mixtures with as little as 10% mammalian gelatin still exhibit barrier properties that appear largely dominated by the mammalian gelatin barrier properties, even at temperatures well above the melting point of cold-water fish gelatin. At the same time, the release from the gels in an aqueous environment also indicates that the barrier properties of a mixture containing up to 50% cold-water fish gelatin is still highly similar to those seen for pure mammalian gelatin. FRAP experiments conducted on gelatin-oil emulsions made using a mixture of mammalian and cold-water fish gelatin showed no significant change in the gelatin matrix when compared to mammalian gelatin gels.

These experiments all also indicate that the cold-water fish gelatin and mammalian gelatin were able to form a mixed system without any noticeable phase separation. Across all three methods used, there were no signs of phase separation occurring. The particle tracking experiments in particular appear to show no phase separation even with as much as 90% cold-water fish gelatin in the mixture. All of these findings strongly suggest that mammalian gelatin and cold-water fish gelatin are able to form mixed matrices without any additional cross-linkers needed, and that very little mammalian gelatin is needed to stabilise a cold-water fish gelatin gel at temperatures significantly higher than the melting point of cold-water fish gelatin. All results point to the idea these gelatin mixtures are extremely similar to pure mammalian gelatin, at least in terms of barrier properties, which could potentially open for new and broader applications for cold-water fish gelatin in an industrial context.

5 Possible implications of findings

The findings in this thesis could have a number of different implications, though the most obvious is that they clearly show that very little mammalian gelatin is needed to provide strong barrier properties when it is mixed with cold-water fish gelatin. The particle tracking experiments performed for the gelatin mixture containing just 10% mammalian gelatin is the biggest indicator of this, as it still showed diffusion behaviour close to those for pure mammalian gelatin. There was a small shift towards cold-water fish gelatin when compared to the 50% mixture, though this is not surprising given that the barrier properties are generally expected to go down with decreasing levels of mammalian gelatin.³⁷ It is worth noting that for the 10% mammalian gelatin gel, the actual weight percentage of mammalian gelatin was just 1.8 w%, which is starting to approach the critical gelling concentration, generally assumed to be around 1 w%.⁵ It is quite interesting that the mixed gel is able to form a gel network dense enough to contain the particles at such a low concentration of mammalian gelatin, which might suggest that the cold-water fish gelatin is not just passively bound to the mammalian gelatin, but rather actively taking part in gelling and stabilising. This comes back to the theory that the mammalian gelatin might act as a form of crystallisation nucleus, inducing gelling in the cold-water fish gelatin portions of the gel. This is purely speculative, and the exact kinetics behind it would be hard to specify, though it is a potential approach to the mystery of how the gelling does happen in these systems.

These results could mean that cold-water fish gelatin may potentially be able to serve as a partial substituent for mammalian gelatin in industrial products, at least if it is beneficial in terms of price or availability. Given that the barrier properties are not heavily affected, it is possible that it might even be used in gelatin films for food packaging. If other properties such as the gelling and melting temperatures, gel strength and so on see similar patterns as the barrier properties, it potentially opens up for cold-water fish gelatin to be used as a partial substituent in nearly any product that utilises mammalian gelatin. It is also important to think in terms of availability, as there is a limit to the amount of mammalian gelatin that can be produced. Seeing as gel-based films for food packaging are a relatively popular and desired topic, it is not unreasonable to think that gelatin might see more use within food packaging in the coming years either.^{40, 41} If this does happen, it will only drive up the demand for gelatin, and if so it might lead to a shortage of supply. Simply put, having the option to use cold-water fish gelatin only increases the amount of available gelatin on the market, which could potentially be very important if the demand for gelatin keeps increasing.

6 Further work

The findings in this thesis have shown that there is a high probability that mammalian gelatin is able to form a mixed network with cold-water fish gelatin, and that little mammalian gelatin is needed to obtain a gel with relatively good barrier properties. While these findings are interesting, there is still many aspects of these mixed gelatin systems that are not known.

The gelation kinetics of these mixtures might be something that could be worth investigating, as understanding how the networks form might help to better understand them as a whole. It could in that line also be interesting to see how the gelling temperature affects the resulting gels, and if the cold-water fish gelatin portions of the gel still gel at higher temperatures. It could also be highly interesting to further study the particle movement of smaller particles in the gel, to see if the same similarities between the mixtures and the mammalian gels are seen for smaller particles as well.

Outside of the diffusion properties as well, plenty of other factors such as the gel strength and the specific gelling temperatures are still unknown. Given that the desire is to utilise such mixtures, it is important for these factors to be investigated as well. The same thing goes for many other factors too, such as the antimicrobial properties and water retention capabilities. With the FRAP measurements giving no clear conclusions in this thesis as well, it is also still unknown if the cold-water fish gelatin is more surface active than mammalian gelatin. Simply put, there are a vast number of different properties that would be interesting to investigate for these gelatin mixtures. The general goal should be to gain a better and more complex understanding of how exactly these mixtures work.

References

- [1] 24 - mesoporous nanomaterials as carriers in drug delivery. In Inamuddin, A. M. Asiri, and A. Mohammad, editors, *Applications of Nanocomposite Materials in Drug Delivery*, Woodhead Publishing Series in Biomaterials, pages 589–604. Woodhead Publishing, 2018. doi:<https://doi.org/10.1016/B978-0-12-813741-3.00025-X>.
- [2] Chapter 18 - dissolution. In C. M. Riley, T. W. Rosanske, and G. Reid, editors, *Specification of Drug Substances and Products (Second Edition)*, pages 481–503. Elsevier, second edition edition, 2020. doi:<https://doi.org/10.1016/B978-0-08-102824-7.00018-X>.
- [3] I. Alshareedah, T. Kaur, and P.R. Banerjee. Methods for characterizing the material properties of biomolecular condensates. In *Methods in Enzymology*, pages 143–183. Academic Press, 2021. Vol. 646.
- [4] M. Araghi, Z. Moslehi, A. Mohammadi Nafchi, and et.al. Cold water fish gelatin modification by a natural phenolic cross-linker (ferulic acid and caffeic acid). *Food science & nutrition*, 3(5):370–375, 2015.
- [5] P. R. Avallone, E. Raccone, S. Costanzo, and et.al. Gelation kinetics of aqueous gelatin solutions in isothermal conditions via rheological tools. *Food Hydrocolloids*, 111:106248, 2021. doi:<https://doi.org/10.1016/j.foodhyd.2020.106248>.
- [6] D. Axelrod, D.E. Koppel, J. Schlessinger, E. Elson, and W.W. Webb. Mobility measurement by analysis of fluorescence photobleaching recovery kinetics. *Biophysical Journal*, 16(9):1055–1069, 1976.
- [7] S.M Baumler. *Diffusional Motion as a Gauge of Interfacial Fluidity and Adhesion of Supported Model Membrane Films*. PhD thesis, Michigan State University, 2017.
- [8] D. Blair and E. Dufresne. The matlab particle tracking code repository. <https://site.physics.georgetown.edu/matlab/>. (accessed: 17.06.2023).
- [9] S. E. Braslavsky. Glossary of terms used in photochemistry. *Pure and Applied Chemistry*, 79(3):293–465, 2007.
- [10] Britannica, The Editors of Encyclopaedia. Brownian motion. <https://www.britannica.com/science/Brownian-motion>, 4. May 2023. Accessed 14 June 2023.
- [11] A. Canette and R. Briandet. Microscopy | confocal laser scanning microscopy. In *Encyclopedia of Food Microbiology*, pages 676–683. Academic Press, 2 edition, 2014.
- [12] B. Chiou, R. J. Avena-Bustillos, P. J. Bechtel, and et.al. Cold water fish gelatin films: Effects of cross-linking on thermal, mechanical, barrier, and biodegradation properties. *European Polymer Journal*, 44(11):3748–3753, 2008. URL: <https://www.sciencedirect.com/science/article/pii/S0014305708004084>, doi:<https://doi.org/10.1016/j.eurpolymj.2008.08.011>.
- [13] A. H Clark. Biopolymer gels. *Current Opinion in Colloid & Interface Science*, 1(6):712–717, 1996. doi:[https://doi.org/10.1016/S1359-0294\(96\)80072-0](https://doi.org/10.1016/S1359-0294(96)80072-0).
- [14] Sigma Aldrich Co. Blue dextran. <https://www.sigmaaldrich.com/NO/en/product/sigma/d4772>. (accessed: 17.06.2023).
- [15] Sigma Aldrich Co. Fluorescein isothiocyanate-dextran. <https://www.sigmaaldrich.com/NO/en/technical-documents/technical-article/cell-culture-and-cell-culture-analysis/cell-based-assays/fluorescein-isothiocyanate-dextran>. (accessed: 17.06.2023).
- [16] Custom Collagen. Gelatin bloom strength types and uses. <https://customcollagen.com/gelatin-bloom-strength-types-and-uses/>. (accessed: 07.06.2023).
- [17] A. Cooper. Thermal stability of tropocollagens—are hydrogen bonds really important? *Journal of Molecular Biology*, 55(1):123–127, 1971.

-
- [18] D. Coppola, C. Lauritano, F. P. Esposito, and et.al. Fish waste: From problem to valuable resource. *Marine Drugs*, 19(2), 2021. URL: <https://www.mdpi.com/1660-3397/19/2/116>, doi: 10.3390/md19020116.
- [19] D. Coppola, C. Lauritano, F. Palma Esposito, and et.al. Fish waste: From problem to valuable resource. *Marine drugs*, 19(2):116, 2021.
- [20] C.S. Baird. Absorption of electromagnetic radiation. <https://doi.org/10.1036/1097-8542.001600>, 2019. Accessed 15 June 2023.
- [21] M. J. Dille, I. J. Haug, and K. I. Draget. Gelatin and collagen. In *Handbook of Hydrocolloids*, pages 1073–1097. Elsevier LTD., 2021.
- [22] M.J. Dille, M.N. Hattrem, and K.I. Draget. Soft, chewable gelatin-based pharmaceutical oral formulations: a technical approach. *Pharmaceutical Development and Technology*, 23(5):504–511, 2018.
- [23] A. Duconseille, T. Astruc, N. Quintana, and et al. Gelatin structure and composition linked to hard capsule dissolution: A review. *Food Hydrocolloids*, 43:360–376, 2015. doi:<https://doi.org/10.1016/j.foodhyd.2014.06.006>.
- [24] M. W. Edelman, E. van der Linden, E. de Hoog, and R. H. Tromp. Compatibility of gelatin and dextran in aqueous solution. *Biomacromolecules*, 2(4):1148–1154, 2001. doi:10.1021/bm015545f.
- [25] D. Ernst and J. Köhler. Measuring a diffusion coefficient by single-particle tracking: statistical analysis of experimental mean squared displacement curves. *Phys. Chem. Chem. Phys.*, 15:845–849, 2013. URL: <http://dx.doi.org/10.1039/C2CP43433D>, doi:10.1039/C2CP43433D.
- [26] FAO. The state of world fisheries and aquaculture 2022. Towards blue transformation. <https://doi.org/10.4060/cc0461en>, 2022. Rome.
- [27] National Center for Biotechnology Information. PubChem Compound Summary for CID 164825, Tartrazine. <https://pubchem.ncbi.nlm.nih.gov/compound/Tartrazine>. (accessed: 19.06.2023).
- [28] Gelatine.org. Gelatine: An all-rounder. <https://www.gelatine.org/en/gelatine/properties-advantages.html>. (accessed: 07.06.2023).
- [29] L. C. Geonzon, X. Zhuang, A. M. Santoya, and et.al. Gelation mechanism and network structure of mixed kappa carrageenan/lambd carrageenan gels studied by macroscopic and microscopic observation methods. *Food Hydrocolloids*, 105:105759, 2020. doi:<https://doi.org/10.1016/j.foodhyd.2020.105759>.
- [30] M.C. Gómez-Guillén, B. Giménez, M.E. López-Caballero, and M.P. Montero. Functional and bioactive properties of collagen and gelatin from alternative sources: A review. *Food Hydrocolloids*, 25(8):1813–1827, 2011. doi:<https://doi.org/10.1016/j.foodhyd.2011.02.007>.
- [31] Z.A. Nur Hanani, Y.H. Roos, and J.P. Kerry. Use and application of gelatin as potential biodegradable packaging materials for food products. *International Journal of Biological Macromolecules*, 71:94–102, 2014.
- [32] P. Harris, V. Normand, and I.T. Norton. Gelatin. In *Encyclopedia of Food Sciences and Nutritions*, page 2865. Elsevier LTD., 2 edition, 2003.
- [33] Fortune Business Insights. Gelatin Market Size, Share & COVID-19 Impact Analysis, By Source (Porcine, Bovine, and Others), By Application (Food & Beverages, Healthcare & Pharmaceuticals, Cosmetics, and Others), and Regional Forecast, 2022-2029. <https://www.fortunebusinessinsights.com/gelatin-market-107012>. (accessed: 19.06.2023).
- [34] F. A. Johnston-Banks. Gelatine. In *FOOD GELS*, pages 233–289. ELSEVIER SCIENCE PUBLISHERS LTD, 1990.
-

-
- [35] T.R. Keenan. *Polymer science: A comprehensive reference*. volume 10, pages 237–247. Elsevier, 2012.
- [36] G. Koulouras, A. Panagopoulos, M.A. Rapsomaniki, and et.al. Easyfrap-web: a web-based tool for the analysis of fluorescence recovery after photobleaching data. <https://easyfrap.vmnnet.upatras.gr/>. *Nucleic Acids Res.* 2018;46(W1):W467-W472.
- [37] K. G. Landsem. *Diffusion in mixtures of mammalian and cold-water fish gelatin*. PhD thesis, Norwegian University of Science and technology, 2022.
- [38] P. A. Levin and E. R. Angert. Small but mighty: Cell size and bacteria. *Cold Spring Harbor perspectives in biology*, 7:a019216, 2015. doi:10.1101/cshperspect.a019216.
- [39] Kenney % Ross Ltd. Testing and specifications. http://kenneyandrosslimited.com/index.php?option=com_content&view=article&id=18&Itemid=250. (accessed: 17.06.2023).
- [40] Y. Lu, Q. Luo, Y. Chu, and et.al. Application of gelatin in food packaging: A review. *Polymers*, 14(3):436, 2022.
- [41] Q. Luo, Md A. Hossen, Y. Zeng, and et.al. Gelatin-based composite films and their application in food packaging: A review. *Journal of Food Engineering*, 313:110762, 2022.
- [42] A.S. Maddox and P.S. Maddox. High-resolution imaging of cellular processes in caenorhabditis elegans. *Methods in Cell Biology*, 107:1–34, 2012.
- [43] Y. Maki and M. Annaka. Gelation of fish gelatin studied by multi-particle tracking method. *Food Hydrocolloids*, 101:105525, 2020. doi:<https://doi.org/10.1016/j.foodhyd.2019.105525>.
- [44] A. A. Mariod and H. F. Adam. Review: Gelatin, source, extraction and industrial applications. *Acta Scientiarum Polonorum Technologia Alimentaria*, 12(2):135–147, 2013.
- [45] R. Metzler, Jeon J, A. G. Cherstvy, and E. Barkai. Anomalous diffusion models and their properties: non-stationarity, non-ergodicity, and ageing at the centenary of single particle tracking. *Physical Chemistry Chemical Physics*, 16:24128–24164, 2014. URL: <http://dx.doi.org/10.1039/C4CP03465A>, doi:10.1039/C4CP03465A.
- [46] J. Miné and I. Chiolo. Complex chromatin motions for dna repair. *Frontiers in Genetics*, 11, 08 2020. doi:10.3389/fgene.2020.00800.
- [47] R. Moučka, M. Sedlačik, and Z. Pátiková. Fractional viscoelastic models of porcine skin and its gelatin-based surrogates. *Mechanics of Materials*, 177:104559, 2023. doi:<https://doi.org/10.1016/j.mechmat.2023.104559>.
- [48] Alan H. Muhr and John M.V. Blanshard. Diffusion in gels. *Polymer*, 23(7):1012–1026, 1982. doi:[https://doi.org/10.1016/0032-3861\(82\)90402-5](https://doi.org/10.1016/0032-3861(82)90402-5).
- [49] T. Petcharat, S. Benjakul, and Y. Hemar. Improvement of gel properties of fish gelatin using gellan. *INTERNATIONAL JOURNAL OF FOOD ENGINEERING*, 13(8), AUG 2017. doi:10.1515/ijfe-2016-0410.
- [50] G. Renaldi, N. Sirinupong, and R. S. Samakradhamrongthai. Gelation. *Food Science Technology Today*, 6(4):236–241, 1992.
- [51] G. Renaldi, N. Sirinupong, and R. S. Samakradhamrongthai. Effect of extraction ph and temperature on yield and physicochemical properties of gelatin from atlantic salmon (salmo salar) skin. *AGRICULTURE AND NATURAL RESOURCES*, 56:687–696, 2022.
- [52] Grand View Research. Gelatin market size, share & trends analysis report by source (bovine, porcine), by function (stabilizer, thickener), by application (food & beverages), by region, and segment forecasts, 2022 - 2030. <https://www.grandviewresearch.com/industry-analysis/gelatin-market-analysis>. (accessed: 07.06.2023).
-

-
- [53] Grand View Research. Hydrocolloids market size, share & trends analysis report by product (gelatin, xanthan gum, carrageenan, alginates, pectin, guar gum, carboxy methyl cellulose), by function, by application, and segment forecasts, 2020 - 2025. <https://www.grandviewresearch.com/industry-analysis/hydrocolloids-market>. (accessed: 07.06.2023).
- [54] Sylvie Ricard-Blums. The collagen family. *Cold Spring Harb Perspect Biol*, 3(1), 2011. doi: <https://cshperspectives.cshlp.org/content/3/1/a004978>.
- [55] I.F. Sbalzarini and P. Koumoutsakos. Feature point tracking and trajectory analysis for video imaging in cell biology. *Journal of Structural Biology*, 151(2):182–195, 2005. doi:<https://doi.org/10.1016/j.jsb.2005.06.002>.
- [56] H. Shen, L.J. Tauzin, R. Baiyasi, and et.al. Single particle tracking: From theory to biophysical applications. *Chemical Reviews*, 117(11):7331–7376, 2017. doi:10.1021/acs.chemrev.6b00815.
- [57] M.D. Shoulders and R.T. Raines. Collagen structure and stability. *Annu Rev Biochem*, 78:929–958, 2009.
- [58] S. Song, J. Wang, Z. Cheng, and et.al. Directional molecular sliding movement in peptide hydrogels accelerates cell proliferation. *Chemical Science*, 11:1383–1393, 2020. doi:10.1039/C9SC05808G.
- [59] Toyochi Tanaka. Gels. *Scientific American*, 244(1):124–S–17, 1981. URL: <http://www.jstor.org/stable/24964265>.
- [60] C. Tang, K. Zhou, Y. Zhu, and et.al. Collagen and its derivatives: From structure and properties to their applications in food industry. *Food Hydrocolloids*, 131:107748, 2022. doi: <https://doi.org/10.1016/j.foodhyd.2022.107748>.
- [61] N. Tarantino, J. Tinevez, E. F. Crowell, and et.al. TNF and IL-1 exhibit distinct ubiquitin requirements for inducing NEMO–IKK supramolecular structures. *Journal of Cell Biology*, 204(2):231–245, 2014. doi:10.1083/jcb.201307172.
- [62] The United States Pharmacopeial Convention. (711) DISSOLUTION. https://www.usp.org/sites/default/files/usp/document/harmonization/gen-method/stage_6_monograph_25_feb_2011.pdf, December 1, 2011.
- [63] B. Valeur and M. N B. Santos. A brief history of fluorescence and phosphorescence before the emergence of quantum theory. *Journal of Chemical Education*, 88(3):731–738, 2011. doi: 10.1021/ed100182h.
- [64] W. Ockenga and J. DeRose. An introduction to fluorescence. <https://www.leica-microsystems.com/science-lab/life-science/an-introduction-to-fluorescence/>, May 31, 2011.
- [65] Y. Wang, X. Liu, X. Li, and et.al. Directional and path-finding motion of polymer hydrogels driven by liquid mixing. *Langmuir*, 28(31):11276–11280, 2012. doi:10.1021/1a301972r.
- [66] L. Wu. Chapter 7 - analysis of food additives. In C. M. Galanakis, editor, *Innovative Food Analysis*, pages 157–180. Academic Press, 2021. doi:<https://doi.org/10.1016/B978-0-12-819493-5.00007-8>.
- [67] M. Xavier. Mean square displacement analysis of single-particle trajectories with localization error: Brownian motion in an isotropic medium. *Physical review. E, Statistical, nonlinear, and soft matter physics*, 82,4, 2010. doi:10.1103/PhysRevE.82.041914.
- [68] T. Zhang, R. Sun, M. Ding, and et.al. Commercial cold-water fish skin gelatin and bovine bone gelatin: Structural, functional, and emulsion stability differences. *Methods in Cell Biology*, 125:109207, 2020.
-

Appendix

A Particle tracking MSD data

Below are all raw and drift corrected MSD curves. All drift corrected data is presented alongside the respective raw data.

A.1 Particle tracking performed at TUMSAT

A.1.1 Particle tracking at 5 °C

A.1.1.1 Porcine gels

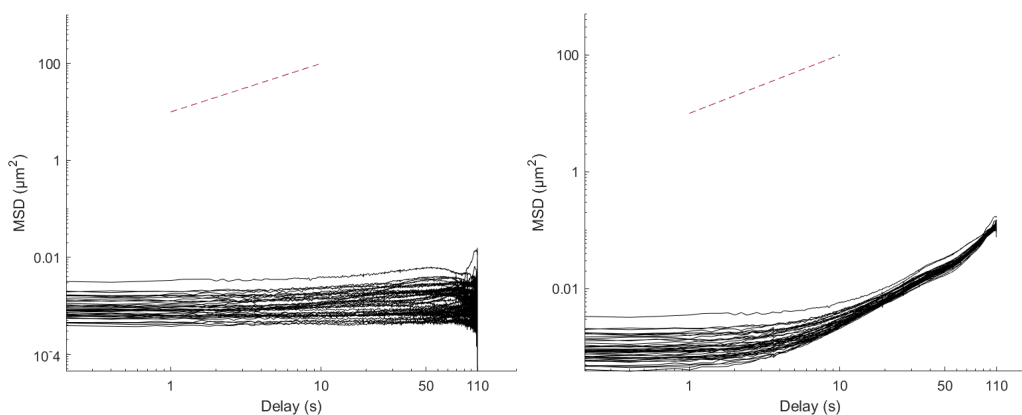


Figure 50: Parallel 1: MSD curves for particles tracked in porcine gelatin of 18 w% concentration, measured at 5 °C. Raw MSD curves are shown on the right, with drift corrected curves on the left.

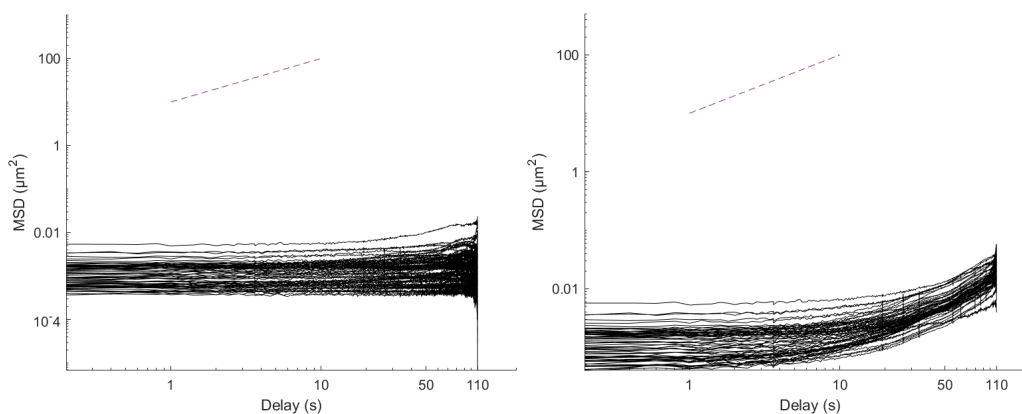


Figure 51: Parallel 2: MSD curves for particles tracked in porcine gelatin of 18 w% concentration, measured at 5 °C. Raw MSD curves are shown on the right, with drift corrected curves on the left.

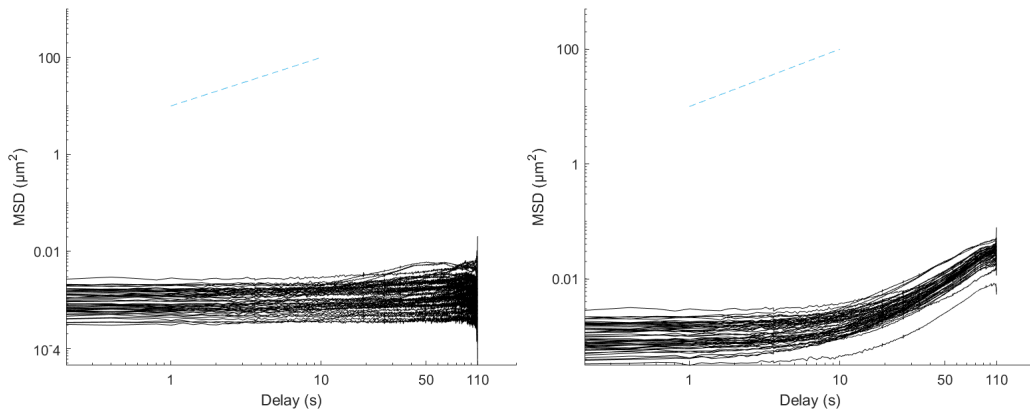


Figure 52: Parallel 3: MSD curves for particles tracked in porcine gelatin of 18 w% concentration, measured at 5 °C. Raw MSD curves are shown on the right, with drift corrected curves on the left.

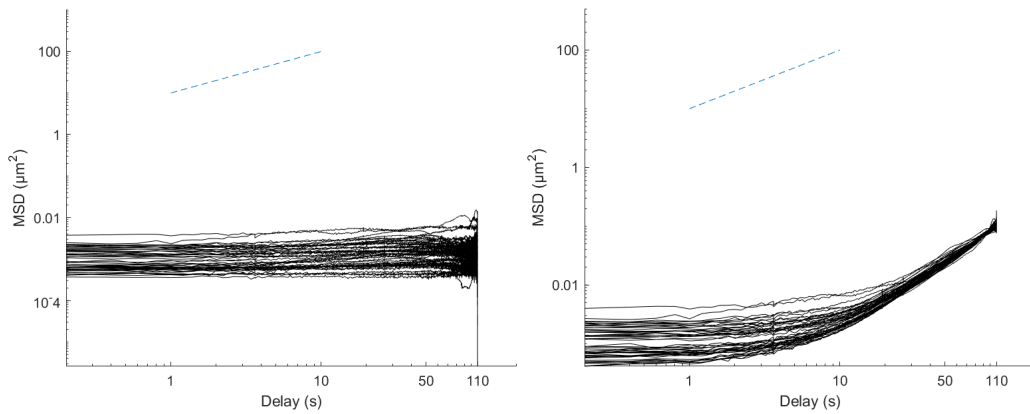


Figure 53: Parallel 4: MSD curves for particles tracked in porcine gelatin of 18 w% concentration, measured at 5 °C. Raw MSD curves are shown on the right, with drift corrected curves on the left.

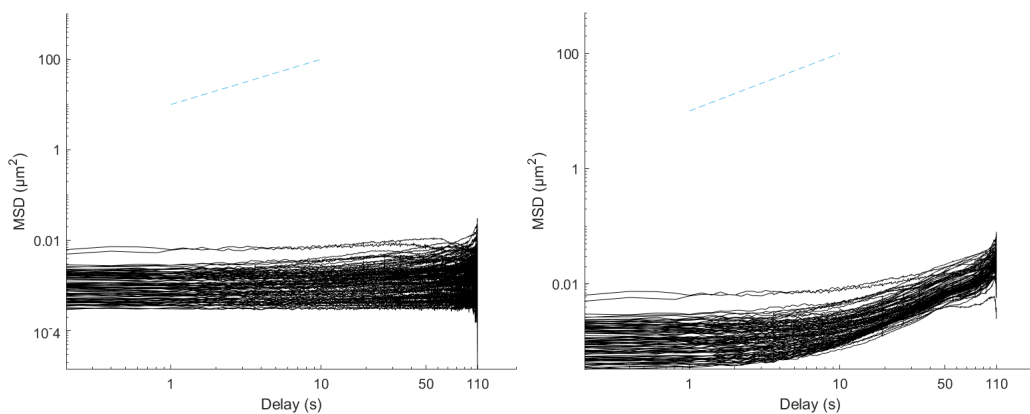


Figure 54: Parallel 5: MSD curves for particles tracked in porcine gelatin of 18 w% concentration, measured at 5 °C. Raw MSD curves are shown on the right, with drift corrected curves on the left.

A.1.1.2 Cold-water fish gels

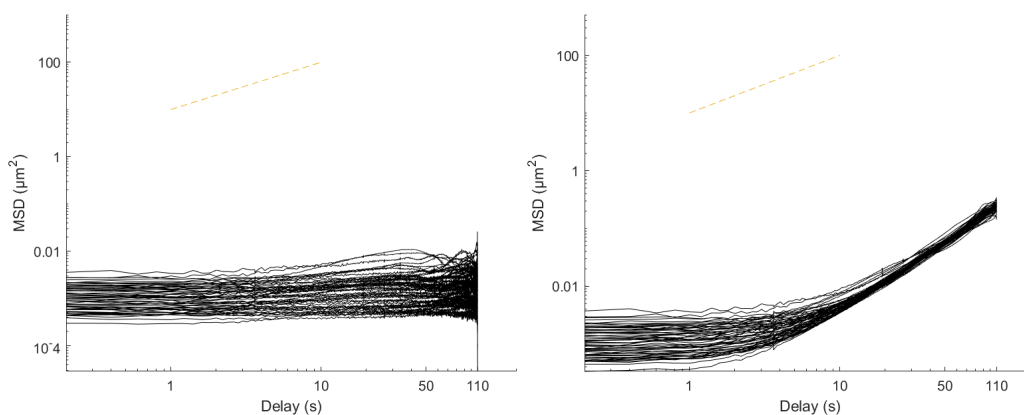


Figure 55: Parallel 1: MSD curves for particles tracked in cold-water fish gelatin of 18 w% concentration, measured at 5 °C. Raw MSD curves are shown on the right, with drift corrected curves on the left.

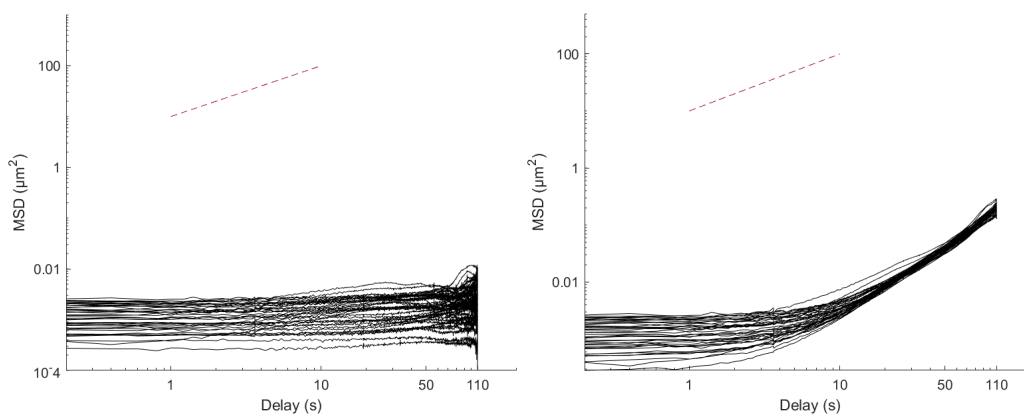


Figure 56: Parallel 2: MSD curves for particles tracked in cold-water fish gelatin of 18 w% concentration, measured at 5 °C. Raw MSD curves are shown on the right, with drift corrected curves on the left.

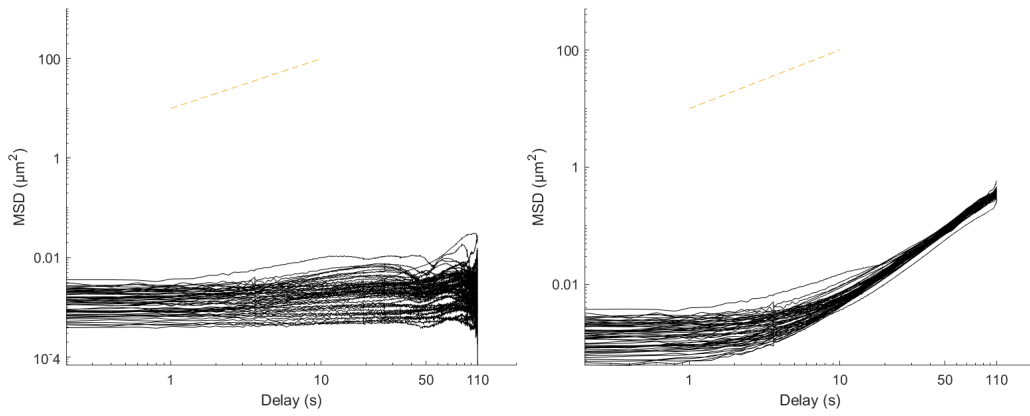


Figure 57: Parallel 3: MSD curves for particles tracked in cold-water fish gelatin of 18 w% concentration, measured at 5 °C. Raw MSD curves are shown on the right, with drift corrected curves on the left.

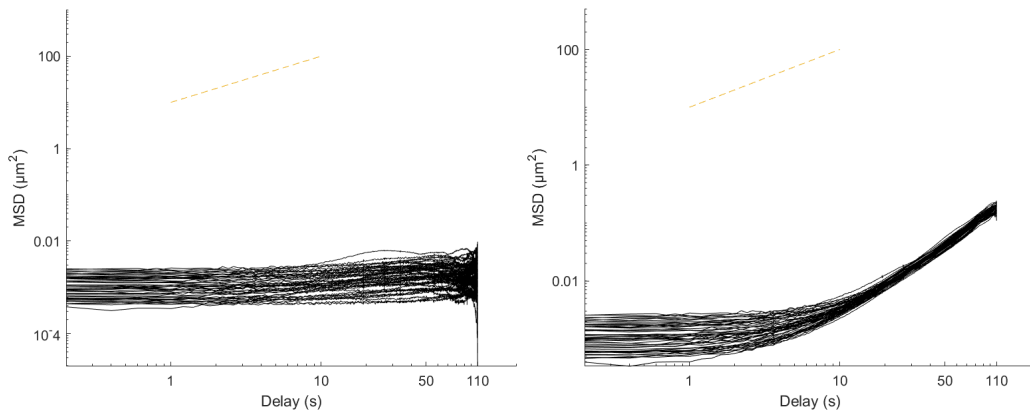


Figure 58: Parallel 4: MSD curves for particles tracked in cold-water fish gelatin of 18 w% concentration, measured at 5 °C. Raw MSD curves are shown on the right, with drift corrected curves on the left.

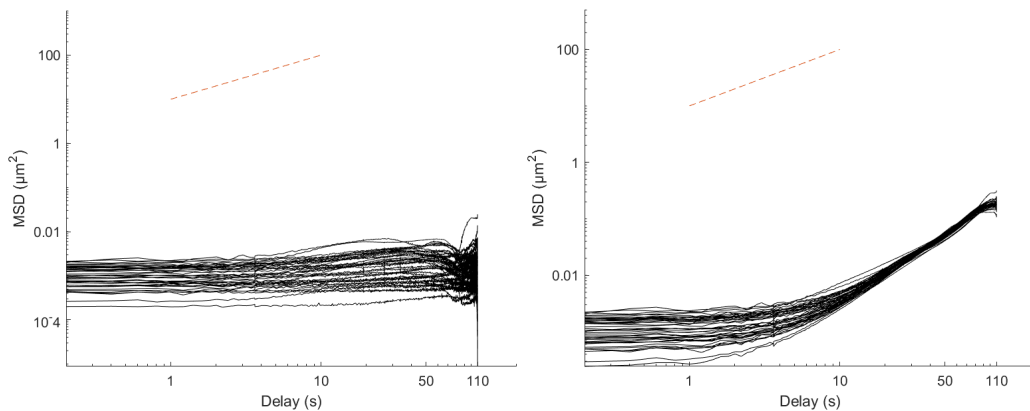


Figure 59: Parallel 5: MSD curves for particles tracked in cold-water fish gelatin of 18 w% concentration, measured at 5 °C. Raw MSD curves are shown on the right, with drift corrected curves on the left.

A.1.1.3 50-50 mixed gels

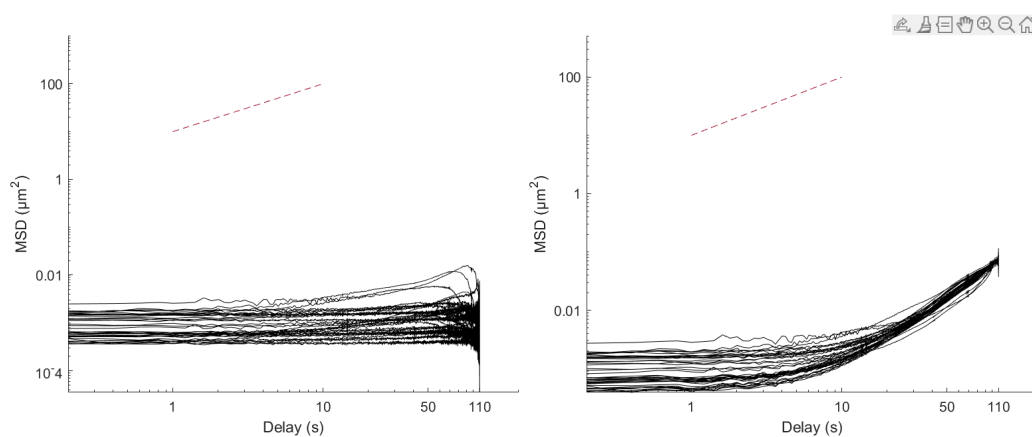


Figure 60: Parallel 1: MSD curves for particles tracked in a mixture of equal parts porcine and cold-water fish gelatin with a total gelatin concentration of 18 w%, measured at 5 °C. Raw MSD curves are shown on the right, with drift corrected curves on the left.

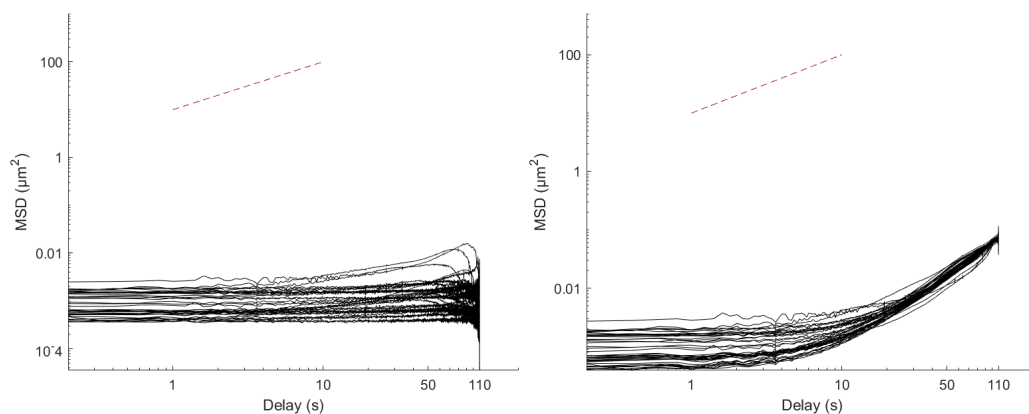


Figure 61: Parallel 2: MSD curves for particles tracked in a mixture of equal parts porcine and cold-water fish gelatin with a total gelatin concentration of 18 w%, measured at 5 °C. Raw MSD curves are shown on the right, with drift corrected curves on the left.

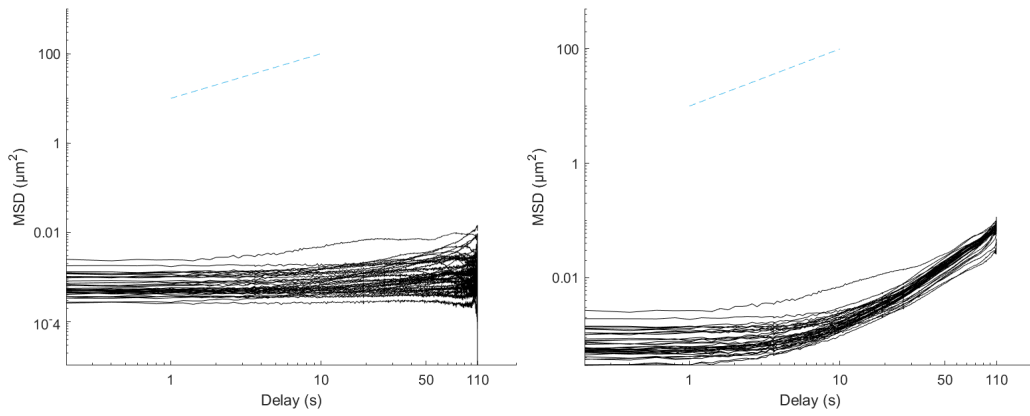


Figure 62: Parallel 3: MSD curves for particles tracked in a mixture of equal parts porcine and cold-water fish gelatin with a total gelatin concentration of 18 w%, measured at 5 °C. Raw MSD curves are shown on the right, with drift corrected curves on the left.

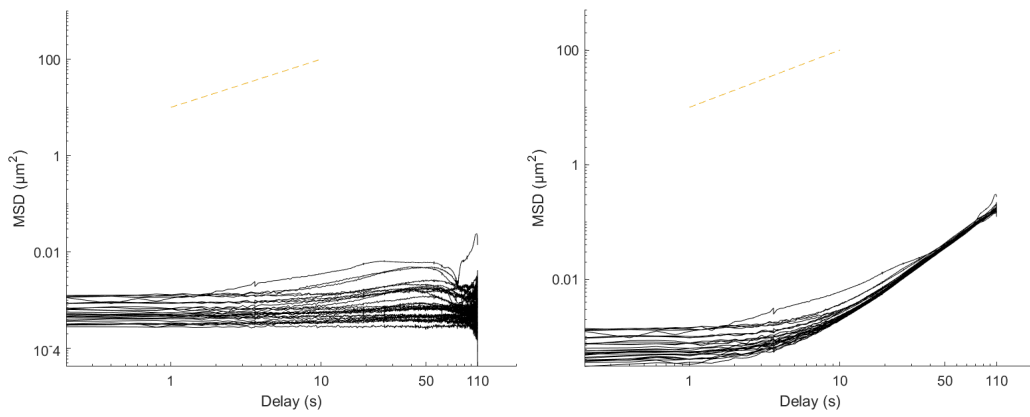


Figure 63: Parallel 4: MSD curves for particles tracked in a mixture of equal parts porcine and cold-water fish gelatin with a total gelatin concentration of 18 w%, measured at 5 °C. Raw MSD curves are shown on the right, with drift corrected curves on the left.

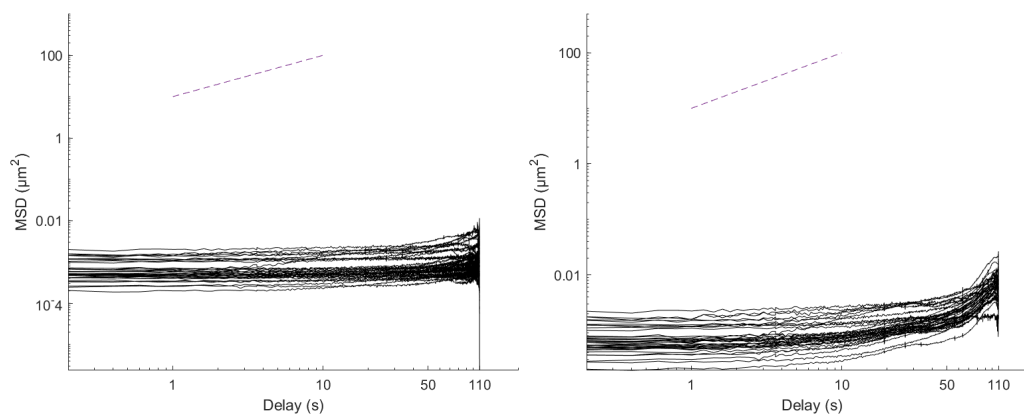


Figure 64: Parallel 5: MSD curves for particles tracked in a mixture of equal parts porcine and cold-water fish gelatin with a total gelatin concentration of 18 w%, measured at 5 °C. Raw MSD curves are shown on the right, with drift corrected curves on the left.

A.1.2 Particle tracking at 20 °C

A.1.2.1 Porcine gels

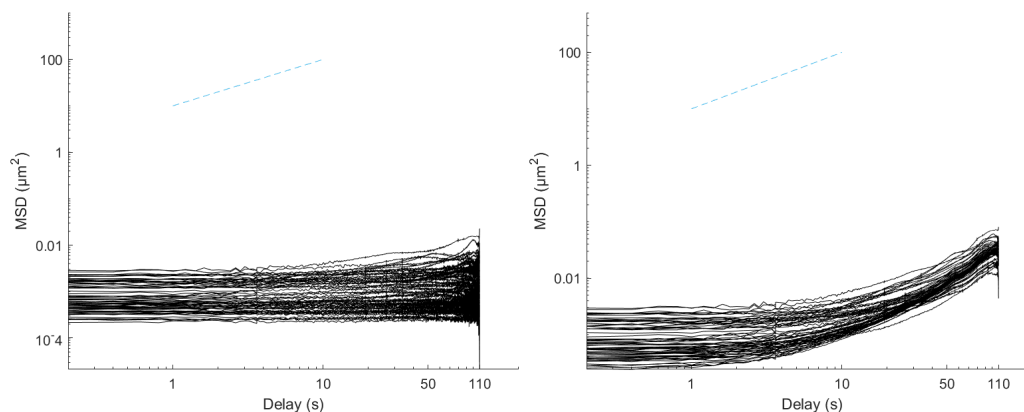


Figure 65: Parallel 1: MSD curves for particles tracked in porcine gelatin of 18 w% concentration, measured at 20 °C. Raw MSD curves are shown on the right, with drift corrected curves on the left.

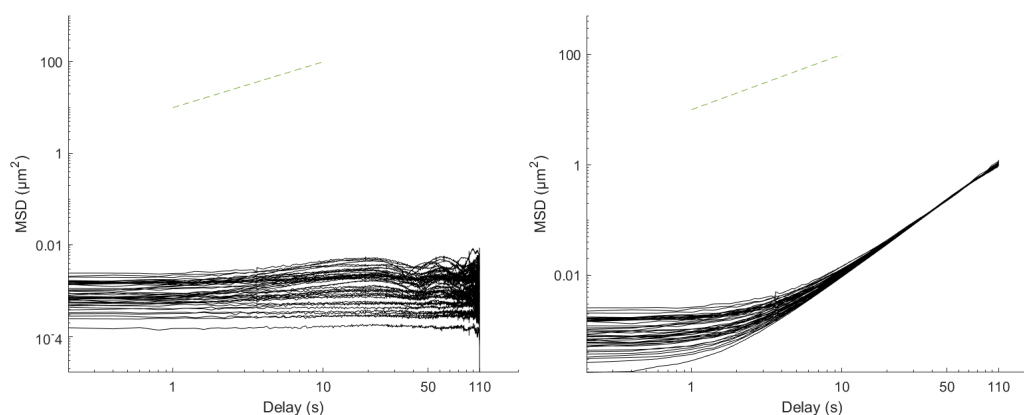


Figure 66: Parallel 2: MSD curves for particles tracked in porcine gelatin of 18 w% concentration, measured at 20 °C. Raw MSD curves are shown on the right, with drift corrected curves on the left.

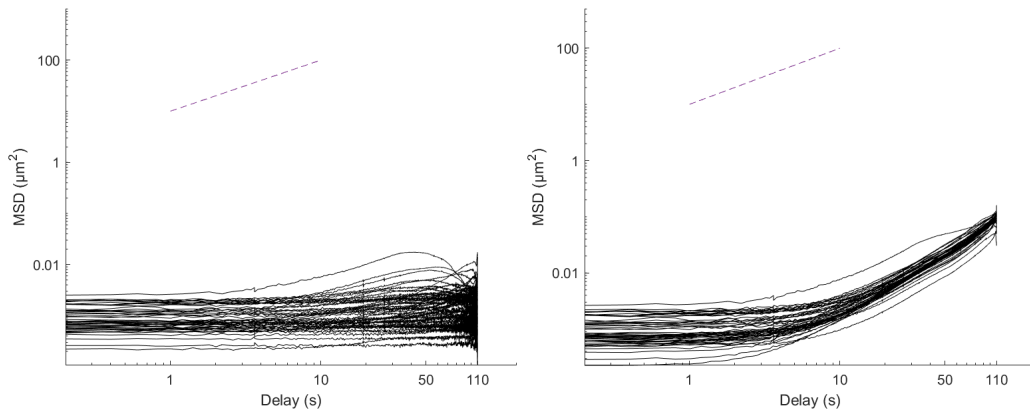


Figure 67: Parallel 3: MSD curves for particles tracked in porcine gelatin of 18 w% concentration, measured at 20 °C. Raw MSD curves are shown on the right, with drift corrected curves on the left.

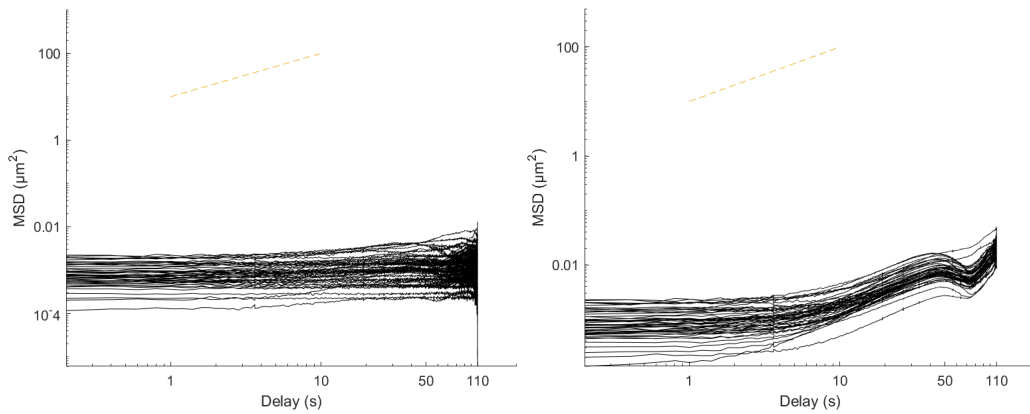


Figure 68: Parallel 4: MSD curves for particles tracked in porcine gelatin of 18 w% concentration, measured at 20 °C. Raw MSD curves are shown on the right, with drift corrected curves on the left.

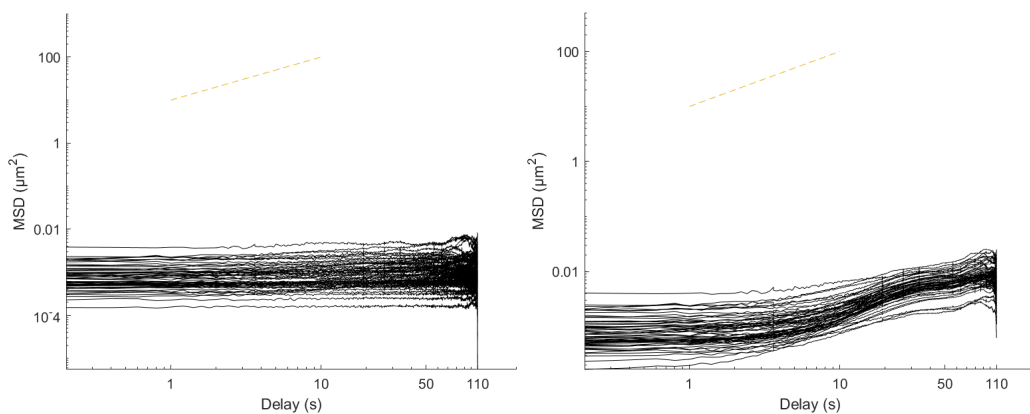


Figure 69: Parallel 5: MSD curves for particles tracked in porcine gelatin of 18 w% concentration, measured at 20 °C. Raw MSD curves are shown on the right, with drift corrected curves on the left.

A.1.2.2 Cold-water fish gels

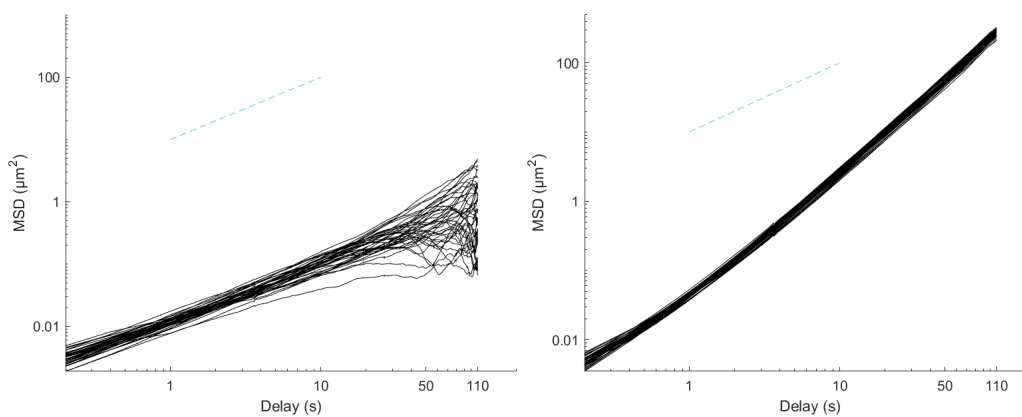


Figure 70: Parallel 1: MSD curves for particles tracked in cold-water fish gelatin of 18 w% concentration, measured at 20 °C. Raw MSD curves are shown on the right, with drift corrected curves on the left.

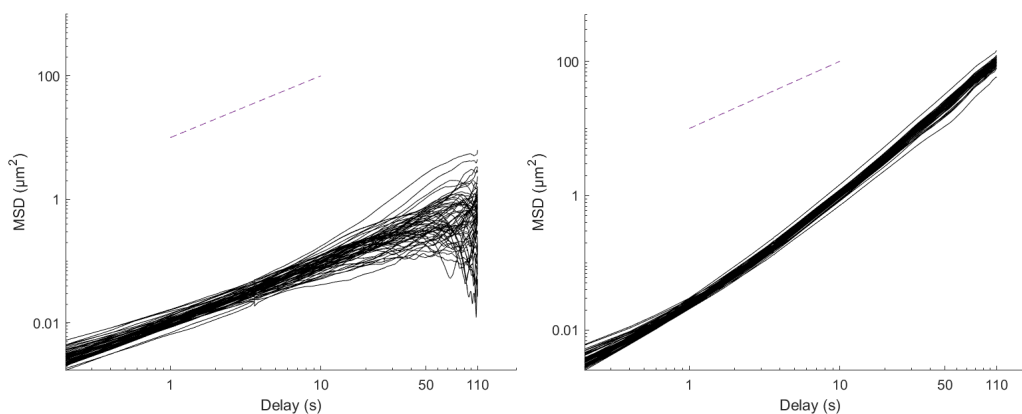


Figure 71: Parallel 2: MSD curves for particles tracked in cold-water fish gelatin of 18 w% concentration, measured at 20 °C. Raw MSD curves are shown on the right, with drift corrected curves on the left.

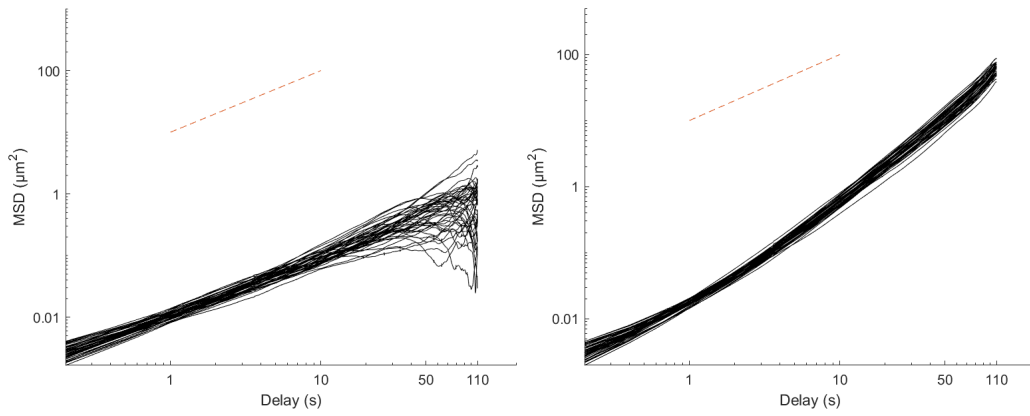


Figure 72: Parallel 3: MSD curves for particles tracked in cold-water fish gelatin of 18 w% concentration, measured at 20 °C. Raw MSD curves are shown on the right, with drift corrected curves on the left.

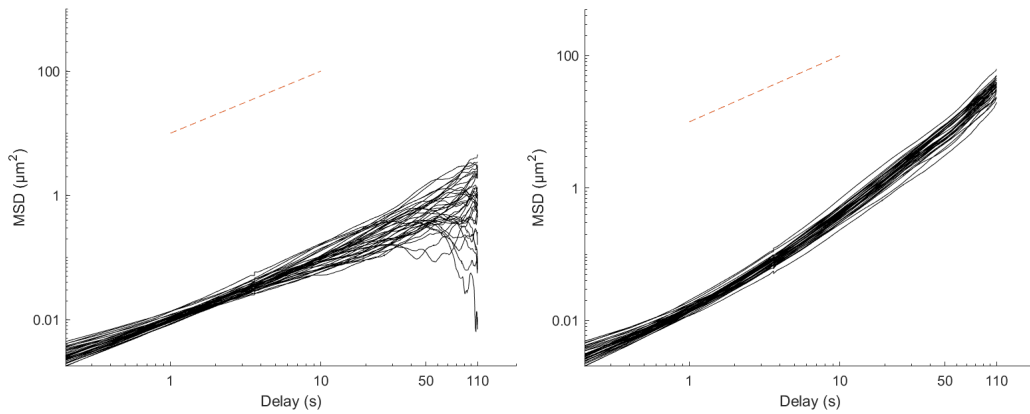


Figure 73: Parallel 4: MSD curves for particles tracked in cold-water fish gelatin of 18 w% concentration, measured at 20 °C. Raw MSD curves are shown on the right, with drift corrected curves on the left.

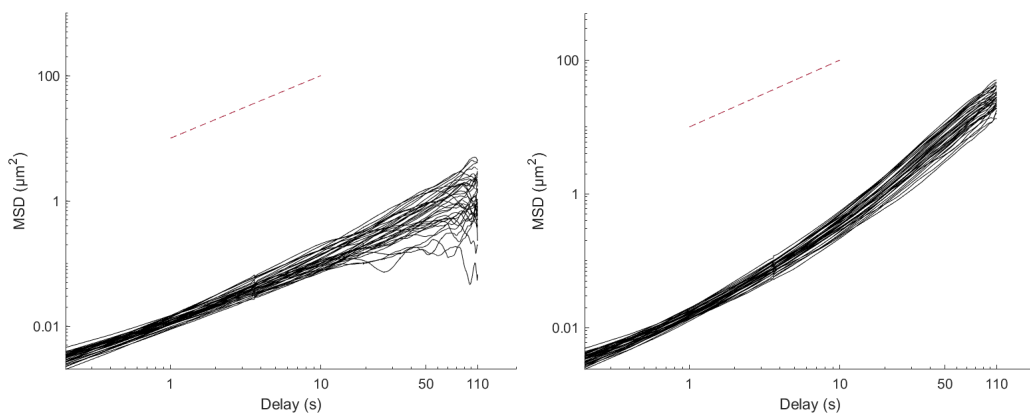


Figure 74: Parallel 5: MSD curves for particles tracked in cold-water fish gelatin of 18 w% concentration, measured at 20 °C. Raw MSD curves are shown on the right, with drift corrected curves on the left.

A.1.2.3 50-50 mixed gels

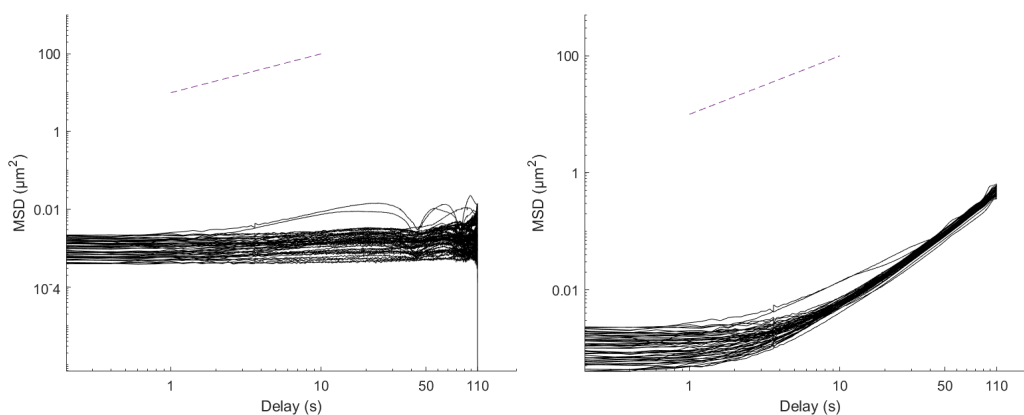


Figure 75: Parallel 1: MSD curves for particles tracked in a mixture of equal parts porcine and cold-water fish gelatin with a total gelatin concentration of 18 w%, measured at 20 °C. Raw MSD curves are shown on the right, with drift corrected curves on the left.

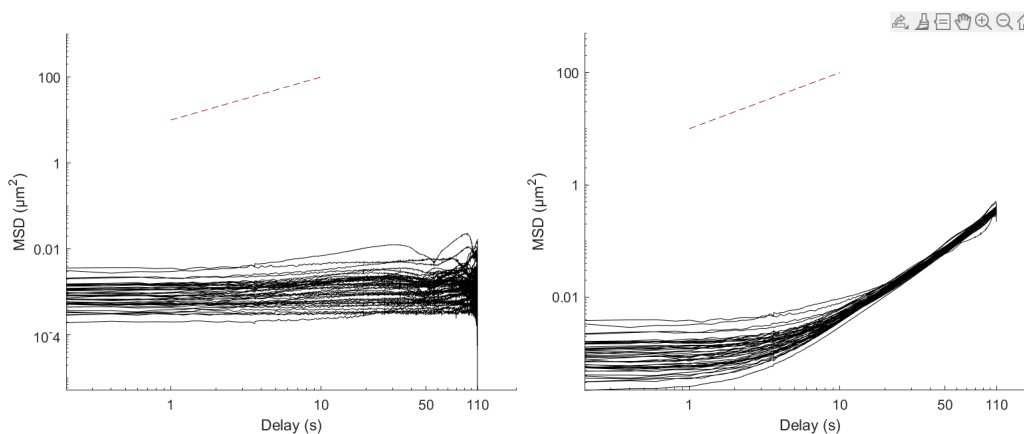


Figure 76: Parallel 2: MSD curves for particles tracked in a mixture of equal parts porcine and cold-water fish gelatin with a total gelatin concentration of 18 w%, measured at 20 °C. Raw MSD curves are shown on the right, with drift corrected curves on the left.

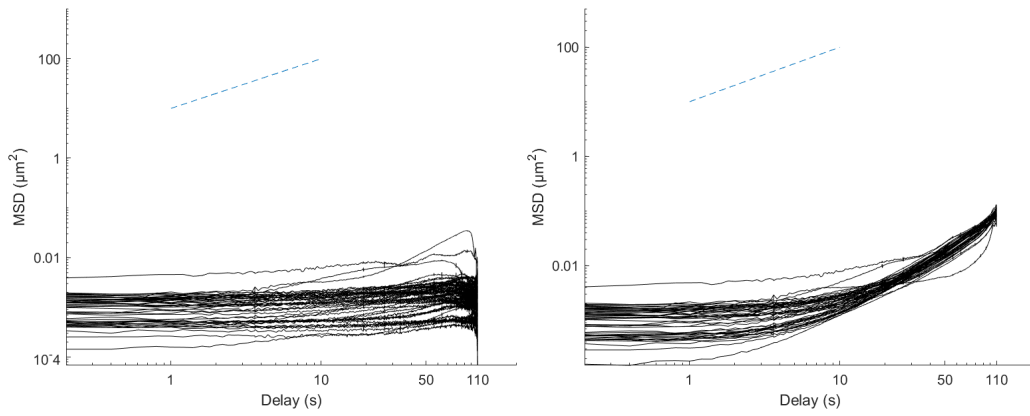


Figure 77: Parallel 3: MSD curves for particles tracked in a mixture of equal parts porcine and cold-water fish gelatin with a total gelatin concentration of 18 w%, measured at 20 °C. Raw MSD curves are shown on the right, with drift corrected curves on the left.

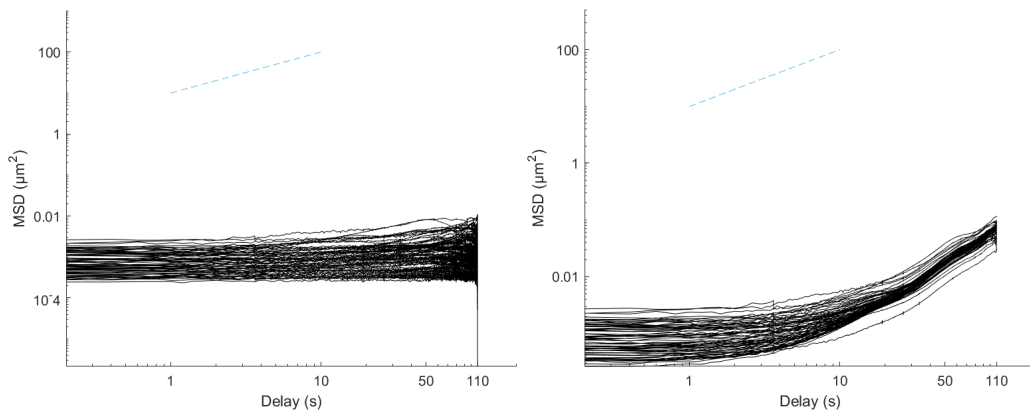


Figure 78: Parallel 4: MSD curves for particles tracked in a mixture of equal parts porcine and cold-water fish gelatin with a total gelatin concentration of 18 w%, measured at 20 °C. Raw MSD curves are shown on the right, with drift corrected curves on the left.

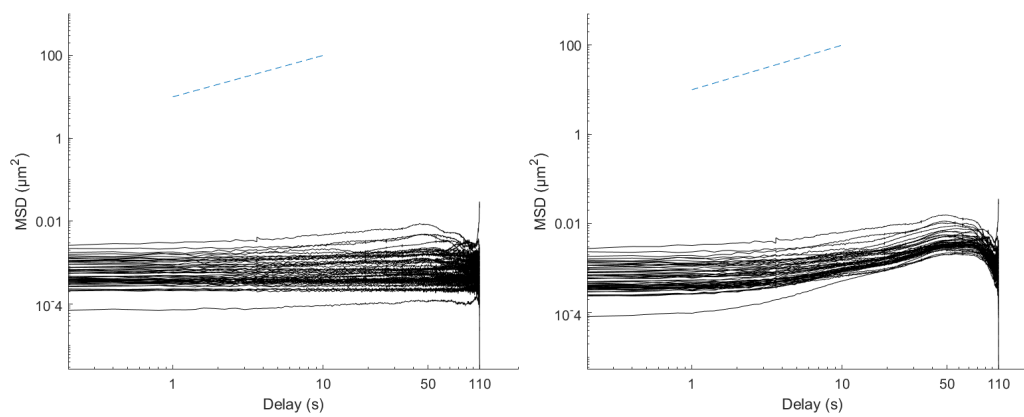


Figure 79: Parallel 5: MSD curves for particles tracked in a mixture of equal parts porcine and cold-water fish gelatin with a total gelatin concentration of 18 w%, measured at 20 °C. Raw MSD curves are shown on the right, with drift corrected curves on the left.

A.2 Particle tracking performed at NTNU

A.2.1 Porcine gels

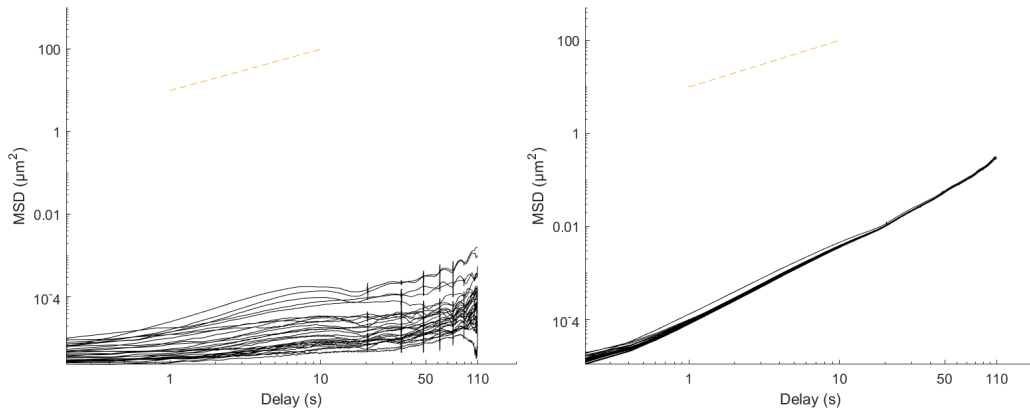


Figure 80: Parallel 1: MSD curves for particles tracked in porcine gelatin of 18 w% concentration, measured at room temperature. Raw MSD curves are shown on the right, with drift corrected curves on the left.

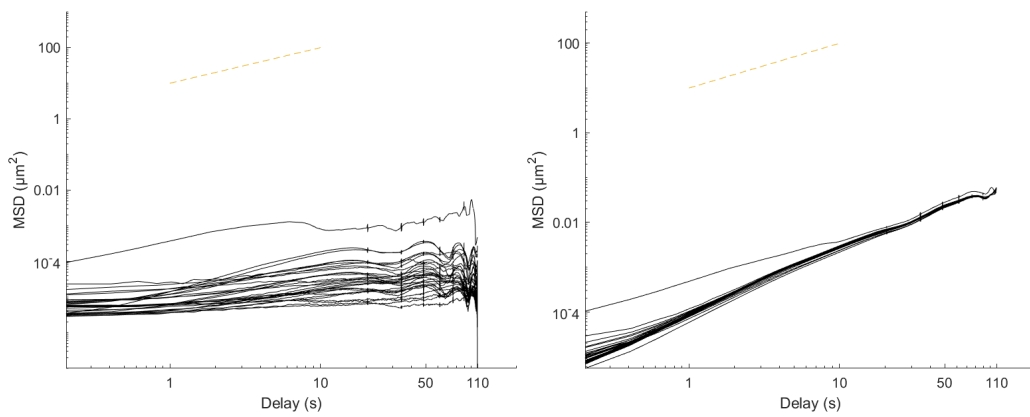


Figure 81: Parallel 2: MSD curves for particles tracked in porcine gelatin of 18 w% concentration, measured at room temperature. Raw MSD curves are shown on the right, with drift corrected curves on the left.

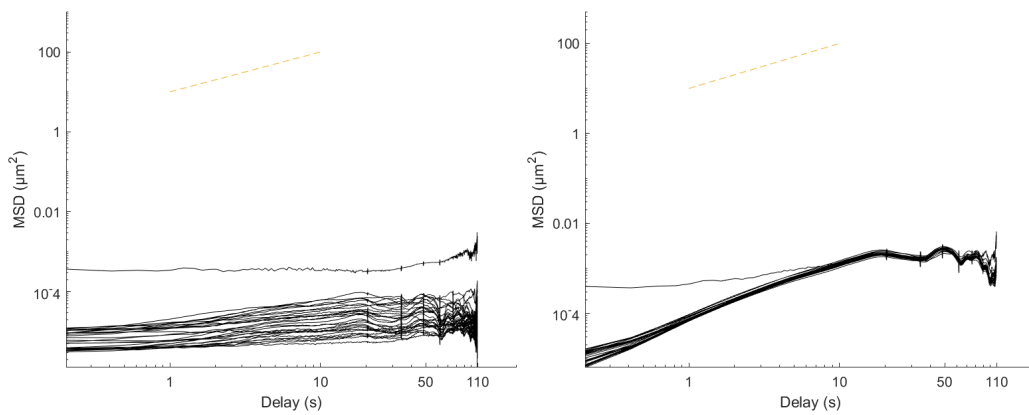


Figure 82: Parallel 3: MSD curves for particles tracked in porcine gelatin of 18 w% concentration, measured at room temperature. Raw MSD curves are shown on the right, with drift corrected curves on the left.

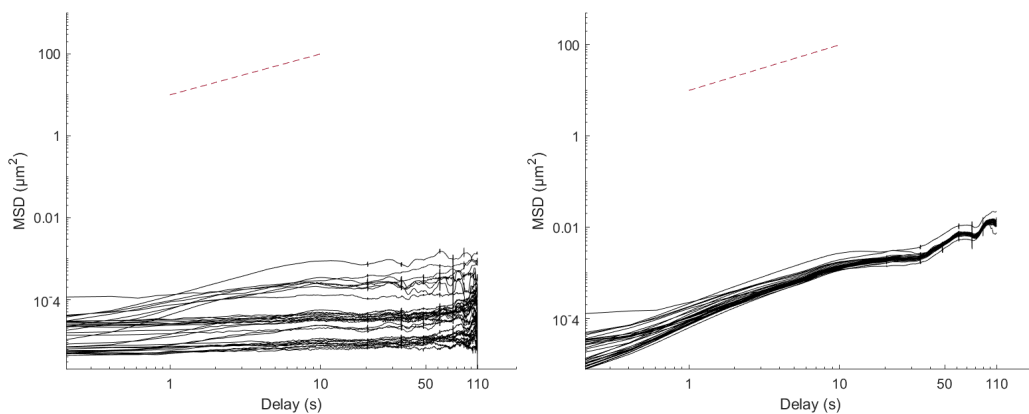


Figure 83: Parallel 4: MSD curves for particles tracked in porcine gelatin of 18 w% concentration, measured at room temperature. Raw MSD curves are shown on the right, with drift corrected curves on the left.

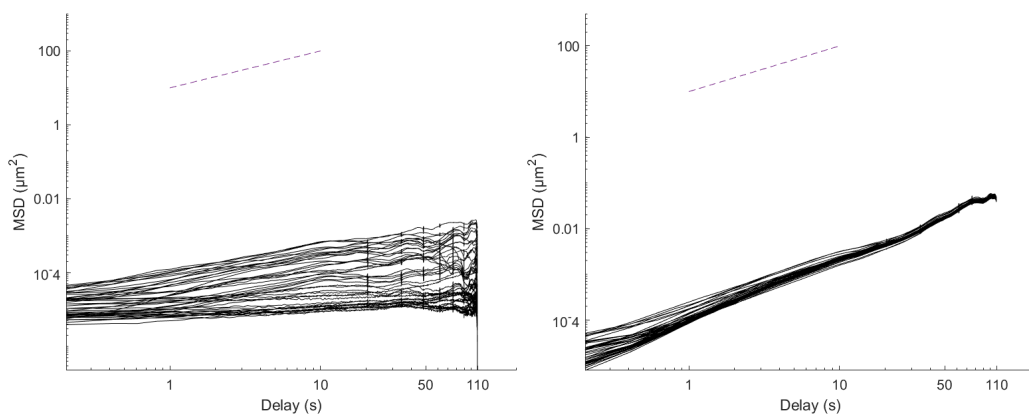


Figure 84: Parallel 5: MSD curves for particles tracked in porcine gelatin of 18 w% concentration, measured at room temperature. Raw MSD curves are shown on the right, with drift corrected curves on the left.

A.2.2 Cold-water fish gels

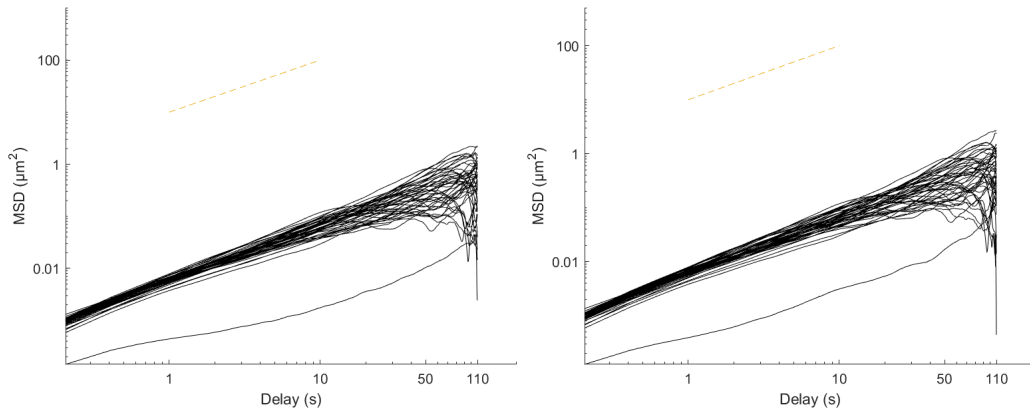


Figure 85: Parallel 1: MSD curves for particles tracked in cold-water fish gelatin of 18 w% concentration, measured at room temperature. Raw MSD curves are shown on the right, with drift corrected curves on the left.

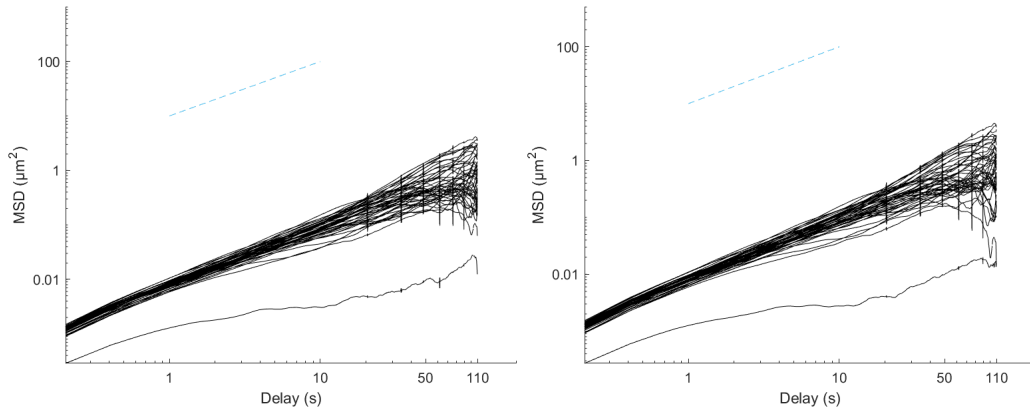


Figure 86: Parallel 2: MSD curves for particles tracked in cold-water fish gelatin of 18 w% concentration, measured at room temperature. Raw MSD curves are shown on the right, with drift corrected curves on the left.

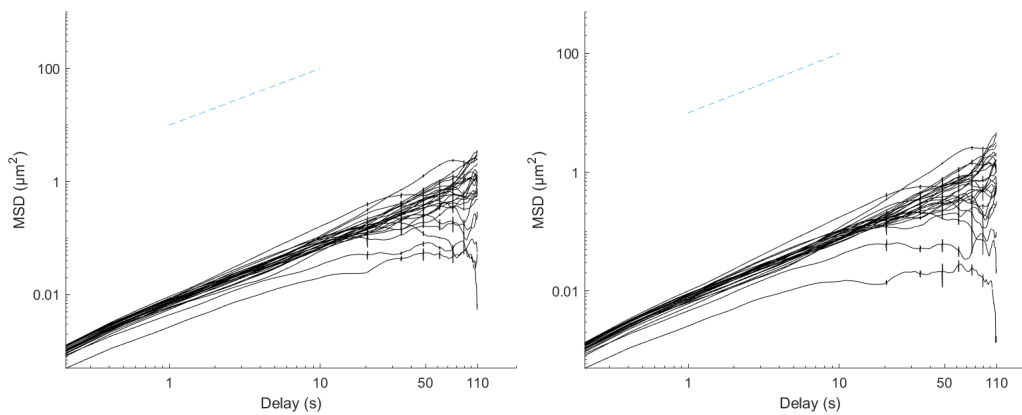


Figure 87: Parallel 3: MSD curves for particles tracked in cold-water fish gelatin of 18 w% concentration, measured at room temperature. Raw MSD curves are shown on the right, with drift corrected curves on the left.

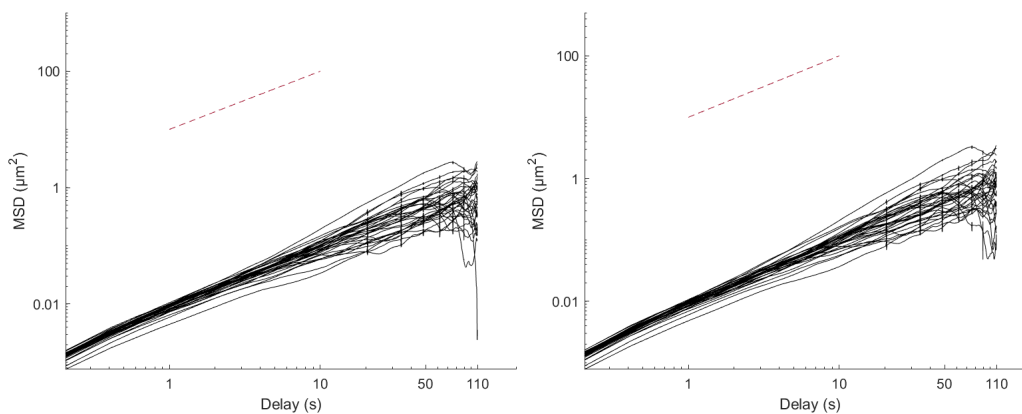


Figure 88: Parallel 4: MSD curves for particles tracked in cold-water fish gelatin of 18 w% concentration, measured at room temperature. Raw MSD curves are shown on the right, with drift corrected curves on the left.

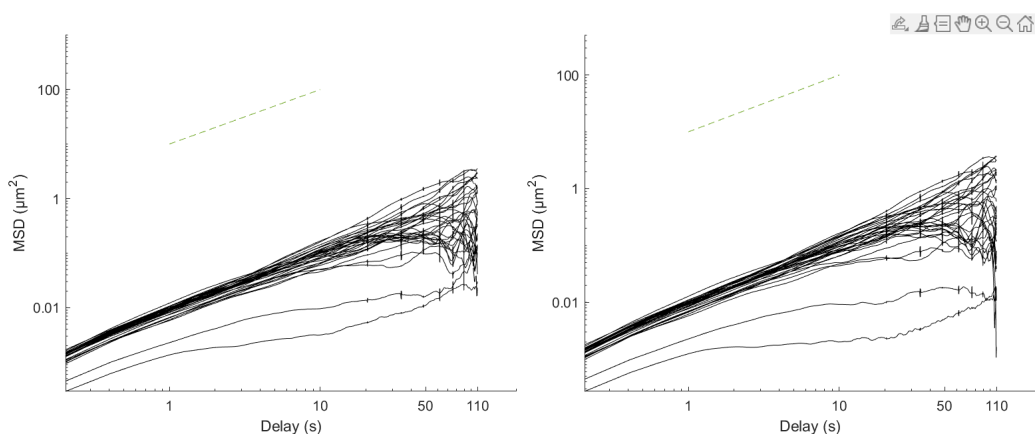


Figure 89: Parallel 5: MSD curves for particles tracked in cold-water fish gelatin of 18 w% concentration, measured at room temperature. Raw MSD curves are shown on the right, with drift corrected curves on the left.

A.2.3 50-50 mixed gels

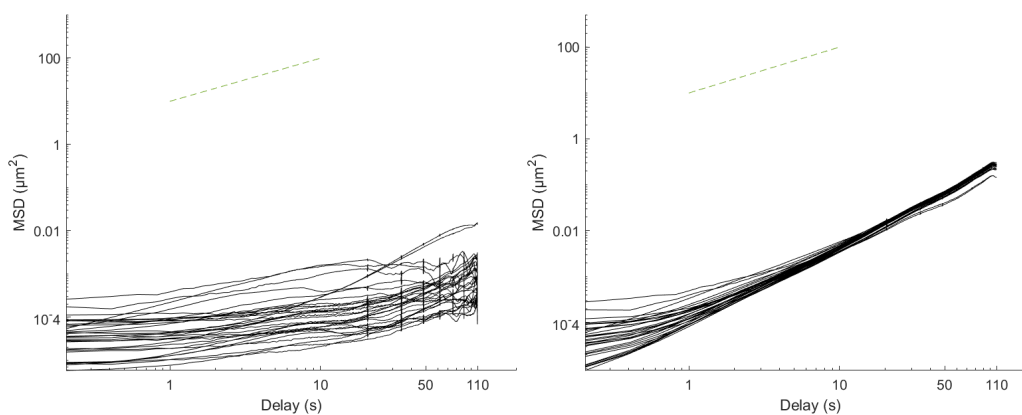


Figure 90: Parallel 1: MSD curves for particles tracked in a mixture of equal parts porcine and cold-water fish gelatin with a total gelatin concentration of 18 w%, measured at room temperature. Raw MSD curves are shown on the right, with drift corrected curves on the left.

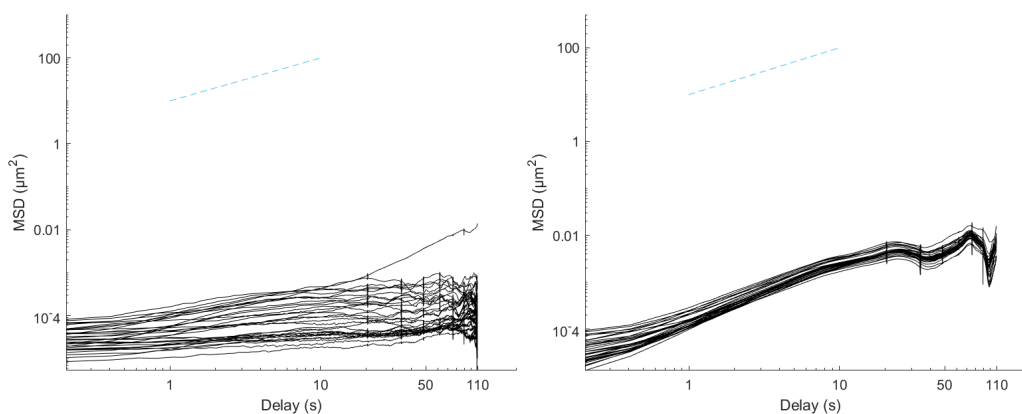


Figure 91: Parallel 2: MSD curves for particles tracked in a mixture of equal parts porcine and cold-water fish gelatin with a total gelatin concentration of 18 w%, measured at room temperature. Raw MSD curves are shown on the right, with drift corrected curves on the left.

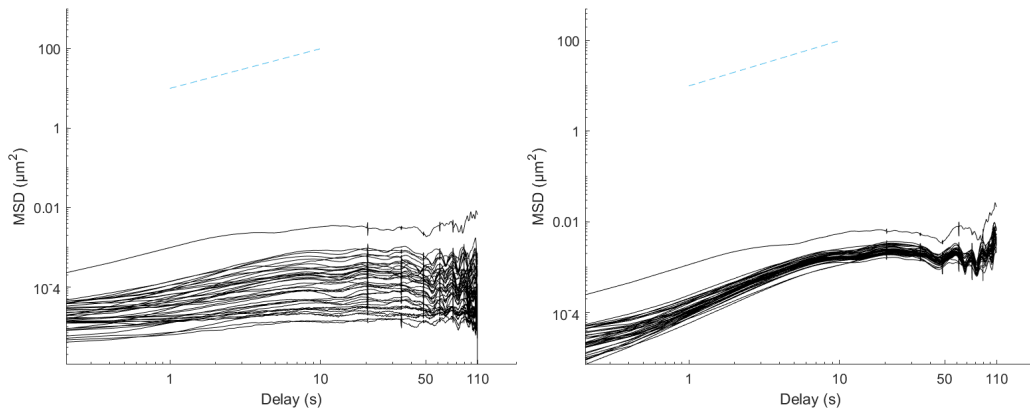


Figure 92: Parallel 3: MSD curves for particles tracked in a mixture of equal parts porcine and cold-water fish gelatin with a total gelatin concentration of 18 w%, measured at room temperature. Raw MSD curves are shown on the right, with drift corrected curves on the left.

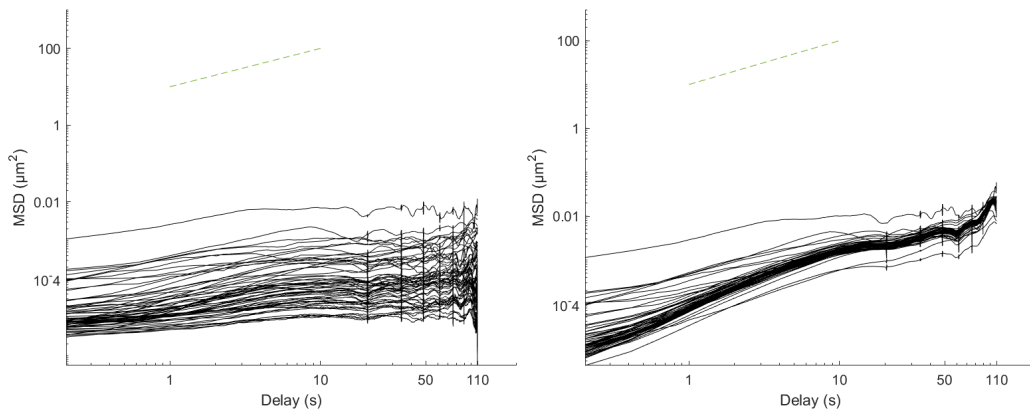


Figure 93: Parallel 4: MSD curves for particles tracked in a mixture of equal parts porcine and cold-water fish gelatin with a total gelatin concentration of 18 w%, measured at room temperature. Raw MSD curves are shown on the right, with drift corrected curves on the left.

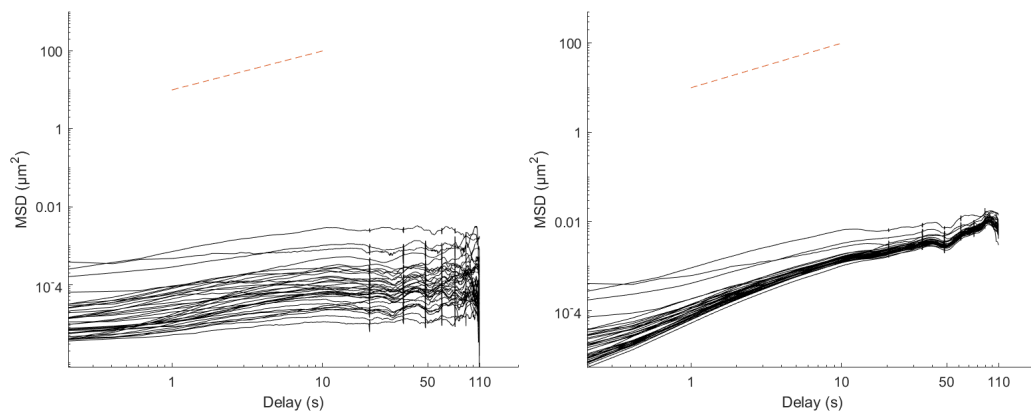


Figure 94: Parallel 5: MSD curves for particles tracked in a mixture of equal parts porcine and cold-water fish gelatin with a total gelatin concentration of 18 w%, measured at room temperature. Raw MSD curves are shown on the right, with drift corrected curves on the left.

A.2.4 90-10 mixed gels

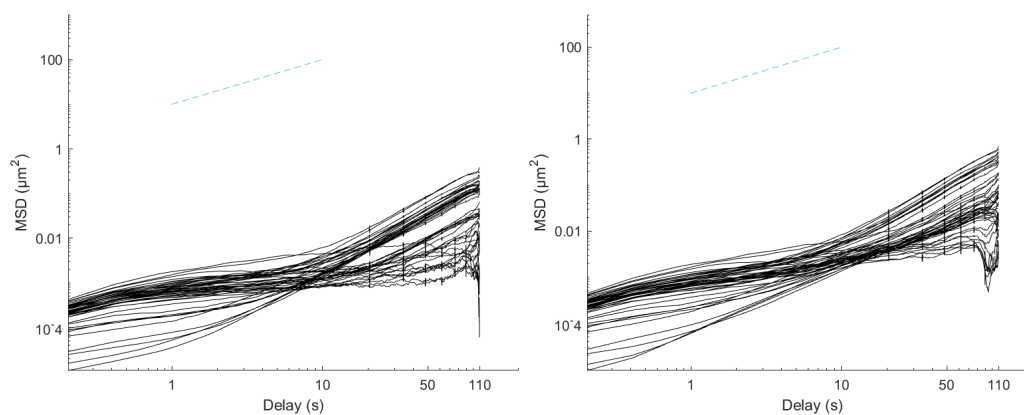


Figure 95: Parallel 1: MSD curves for particles tracked in a mixture of 10% porcine and 90% cold-water fish gelatin with a total gelatin concentration of 18 w%, measured at room temperature. Raw MSD curves are shown on the right, with drift corrected curves on the left.

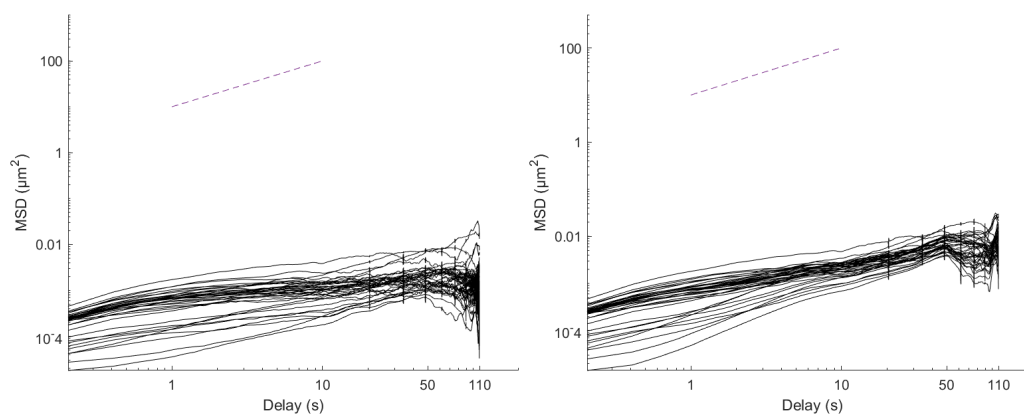


Figure 96: Parallel 2: MSD curves for particles tracked in a mixture of 10% porcine and 90% cold-water fish gelatin with a total gelatin concentration of 18 w%, measured at room temperature. Raw MSD curves are shown on the right, with drift corrected curves on the left.

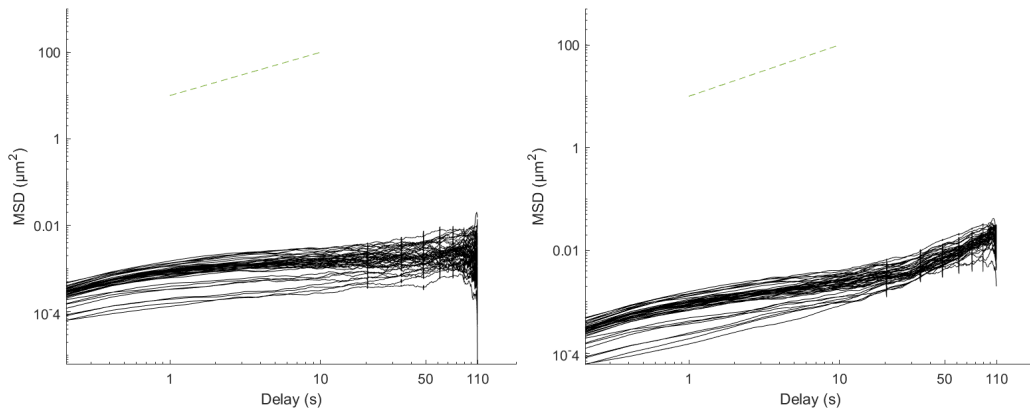


Figure 97: Parallel 3: MSD curves for particles tracked in a mixture of 10% porcine and 90% cold-water fish gelatin with a total gelatin concentration of 18 w%, measured at room temperature. Raw MSD curves are shown on the right, with drift corrected curves on the left.

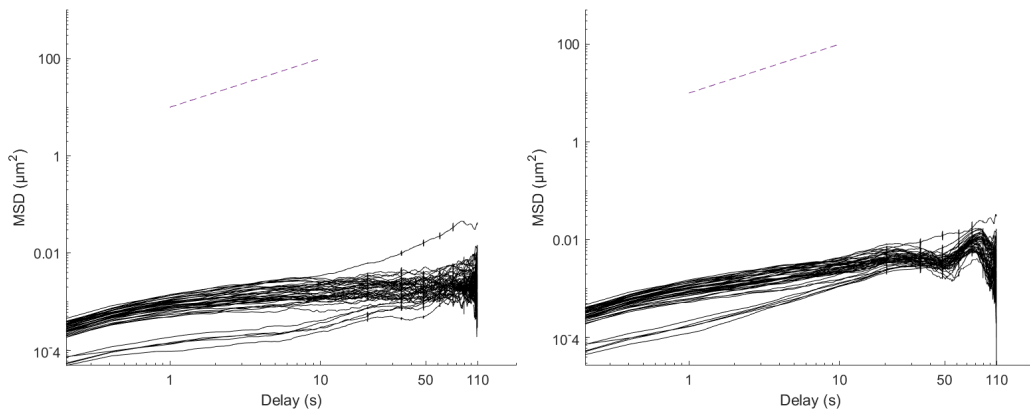


Figure 98: Parallel 4: MSD curves for particles tracked in a mixture of 10% porcine and 90% cold-water fish gelatin with a total gelatin concentration of 18 w%, measured at room temperature. Raw MSD curves are shown on the right, with drift corrected curves on the left.

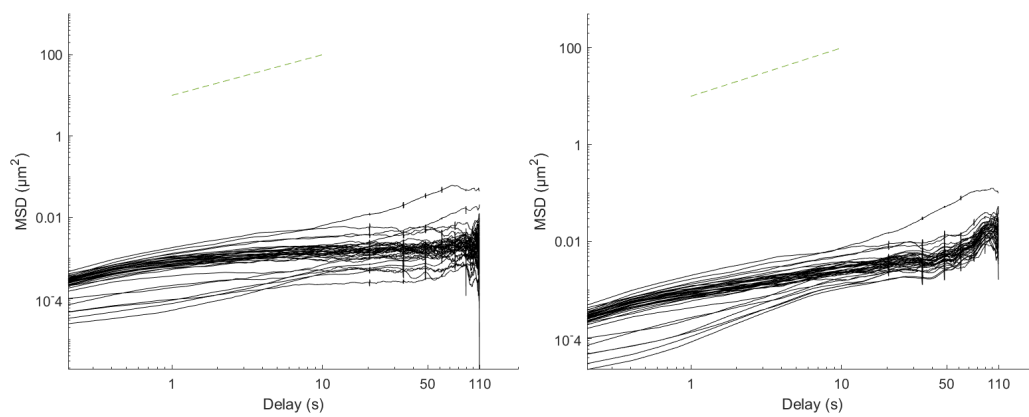


Figure 99: Parallel 5: MSD curves for particles tracked in a mixture of 10% porcine and 90% cold-water fish gelatin with a total gelatin concentration of 18 w%, measured at room temperature. Raw MSD curves are shown on the right, with drift corrected curves on the left.

B MATLAB code used for particle tracking

```
clear all;
tr = DETracker();
%%
5 tr.getPTrace(21,0.6,0,1);
tr.traceNum;
tr.setShowId(1:1:tr.traceNum);
tr.save("Trackingdata"); %Saves tracking data in the same folder as image
    series
10 %%
folder = "E:\"; %Folder containing tracking data.
Image_number = 536; %Number of images
Tracking_sec = 110; %Tracking time in seconds
15 trackingdataloc=append(folder, "\Trackingdata.csv");
framerate = Image_number/Tracking_sec;
frame2sec = 1/framerate;
pixels2um = 0.18; %||100x = 0.107||40x = 0.270||40x = 0.18||
opts = untitled;
20
A = readmatrix(trackingdataloc, opts);
A = circshift(A,[0 2]);
A(:,[1,2]) = A(:,[2,1]);
G = findgroups(A(:,1));
25 C=splitapply(@(m){m},A,G);
C{:};
C = C(cellfun('length', C) >= Image_number);
length(C)
N=length(C);
30 for n=1:N
    C{n}(:,1) = [];
    if n>N/2
        for a=2:length(C{n}(:,2))
            C{n}(a,2) = C{n}(a,2) + 5;
35         end
        for a=2:length(C{n}(:,3))
            C{n}(a,3) = C{n}(a,3) + 5;
        end
    else
40         for a=2:length(C{n}(:,2))
            C{n}(a,2) = C{n}(a,2) + 4;
        end
        for a=2:length(C{n}(:,3))
            C{n}(a,3) = C{n}(a,3) + 4;
45         end
    end
    C{n}(:,1) = frame2sec*C{n}(:,1);
    C{n}(:,2) = pixels2um*C{n}(:,2);
    C{n}(:,3) = pixels2um*C{n}(:,3);
50    my_field = strcat('p',num2str(n));
    particle.(my_field) = C{n};
end
figure()
55 ma = msdanalyzer(2, ' m ', 's');
ma = ma.addAll(C);
set(gca,'DefaultLineLineWidth',2)
[hps, ha] = ma.plotTracks;
ma.labelPlotTracks(ha);
```

```

60 trackloc=append(folder, "\Tracks.tif");
exportgraphics(gcf,trackloc);

for i = [0.1, 0.5, 0.8, 0.9] %Preforms curve fits
    ma = ma.fitLogLogMSD(i);
65     fit = ma.loglogfit;
        slopes = fit.alpha;
        if i == 0.1
            slopes4img = slopes;
        end
70
        fitloc=append(folder, "\Fits", num2str(i), ".xml");
        CSVloc=append(folder, "\Fits", num2str(i), ".CSV");
        mval4disp = append("For fraction ", num2str(i), ", mean MSD = ",
            num2str(mean(ma.loglogfit.alpha)));
        disp(mval4disp)
75     disp(" ")

        writestruct(fit, fitloc);
        S = readstruct(fitloc);
        S = struct2table(S);
80     writetable(S,CSVloc)
end

figure()
85 xlim([1 200])
    ylim([0 500])
    set(gca, 'YScale', 'log')
    set(gca, 'XScale', 'log')
    yticks([0.0001 0.01 1 100])
90 yticklabels({'10^-4','0.01', "1", "100"})
    xticks([1 10 50 110])
    xticklabels({'1','10', "50", "110"})
    msd = ma.plotMSD;
    plot([1 10], [10 100], "--")
95 MSDloc=append(folder, "\MSD.tif");
exportgraphics(gcf,MSDloc); %Gives MSD curves

figure()
xlim([1 200])
100 ylim([0 500])
    set(gca, 'YScale', 'log')
    set(gca, 'XScale', 'log')
    yticks([0.0001 0.01 1 100])
    yticklabels({'10^-4','0.01', "1", "100"})
105 xticks([1 10 50 110])
    xticklabels({'1','10', "50", "110"})
    Mmsd = ma.plotMeanMSD(gca, true);
    plot([1 10], [10 100], "--")
    MMSDloc=append(folder, "\MSD-Mean.tif");
110 exportgraphics(gcf,MMSDloc); %Gives mean MSD curves

figure
dr = ma.computeDrift('velocity');
dr.plotDrift
115 dr.labelPlotTracks;
dr = dr.computeMSD;
figure
xlim([1 200])
ylim([0 1000])
120 set(gca, 'YScale', 'log')
    set(gca, 'XScale', 'log')

```

```

yticks([0.0001 0.01 1 100])
yticklabels({'10^-4','0.01', "1", "100"})
xticks([1 10 50 110])
125 xticklabels({'1','10', "50", "110"})
drplot = dr.plotMSD;
plot([1 10], [10 100], "--")
DCMSDloc=append(folder, "\MSD-DriftCorrected.tif");
exportgraphics(gcf,DCMSDloc); %Gives drift corrected MSD curves
130
for i = [0.1, 0.5, 0.8, 0.9] %Gives curve fits for fractions 0.1, 0.5, 0.8
and 0.9 of total data.
    dr = dr.fitLogLogMSD(i);
    DCfit = dr.loglogfit;

135    DCfitloc=append(folder, "\Fits_DC", num2str(i), ".xml");
    DCCSVloc=append(folder, "\Fits_DC", num2str(i), ".CSV");
    mval4disp = append("For fraction ", num2str(i), ", Drift corrected MSD
    = ", num2str(mean(dr.loglogfit.alpha)));
    disp(mval4disp)
    disp(" ")

140    writestruct(DCfit, DCfitloc);
    S = readstruct(DCfitloc);
    S = struct2table(S);
    writetable(S,DCCSVloc)
145    if i == 0.1
        DCslopes4img = DCfit;
    end

end
150 %Code below is for exporting particle trajectories
%%
DCslopes = DCslopes4img.alpha;
tracks = [];
for i = 1:N %Plots all trajectories individually
155    D = {C{i}};
    ta = msdalyzer(2, ' m ', 's');
    ta = ta.addAll(D);
    set(gca,'DefaultLineLineWidth',2)

160    figure(Visible="off")
    ta.plotTracks;
    ta.labelPlotTracks();

    slopeval = append(" = ", num2str(round(slopes4img(i),5)));
165    DCslopeval = append("Drift c. = ", num2str(round(DCslopes(i),5)));
    yli=get(gca,'ylim');
    xli=get(gca,'xlim');

    xpos = xli(2) - (xli(2)-xli(1))*0.845;
170    ypos = yli(2) - (yli(2)-yli(1))*0.90;
    text(xpos,ypos,slopeval, "FontSize",15)

    xpos = xli(2) - (xli(2)-xli(1))*0.99;
175    ypos = yli(2) - (yli(2)-yli(1))*0.95;
    text(xpos,ypos,DCslopeval, "FontSize",15)

    imname = append("/Track", num2str(i), ".TIF");
    trackloc=append(folder, imname);
    tracks{end+1} = trackloc;
180    exportgraphics(gcf,trackloc, "Resolution",800);
end

```

```

%%
il = 9;
185 ll = 1;

while il<N %Plots 9 and 9 trajectories together
    figure
    montage(tracks,Indices=ll:il, ThumbnailSize=[800 1000], BackgroundColor
190         ="white");
    name = append("/Tracks ",num2str(ll),"-",num2str(il),".PDF");
    collloc = append(folder,name);
    exportgraphics(gcf,collloc);
    ll = il+1;
    il = il+9;
195 end

if il>N %Plots all trajectories together
    montage(tracks, Indices=ll:N, ThumbnailSize=[800 1000])
    name = append("/Tracks ",num2str(ll),"-",num2str(N),".PDF");
200    collloc = append(folder,name);
    exportgraphics(gcf,collloc);
end

205
%%

montage(tracks, ThumbnailSize=[])
collloc = append(folder,"/SeparatedTracks.PDF");
210 exportgraphics(gcf,collloc);

%%
close("all")
215

function opts = untitled
220
varNames = {'x','y','t','id'} ;
varTypes = {'double','double','double','double'} ;
delimiter = ',';
dataStartLine = 13;
225 extraColRule = 'ignore';

opts = delimitedTextImportOptions('VariableNames',varNames,...
    'VariableTypes',varTypes,...
    'Delimiter',delimiter,...
230    'DataLines', dataStartLine,...
    'ExtraColumnsRule',extraColRule);
end

```

C Release in aqueous environment - Raw data

C.1 Release after heating to 40 °C

The measured release from the gels when increasing the temperature to 40 °C is shown in the figures below.

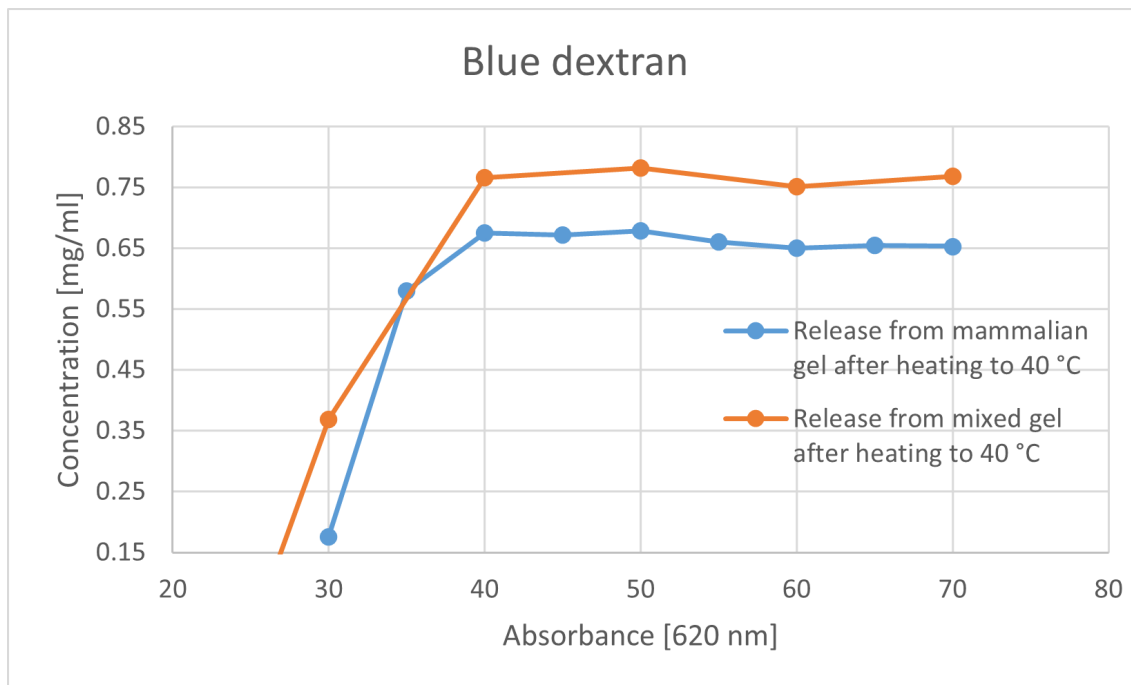


Figure 100: The release measured from gels containing blue dextran when heating to 40 °C.

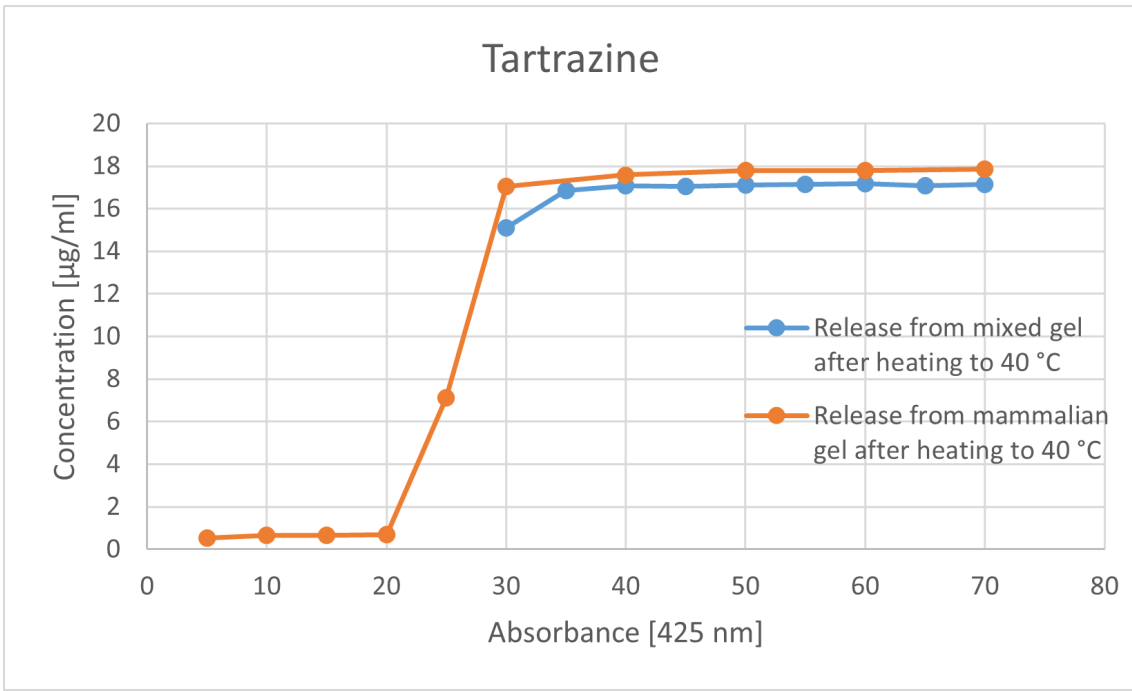
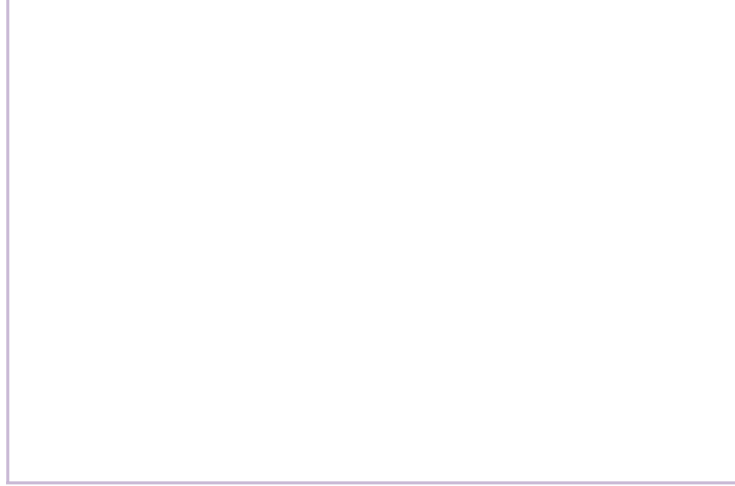
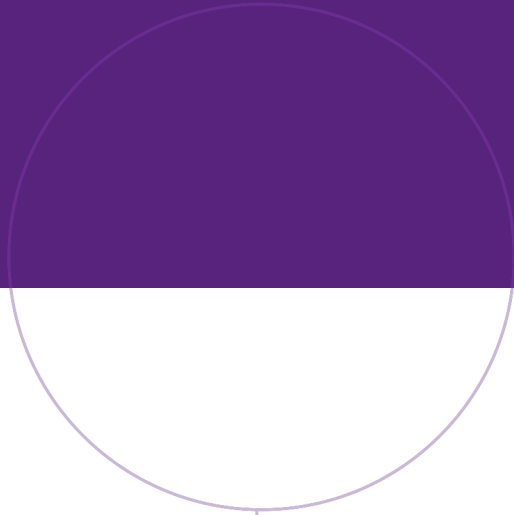


Figure 101: The release measured from gels containing tartrazine when heating to 40 °C.



Norwegian University of
Science and Technology